DOWNSCALING GLOBAL CLIMATE MODELS STATISTICALLY AND GENERATING PROJECTIONS OF CHANGES IN PRECIPITATION AND TEMPERATURE AT METEOROLOGICAL STATIONS IN ZAMBIA

BY

MONDAY CHOTA

A dissertation submitted to the University of Zambia in partial fulfilment of the requirements for the award of the degree of Master of Science in Statistics

THE UNIVERSITY OF ZAMBIA

LUSAKA

2019

COPYRIGHT

DECLARATION

I, **Monday Chota**, declare that this dissertation is my own work and that it has not been submitted for the award of any degree at this or any other institution of learning or research. All other person's works have been acknowledged accordingly.

Student's Signature……...Date……

Supervisor's Signature……..……Date…….

APPROVAL

This dissertation by Monday Chota has been approved as the partial fulfilment of the requirements for the award of the degree of Master of Science in Statistics of the University of Zambia.

Examiner 1

Name:…….

Signature:…… Date:……..

Examiner 2

Name:…….....

Signature:…… Date:……..

Examiner 3

Name:…….

Signature:……... Date:……..

Chairperson Board of Examiners

Name:……...

Signature:……..... Date:……..

Supervisor

Name:…….

Signature:…… Date:…….....

ABSTRACT

Zambia has been experiencing adverse impacts of climate change. Generation of climate information about changes in future precipitation and temperature is useful in designing adaptive measures. Currently, global climate models (GCMs) are primary tools utilized to simulate the present and future climate under different greenhouse emission scenarios. Owing to their coarse resolution of approximately 100 – 300 km per grid box, GCMs outputs are not suitable for direct use in assessing climate change impacts and designing adaptation strategies at local-scale. In this study, a statistical downscaling approach has been used to downscale GCMs at meteorological station level in order to improve GCMs coarse resolution to match with local needs for impact assessment. Further, the study used the downscaled time series to generate projected changes in precipitation and temperature at meteorological stations of Zambia for the period 2020 – 2049 relative to 1971 – 2000. A non-parametric analogue method based on nearest neighbour was used to downscale daily precipitation, minimum temperature and maximum temperature over 19, 13 and 11 meteorological stations, respectively, across Zambia from three GCMs: CanESM2, CNRM-CM5 and MPI-ESM-MR under RCP4.5 and RCP8.5 emission scenarios. ERA-Interim reanalysis and station datasets for a common period 1981 – 2010 were used to train the downscaling model. Findings presented are based on the ensemble of models. The ensemble mean at each station and local variable was computed from at least two GCMs with the same sign of change. Minimum and maximum temperatures are projected to increase at each meteorological station under both emission scenarios. The increase is higher towards the south of Zambia and for emission scenario RCP8.5 as compared to RCP4.5 scenario. Results also show decrease in precipitation over most stations in the Northern and Eastern parts of the country, increase in the western and Southern parts and exhibit a mixed signal for stations in the central part of the country. The downscaled precipitation and temperature scenarios can be used as inputs in climate impact models such as crop and hydrological models.

Key words: CMIP5 models, Statistical downscaling, Temperature, Precipitation, Climate models, Representative concentration pathways

DEDICATION

To mum **Edwis Kabwela Makaliki Chota**

and

late dad **Bartholomew Kasafya Chota.**

I will forever remain deeply indebted to your parental love, care and guidance. This is what your unwavering support has yielded.

To my beloved wife **Annety Mwila Kalengule Chota**

Your tolerance, love and patience have finally paid off.

ACKNOWLEDGEMENTS

I would like to express my sincere gratitude to all members of staff in the Department of Mathematics and Statistics of the University of Zambia for their support. I am highly indebted to my supervisor, Mrs. Jain Suman for her academic guidance, inspiration and trust in me. Special thanks also go to my employer, Ministry of General Education for the support and granting me study leave to take up full-time studies.

I am also grateful to Food and Agriculture Organisation (Zambia) for the financial support rendered towards this research. Dr. Chisanga Bwalya Charles (a Post-Doctoral Fellow in school of Agriculture - UNZA) deserves special mention for his assistance in writing R scripts for data analysis. His insights were valuable and made data analysis a lot easier.

Special appreciation goes to Zambia Meteorological Department for making their station data available through the downscaling portal for Santander Meteorology Group of the University of Cantabria, Spain. Manzanas Rodrigo Garcia (PhD) of the Santander Meteorology Group, Spain, I owe you great appreciation for your support and most importantly for granting me permission to use the web based statistical downscaling portal for data simulations.

To all postgraduate students that we shared the computer laboratory together, I say thank you for your inspiration and moral support. We endured together long hours studying and kept on encouraging one another. May God richly bless you all.

TABLE OF CONTENTS

LIST OF TABLES

LIST OF FIGURES

LIST OF APPENDICES

LIST OF SYMBOLS

$\sim$	Approximately
°	Degree
°C	Degrees Celsius
°E	Degrees East
°N	Degrees North
°S	Degrees South
Δ	Delta (change)
hPa	Hectopascal
Km	Kilometre
$\overline{Y}_B$	Long-term mean for baseline period
$\overline{Y}_f$	Long-term mean for the future period
m	Metre
ppm	ppm
mm	Milimetre
Parts per million	Parts per million
Δ_p	Projected change in precipitation
%	Percent
ρ	Rho (Pearson correlation coefficient)
r_s	Spearman rank correlation coefficient
$\sum$	Summation
W/m^2	Watts per square metre

OPERATIONAL DEFINITIONS OF KEY CONCEPTS AND TERMS

Climate change: A shift in long term mean of climate which is attributed directly or indirectly to human activity that alters the composition of gases in the global atmosphere.

Climate projections: Climate generated from the simulations of GCMs which incorporate response of the climate system to concentration of GHGs and aerosols in the atmosphere.

Climate system: Totality of the atmosphere, hydrosphere, cryosphere, land surface and biosphere including their interactions.

Downscaling: Process of deriving local to regional-scale (10 – 100 km) information from larger scale (100 – 300 km) observed or modeled data.

Emission scenario: Estimates of potential future discharges of substances into the atmosphere that affect the Earth's radiation balance, such as greenhouse gases and aerosols. These are based on projections of population, economic growth and technological advancement.

GCM ensemble mean: arithmetic average of at least two GCMs with same direction of sign of change under a given emission scenario.

Model training/calibration: Process involving adjusting (tuning) the model parameters in order to get a model representation of the process of interest.

Model validation (testing): Assessing the extent to which the downscaling methodology is able to reproduce the observations for a particular station.

Predictand: Local scale climate/weather variable associated with specific large scale variable(s).

Predictor: Large scale atmospheric/surface variable influencing a local climate/weather variable.

Radiative forcing: Net change in the energy balance of the Earth system resulting from some imposed perturbation. It is measured in watts per square meter and quantifies the energy imbalance that occurs when the imposed change takes place.

Reanalysis data: State-of-the-art dataset of past meteorological variables spanning the entire atmosphere produced by using quality controlled observations and data assimilation techniques.

Robust change: Model agreement in terms of the direction projected change in precipitation and/ or temperature. If at least two-thirds of the models agree on the direction of change then projections are robust.

Scenario: Plausible but unverifiable description of how the system and/or its driving forces may develop over time.

Spatial resolution: Size of a grid cell on the earth's surface. It is defined in terms of latitude, longitude and atmospheric layers.

ABBREVIATIONS

AGW	Anthropogenic Global Warming
AERs	Agro-Ecological Regions
CanESM2	Second Generation Canadian Earth System Model
CMIP3	Third Coupled Model Intercomparison Project
CMIP5	Fifth Couple Model Intercomparison Project
CNRM-CM5	Centre National de Researches Meteorological Coupled Model, Version 5
CSO	Central Statistics Office
DJF	December - February
ECMWF	European Centre for Medium Range Weather Forecasts
ENSO	El Nino Southern Oscillation
ERA-Interim	European Reanalysis Interim
GCMs	Global Climate Models
GFDL-ESM-2M	Geophysical Fluid Dynamics Laboratory Earth System Model with Modular Ocean Model version 4.1
GHGs	Greenhouse Gases
HadGEM2-ES	Hadley Centre Global Environmental Model version 2 (Earth System)
IPCC	Intergovernmental Panel on Climate Change
IPSL-CM5A-MR	L'Institut Pierre-Simon Laplace Coupled Model version 5A of Mid-Resolution
ITCZ	Inter-Tropical Convergence Assessment
JJA	June – August
KKIA	Kenneth Kaunda International Airport
KS-p	Kolmogorov Smirnov p-value
LARS-WG	Long Ashton Research Station Weather Generator
LCA	Lusaka City Airport
MAM	March – May
MAP	Mean Annual Precipitation
MENA	Middle East and North Africa

MIROC5	Model for Interdisciplinary Research on Climate Earth System Model version 5
MIROC-ESM	Model for Interdisciplinary Research on Climate Earth System Model
MPI-ESM-MR	Max-Planck Institute Earth System Model of Medium Resolution
NAPA	National Adaptation Programme of Action on Climate Change
NCAR-CCSM4	National Centre for Atmospheric Research – Community Climate System Model version 4
NorESM1-M	Norwegian Earth System model version 1 Medium Resolution
RCM	Regional Climate Model
RCP	Representative Concentration Pathway
SDP	Statistical Downscaling Portal
SDSM	Statistical Downscaling Model
SLP	Sea Level pressure
SON	September - November
SRES	Special Report Emission Scenario
T2m	Temperature at 2 metres
TMAX (Tmax)	Maximum Temperature
TMIN (Tmax)	Minimum Temperature
UNFCCC	United Nations Framework Convention on Climate Change
WMO	World Meteorological Organisation
ZMD	Zambia Meteorological Department

CHAPTER ONE: INTRODUCTION

1.1. Overview

This chapter presents the background to the study on statistical downscaling of precipitation and temperature for Zambia using simulations of global climate models (GCMs). It also highlights the statement of the problem, objectives of the study, hypothesis, and significance of the study, delimitation of the research, definitions of operational terms as well as the structure of the study.

1.2. Background

1.2.1. Climate Change

Unprecedented changes have been observed in the climate of the earth since 1950s. Experts in climate science have established that our climate is changing and there is strong evidence that this change can be largely attributed to human interference (IPCC, 2013). Climate change refers to a shift in the long-term (at least 30 years) mean climate. The United Nations Framework Convention on Climate Change (UNFCCC) distinguishes between human induced climate change and natural variability attributable to natural causes. UNFCCC (1992) defines climate change as a shift in climate observed over extended period and caused directly or indirectly by human interference to the climate system. Indicators of climate change at global level includes warming of the atmosphere and oceans, diminishing of snow and ice, and rise in sea levels (IPCC, 2013). At regional and national levels, climate change manifests as more frequent extreme weather events such as heat waves, droughts, seasonal and flush floods and dry spells occur. These events often lead to poor crop yields, loss of terrestrial and inland water ecosystems and biodiversity (IPCC, 2014).

1.2.2. Climate Models

In order to assess the response of the climate system to the increasing human activities, the scientific community has developed climate models (Hanssen-Bauer et al., 2005). The climate system of the Earth consists of the atmosphere, hydrosphere, biosphere, land surface and cryosphere. Interactions of these components determine the climate of the Earth. A climate model is a mathematical representation of the climate system based on physical, biological and chemical principles. The equations derived from these principles are very complex and solved numerically using computers (Curry, 2017). To solve these equations, GCMs use a three-

dimensional grid system by dividing the atmosphere, oceans and land into grids consisting of a number of cells (Figure 1). The number of cells in a grid system determines the spatial resolution of the model. For each time step making up the simulation period, these equations are computed for each cell in the grid (Curry, 2017). Presently, GCMs are primary tools which are used to understand present climate and future climate scenarios under increased GHGs concentrations (Wibig et al., 2015).

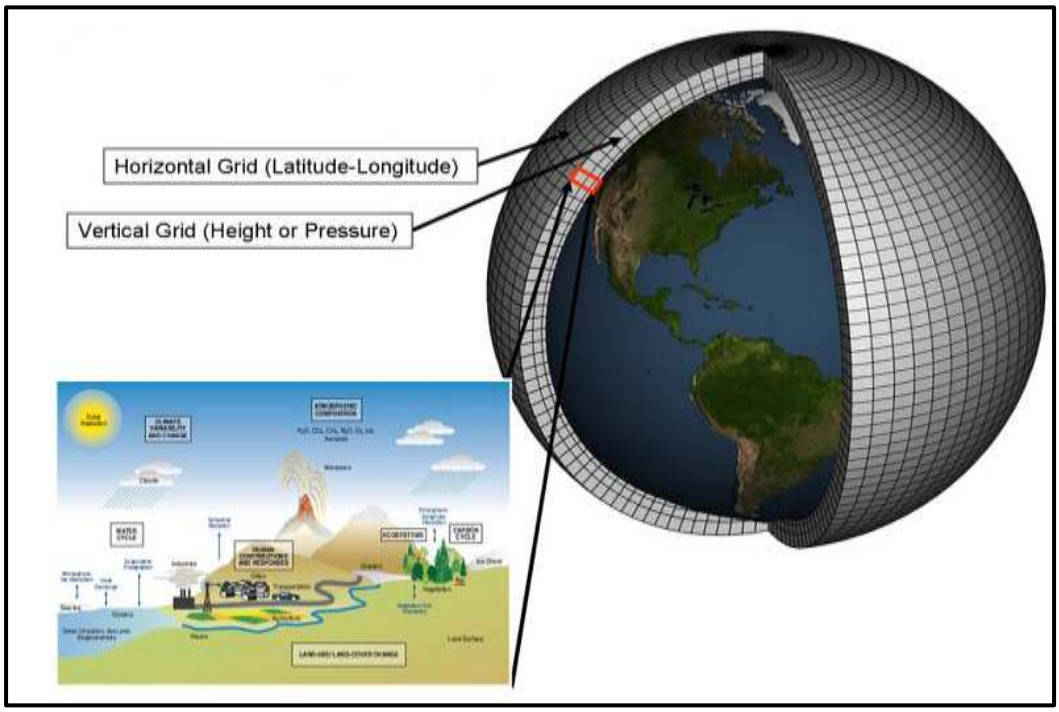

Figure 1: *Schematic diagram of a Global Climate Model (Source: Curry, 2017)*

1.2.3. Meaning and Motivation of Climate Downscaling

Climate downscaling is the process of obtaining local to regional-scale (10 to 100 km) climate information from the coarser spatial resolution (100 to 300 km) of GCMs (Trzaska and Schnarr, 2014) (Figure 2). Downscaling involves linking large-scale climate variables such as temperature, circulation, and moisture with local-scale surface variables such as temperature and precipitation (Wilby et al., 2004; Maraun et al., 2010; Wibig et al., 2015). Downscaling GCM simulations bridges the gap between what is provided by global climate modelers and what is needed for impact assessment at local level where impacts are most felt. Through downscaling, spatial resolution in the region of interest is increased, thereby improving essential aspects of the local/regional climate information. The increasing reliance on finer

resolution climate information for impact studies and policy formulation regarding adaptation justify the need for downscaling GCM simulated outputs.

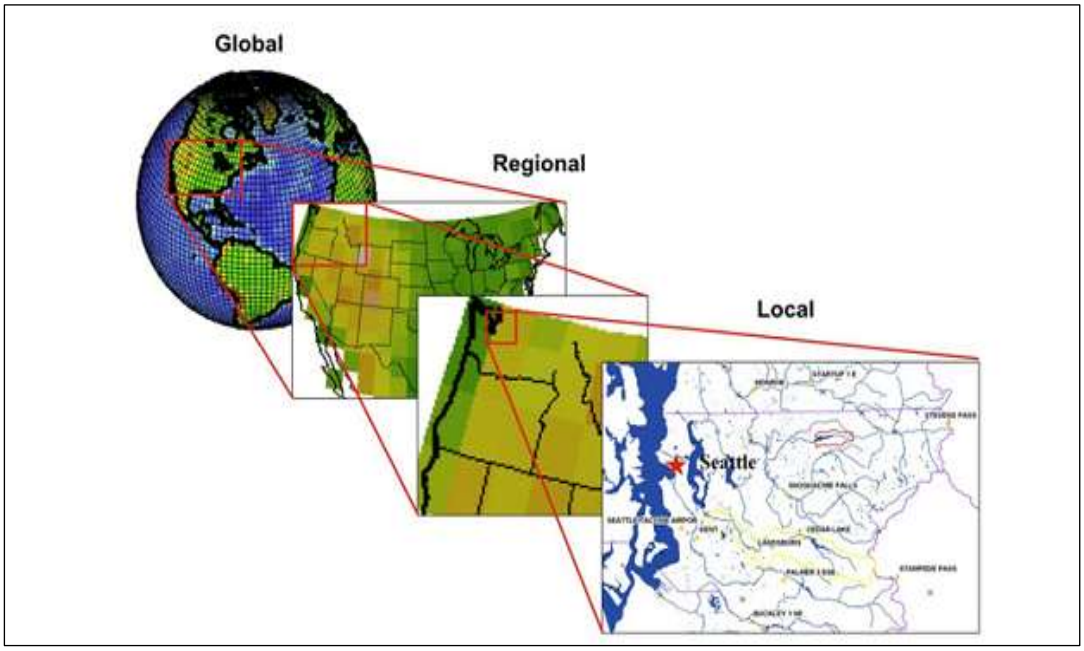

Figure 2: *Climate downscaling from global to regional and local scales*
Source: https://www.earthsystemcog.org/projects/downscaling-2013
(retrieved on 19/02/2018)

Although GCMs are capable of simulating climate variables at global and continental scales, they cannot account for regional to local climate changes that are needed for impact studies (Wilby and Wigley, 2000; Maraun et al., 2010; Trzaska and Schnarr, 2014; Benestad, 2016; Grouillet et al., 2016). This is attributed to their low spatial resolution of about 100km to 300km grid box (Luo et al., 2013; Benestad, 2016). This leads to a consensus among climate scientists that current GCMs cannot resolve important processes such as cloud and topographic effects that occur at local level and are of great importance to impact studies (Hewitson and Crane, 1996; von Storch et al., 2000; Wilby et al., 2004; Maraun et al., 2010; Gutiérrez et al., 2013).

In view of GCMs failure to simulate local characteristics of the region of interest, they cannot be used to describe local climate realistically (Gutiérrez et al., 2013). As a way of circumventing this weakness of GCMs and making them more applicable, downscaling is inevitable. Two major techniques of downscaling have been developed, namely; Dynamical and Statistical (Hewitson and Crane, 1996; Maraun et al., 2010).

In dynamical downscaling high resolution climate information is obtained by nesting a regional climate model (RCM) into a low GCM, which provides initial boundary conditions (Maraun et al., 2010). The RCMs and the driving GCM have similar representation of physical and atmospheric dynamical processes. Therefore, it is expensive to implement dynamical downscaling since it requires huge computing resources and high skilled human resource like that of GCMs (Hewitson and Crane, 1996; Maraun et al., 2010; Trzaska and Schnarr, 2014).

In statistical downscaling, empirical relationships linking some large-scale atmospheric predictor variables to local climate variables of interest are established (Ribalaygua *et al.*, 2013; Trzaska and Schnarr, 2014; von Storch et. al., 2000; Wilby et al., 2004). Statistical downscaling is capable of extracting point-scale climate information from a GCM simulation. The major assumption underlying statistical downscaling methods is that statistical relationships remain unchanged in a changed future climate (von Storch et. al., 2000; Wilby et al., 2004). Based on this assumption, these relationships are then applied to large scale variables simulated by the GCMs to produce local climate change information under different GHG emission scenarios (von Storch et al.2000; Wilby et al., 2004; Evans, 2011; Hewitson et al., 2014).

In climate simulations, the GCMs and GHGs emission scenarios are updated from time to time. The Fifth Phase of the Coupled Models Intercomparison Project (CMIP5) (Taylor et al,. 2012) is the most recent archive of GCMs after the earlier archive CMIP3. Similarly, Representative Concentration Pathways (RCPs) (Moss et al., 2010; Vuuren et al., 2011) are the most recent GHG emission scenarios developed after the Special Report on Emission Scenarios (SRES) (Nakicenovic et al., 2000)

1.2.4. The Coupled Model Intercomparison Project (CMIP)

CMIP was started in 1994 by the Climate Variability and Predictability (CLIVAR) Numerical Experimentation Group2 (Meehl et al., 2000). The objective of CMIP, as noted by (Eyring et al., 2016), was to advance the scientific understanding of the Earth system by assessing the performance of various climate models and better understand past, present, and future climate changes arising from natural, unforced variability or in response to changes in radiative forcing in a multi-model context. Since its inception, CMIP has evolved over five phases into a major international multi-model research activity and formed a central element of climate change assessment at different spatial and temporal scales. The current fifth project dubbed CMIP5

was aimed at understanding factors responsible for differences in model projections, evaluating how realistic models are in simulating recent climate and provide projections for future climate change on near term and long term bases (Taylor et al., 2012; Eyring et al., 2016; Emori et al., 2016).

1.2.5. Emission Scenarios

The IPCC's emission scenarios have evolved in terms of description, structure, development process and context (Girod et al., 2009) since the First Assessment Report in 1990. The latest generation of emission scenarios, Representative Concentration Pathways (RCPs) (Moss et al., 2010), were used in the latest IPCC report, Fifth Assessment Report which was completed in 2014. Table 1 shows the four independently developed RCPs emission scenarios.

Table 1: The Four Representative Concentration Pathways

Name	Description	Concentration
RCP2.6	Peak in radiative forcing at approximately 3 W/m^2 before 2100 and then decline.	~490 ppm CO_2 equivalent
RCP4.5	Stabilization without overshoot pathway to approximately 4.5 W/m^2 at stabilization after 2100.	~650 ppm CO_2 equivalent
RCP6.0	Stabilization without overshoot pathway to approximately 6 W/m^2 at stabilization after 2100.	~850 ppm CO_2 equivalent
RCP8.5	Rising radiative forcing pathway leading to 8.5 W/m^2 By 2100.	~1370 ppm CO_2equivalent

Source: *Adapted from Moss et al. (2010) and Vuuren et al. (2011).*

RCPs differ from the previous emission scenarios in two major ways. First, RCPs are not associated with fixed set of assumptions unlike the previous scenarios. Second, RCPs provide spatial and temporal information about different emissions and land use changes at a better resolution compared to its predecessors(Wayne, 2013).

1.2.6. Use of Climate Model Simulations in Studies on Climate Change Impacts Assessment for Zambia

Some earlier studies assessing impacts of climate change in Zambia on energy generation utilized GCM simulations. A study by (Yamba et al., 2011) assessed climate change implications on hydroelectricity generation in the Zambezi River Basin for the period 2010 to 2070 relative to the baseline period 1970 to 2000. The study used simulations of three CMIP3 GCMs to generate monthly precipitation for stations in the Zambezi river basin. The study

projected decrease in hydroelectricity power potential for Zambezi river basin during the period 2010 – 2070. This was attributed to projected frequent dry years, floods and increasing water demand. Another study undertaken by Stenek et al. (2011) evaluated climate change impacts on the Kafue Gorge Lower River Power Project using six CMIP3 GCMs Projections of precipitation and temperature were done for three time periods 2010 – 2039 (early century), 2040 – 2069 (mid-century) and 2070 – 2099 (late-century) with reference to baseline period 1975 – 2005. The study projected insignificant changes in mean annual precipitation but large increases in temperature.

Libanda et al. (2016) employed a non-parametric analogue method in a study involving assessment of predictors associated with statistical downscaling of precipitation over Zambia. Two CMIP5 GCMs were used in this study which was confined to predictor selection and downscaling of GCM projections was not conducted. A recent study by (Chisanga et al., 2017a) evaluated the suitability of Long Ashton Research Station Weather Generator (LARS-WG) in Zambia. The study used Mt. Makulu agriculture research station as a study site where three weather parameters (precipitation, minimum and maximum temperatures) were simulated using LARS-WG.

It is apparent that there is scanty literature involving statistical downscaling of climate over Zambia. This view is also reflected in other studies (Libanda et al., 2016; Chisanga et al. 2017b). Reviewed studies reveal that CMIP5 GCMs projections over Zambia have not been downscaled. Hence in all these studies, climate projections are generated at a coarse spatial resolution of about 100 to 300km. Moreover, studies in which future climate scenarios were downscaled relied on CMIP3 models. The current study sought to generate future climate information for Zambia at meteorological station level for the period 2020 to 2049 using Zambia Meteorological Department's (ZMD) observation dataset for the period 1981 to 2010 for both model calibration and validation. This was done through statistical downscaling of precipitation, maximum and minimum temperatures using a combination of two RCPs scenarios: RCP4.5 and RCP8.5 and three climate models from the CMIP5 archive. The use of multiple scenarios and GCMs allow better quantification of uncertainties associated with projected climate.

1.3. Statement of the Problem

The Intergovernmental Panel on Climate Change (IPCC) has established that climate change is real as unprecedented changes in the climate have been observed over decades to millennia (IPCC, 2014). Since the 1980s, Zambia has experienced an increase in frequency and intensity of heat waves, droughts and floods which are continuously posing long term threats to the sustainable development of the country. The high variability in temperature and precipitation are adversely impacting many sectors of Zambian economy including agriculture, food security, health and construction among others (National Adaptation Programme of Action on Climate Change - (NAPA, 2007). Therefore, the nation needs to plan and adapt to changing climate to achieve sustainable development. The planning and adaptation process requires future climate change information which is currently available at coarse spatial resolution of GCMs (Arslan et al., 2015). Literature reviewed (Stenek et al., 2011; Yamba et al., 2011; Libanda et al., 2016; Chisanga et al., 2017) showed inadequate information about downscaled future changes in precipitation and temperature at meteorological station level across Zambia.

Thus, adequate scientific climate change information is lacking at finer spatial resolution to empower the decision makers in formulating national policies to reduce harmful impacts of climate change at district and community level. Therefore, this study sought to contribute to closing this gap by projecting changes in precipitation and temperature downscaling of Zambia at meteorological station level for the period 2020 to 2049 relative to the reference period 1971 to 2000 using simulations of Global Climate Models.

1.4. Objectives

1.4.1 Main Objective

The overall objective of this study was to generate mean precipitation and temperature at meteorological stations in Zambia for the period 2020 – 2049.

1.4.2. Specific Objectives.

1. To investigate large scale atmospheric variables which are optimal predictors for temperature and precipitation at weather station level in Zambia.
2. To determine long-term mean precipitation and temperature at meteorological station for periods 1971 – 2000 and 2020 – 2049.

3. To determine the changes in mean precipitation and temperature for the period 2020 to 2049 relative to the reference period 1971 to 2000.

1.5. Hypothesis

Mean temperature and precipitation at the meteorological stations in Zambia would change during 2020 – 2049 with respect to the corresponding means for the baseline period 1971 – 2000.

1.6. Significance of the Study

Findings of this study were envisaged to contribute to the understanding of the plausible climate change in Zambia during the period 2020 to 2049. It endeavoured to provide detailed future climate change projections at smaller spatial scale to enable decision makers to formulate responsive strategies in a quest to mitigate and adapt to adverse impacts of climate change. It was anticipated that this study would provide inputs in the Impacts, Adaptation and Vulnerability assessment models specific to sectors such as agriculture, hydrology, health, insurance, infrastructure, wildlife, forestry and energy of the Zambian economy at smaller spatial resolution.

1.7. Delimitation of the Study

The study was confined to statistical downscaling of daily precipitation and temperature (maximum and minimum) for Zambia, using GCMs from the CMIP5 archive forced by two RCPs (RCP4.5 and RCP8.5). This study relied on three GCMs that cover Zambia and the surrounding region since GCMs use various grid systems. For the period 1981 – 2010, only 11, 13 and 19 stations had continuous data for maximum temperature, minimum temperature and precipitation respectively. Therefore, not all meteorological stations maintained by ZMD were analysed in the study. Predictors for downscaling were supplied by the European Reanalysis (ERA) Interim data, henceforth known as ERA-interim reanalysis data. Simulations from three CMIP5 GCMs were downscaled for the period 2020 to 2049.

1.8. Structure of the Dissertation

This dissertation is organised in six chapters. **Chapter One** has presented background to the study, statement of the problem, objectives, significance of the study and the operational

definitions. In **Chapter Two**, theoretical framework and review of related literature, which is organised thematically, are presented. A brief description of the study area will be given in the **Third Chapter**. Datasets and methodology used are presented in **Chapter Four**. Results are presented and discussed in **Chapter Five**. In **Chapter Six** conclusions and recommendations are presented.

1.9. Chapter Summary

In this chapter, background on statistical downscaling of GCM simulation outputs in Zambia has been presented. Furthermore, statement of the problem, purpose of the study, research objectives and hypothesis, significance of the study, limitations as well as delimitations of the study, conceptual and theoretical frameworks have been highlighted. The chapter has also presented definitions of operational terms used in the study. Lastly, organisation of the study has been given. In the next chapter literature deemed relevant to the study is reviewed so as to put it within the context of similar previous works

CHAPTER TWO: LITERATURE REVIEW

2.1. Overview

In this chapter, literature essential to the study is reviewed. The chapter begins by discussing the theoretical framework guiding the study. A review of literature on the meaning and motivation for downscaling of GCM outputs, approaches to statistical downscaling, predictor variables commonly used in downscaling temperature and precipitation are also presented. Apart from the discussion on the selection of GCMs for downscaling, observed and projected changes in precipitation and temperature at global, regional and national levels are presented.

2.2. Theoretical Framework

The study was guided by Anthropogenic (human induced) Global Warming (AGW) and the principle of uncertainty in the Earth's climate.

2.2.1. The Anthropogenic Global Warming (AGW)

Proponents of AGW theory assert that a rise in global temperature is predominantly caused by increased human emissions of greenhouse gases (GHGs) (Bast, 2010; Collins et al., 2013; IPCC, 2013) since the pre-industrial times. The major GHGs are water vapour, carbon dioxide, nitrous oxide and methane. Human activities such as deforestation, burning wood and fossil fuels contribute to increased concentration of GHGs, especially carbon dioxide, in the atmosphere. It is scientifically established that if emissions do not correspond to natural sinks of carbon dioxide, deforestation and burning of fossil fuels would double the amount of carbon dioxide in the atmosphere. According to the AGW theory, the influence of other external forcings such as variations in solar radiation cannot explain the increase in global temperature (Bast, 2010).

This theory was deemed appropriate for the study based on two reasons. The first reason was that GCMs incorporate response of the climate system to concentration of GHGs and aerosols in the atmosphere. In this case, the increase in human activities would lead to more warming owing to the enhanced emission and concentration of GHGs in the atmosphere. In addition, the theory is strongly supported by the IPCC as evidenced in its reports.

2.2.2. Principle of Uncertainty in Future Climate

Curry and Webster (2011) argued that science is characterised by varying degree of certainty, ranging from nearly true to absolute uncertain. Similarly, climate science is associated with uncertainties. The fact that the future is not known, coupled with complexity of the climate system, makes projections of future climate uncertainty. Uncertainty in climate projections arise from various sources including climate models, emission scenarios, and internal variability to forcing and boundary conditions (Collins et al., 2013). Projections of future climate are characterised by GHG emission scenarios. Studies show that as human understanding of future emissions is limited, climate change projections involve exploring climate response to a wide range of possible futures influenced by societal choices.

2.3. Statistical Downscaling under Perfect Prognosis approach

Under perfect prognosis approach, statistical relationships are trained using large-scale variables (predictors) from the reanalysis dataset and historical observations. The underlying assumption of the perfect prognosis approach is that reanalysis data represent real large-scale atmospheric conditions (Manzanas, 2016). This approach involves the training (calibration) phase and downscaling (prediction) phase. In the training phase, a statistical relationship linking predictors and observed local-scale variables is established using data from a common historical period of the reanalysis time window and the station-based observations period (Gutiérrez et al., 2013; Casanueva et al., 2016).

In the downscaling phase, the resulting model is applied to GCM predictor data forced by different concentration or emission scenarios to obtain target local-scale climate variable(s). For this reason, only large-scale variables which are well simulated by both GCMs and reanalysis are commonly selected as predictors (Wilby and Wigley, 1997; Wilby et al., 2004).

Further, this approach does not consider, as predictors, surface variables such as precipitation since they are directly influenced by model parameterisations and orography (Manzanas, 2016). The major setback for PP is that reanalysis data does not necessarily provide a perfect representation of the large-scale circulations.

2.4. Selection of Global Climate Models for Downscaling

As discussed in Section 1.2.5, GCMs are the main tools for understanding how climate may evolve in future. They are also useful in characterising outcomes and uncertainties under specific assumptions about future forcing scenarios (Flato et al., 2013). Presently, high resolution climate information is greatly sought for climate change impact assessment studies. This information is obtained from GCM outputs using downscaling techniques. However, downscaled climate information is associated with a number of uncertainties. One of the sources of these uncertainties is the choice of GCMs used in the downscaling process (Wibig et al., 2015). Therefore, the choice of GCMs in impact studies is a very important step. In most applications a small ensemble of climate models is chosen for the assessment as it may not be necessary to use all GCMs projections in detailed climate change impact studies. In practice, computational and human resource constraints justify the selection of a subset of GCMs for downscaling (McSweeney et al., 2012; Lutz et al., 2016).

In literature, a number of approaches have been used to select GCMs for impact studies. Pierce et al., (2009) and Lutz et al. (2016) used the past-performance approach. In this approach, the skill of the model to simulate present and near-past climate is the criterion for model selection. Models are assessed in their ability to simulate key climatological variables such as mean annual temperature, total annual precipitation. This approach is referred to as validation approach by Fenech et al. (2002) and Breach et al. (2016). In the context of climate change, GCMs should be able to simulate observed climate phenomena. These may include climatological mean, seasonal cycles, inter - annual variability and frequency of extreme events (Brands et al., 2011). This criteria is supported by (Flato et al., 2013; McSweeney et al. 2012; Lutz et al., 2016; Zubler et al., 2016) who contend that GCM of choice should represent present climate realistically by simulating key processes since such models increase confidence in the generation of projections for future climate. Many studies have used this method and the climate research community encourage its use.

2.5. Assessment of CMIP 5 GCMs Integrated in the Statistical Downscaling Portal (SDP)

Miao et al. (2014) assessed the performance of 24 CMIP5 models in simulating intra-annual, annual and decadal temperature over Northern Eurasia for the period 1901 to 2005. This

ensemble of GCMs included seven (CanESM2, CNRM-CM5, HadGEM2-ES, IPSL-CM5A-MR, MIROC-ESM, MPI-ESM-MR and NorESM1-M) of the eight GCMs that are integrated in the SDP with the exception of GFDL-ESM-2M only. The study established that of these seven models CNRM-CM5, HadGEM2-ES, MPI-ESM-MR and NorESM1-M underestimate annual temperature while CanESM2, IPSL-CM5A-MR and MIROC-ESM overestimates. While Chylek et al. (2011) found similar results for CanESM2 of the arctic temperature over the period 1970 to 2000, Chong-Hai and Ying (2012) established that CanESM2 had a larger warming trend than observations with CNRM-CM5 underestimating annual temperature over China. Further, Hewitson et al. (2014) established that the CanESM2 model was able to capture local scale differences over Africa which is relevant for impact and adaptation studies. This is similar to what Yang et al., (2015) found in East Africa where correlation between observed and modelled precipitation in CNRM-CM5 was high.

A study by Mehran et al. (2014) cross-validated historical precipitation simulations of 34 CMIP5 GCMs against observations for the period 1979 to 2005. Apart from the MPI-ESM-MR, other seven GCMs integrated in the SDP were part of the 34 models assessed. Over regions of complex topography such as Southern Africa and South America, most models overestimate precipitation but underestimate it over arid regions. Further ensemble mean and median were showed to out-perform individual CMIP5 models.

In West Africa, Roehrig et al., (2013) established that the model CNRM-CM5 simulates well the diurnal cycle of low level clouds and appreciable amount of precipitation during most of the day. Furthermore, the onset of monsoon is correctly captured by the three models; CNRM-CM5, MPI-ESM-MR and NorESM1-M. However, the model IPSL-CM5A-MR underestimates maximum precipitation and does not capture the spring precipitation near the Guinea coast but simulates summer rainfall well over the Gulf of Guinea south of the equator.

Ongoma (2017a) used five CMIP5 models, which included CanESM2 and CNRM-CM5, to assess potential future variations of mean rainfall and temperature over East Africa under RCP4.5 and RCP8.5. Although results show that these GCMs tend to underestimate and overestimate seasonal rainfall during MAM and OND respectively, they simulate annual cycle in the entire region fairly well.

A study by McSweeney et al. (2015) sought to identify 8 to 10 GCMs, from CMIP5 models, appropriate for use in the assessment of regional climate change across three regions: Africa, Europe and Southeast Asia. For Southern Africa, the assessment of each of these models was based on the ability to simulate annual cycles of precipitation and temperature. The study classified a model as "biased" if position and timing of features are realistic but magnitude is inaccurate and "significantly biased" when it represents a surface climate variable unrealistically. Table 2 is a summary of an assessment of the seven models that are integrated in the SDP as analysed by McSweeney et al (2015) over Africa. As for Southern Africa, performance was found to be mixed and no models emerged as significantly 'worse' than others generally.

Table 2: Assessment of CMIP5 models integrated in the SDP

Model	Annual cycle of Temperature	Annual cycle of precipitation	Key Teleconnections
CanESM2	Satisfactory	Satisfactory	Biases
CNRM-CM5	Satisfactory	Satisfactory	Satisfactory
GFDL-ESM2M	Satisfactory	Satisfactory	Satisfactory
IPSL-CM5A-MR	Satisfactory	Satisfactory	Satisfactory
MIROC-ESM	Satisfactory	Satisfactory	Satisfactory
MPI-ESM-MR	Satisfactory	Satisfactory	Satisfactory
NorESM1-M	Biases	Biases	Satisfactory

Source: *Adapted from McSweeney et al. (2015)*

A recent study by Munday and Washington (2017) used twenty-one GCMs with a common ensemble member r1i1p1 (same as the one used in the portal) from the CMIP5. Five of these models: CanESM2, MIROC-ESM, IPSL-CM5-MR, MPI-ESM-MR and NorESM1-M are among eight models integrated in the portal. The study established that these models capture the location of Angola Low (AL) well. Moreover, annual cycle of rainfall over Southern Africa is reproduced well by these models despite exhibiting a large spread in rainfall amounts. Good performance of IPSL-CM5A-MR and MPI-ESM-MR is also noticed in East Africa by Yang et al (2015) where correlations and root mean square error (RMSE) between observations and models is greater than 0.8 and less than 0.5 respectively, in each GCM.

Libanda et al., (2016) assessed the performance of two CMIP5 models, namely CNRM-CM5 and CanESM2 by comparing with observed station data for thirty nine meteorological stations across Zambia. The study established that annual cycle of the rain season (October to April) was well captured by both models. Besides representing the dry season (May to September) well, the two models also captured the downward gradient of the distribution of precipitation from North to the South of Zambia. Comparing the two models, the study established that CNRM-CM5 out-performed the CanESM2 as the latter under estimated precipitation over some parts of Eastern Province.

A recent study by Charles et al. (2017a) investigated how statistical bias correction of CMIP5 models impact the future climate change under RCP8.5 for 2020 – 2050, relative to the period 1980 – 2000. This was a single-site study as only Mt. Makulu station was involved. Three bias correction methods: change factor, nudging and quantile mapping were compared using four GCMs from CMIP5 archive, namely: GFDL-ESM2M, MIROC5, MPI-ESM-MR and NCAR-CCSM4. Results show that change factor method performed better in correcting bias of annual precipitation as quantile mapping and nudging methods yielded poor accuracy.

2.6. Selection of Large-scale Variables (Predictors)

The selection of large-scale variables (predictors) is one of the most crucial tasks in statistical downscaling of climate projections. Hofer et al. (2015) argue that there are two ways of selecting predictors for statistical downscaling, namely priori selection and data-based selection. In priori selection, predictors are chosen based on knowledge outside the available data (without data analysis). As for the second method, selection is based on statistical analysis of the relationship between potential predictors and predictand (data based selection). To counter the weaknesses associated with each of these two methods, the use of both methods is common in most studies.

Regardless of the method used in predictor selection, there is consensus among the downscaling community (Hewitson and Crane, 1996; Wilby et al., 2004; Coulibaly et al., 2005; Maraun et al., 2010; Gutiérrez et al., 2013; Manzanas, 2016) that any study involving statistical downscaling of GCM outputs should be preceded by a careful selection of most relevant predictors for the target local variable. Maraun et al., (2010) and Wibig et al., (2015) contend that a predictor of choice should be of high predictive power and can be identified by

some correlation analysis with local-scale variables (predictand). However, Hewitson and Crane (2006) warn against relying on relationships that are completely correlative and demand for knowledge of local physical processes as invaluable in determining meaningful predictor combinations. Further, Tareghian and Rasmussen (2013) cautioned against using excessive number of predictors since some of them may be correlated and lead to poor prediction accuracy and difficulties in interpretation.

In the context of climate change, predictors for downscaling should include large-scale variables that contain relevant climate change signal such as changes in thermodynamic properties. These may include circulation variables, free atmospheric temperature and moisture variables (Huth, 2002; Hewitson and Crane, 2006; Brands et al., 2011; Benestad, 2016). This stand point is consistent with Gutierrez et al. (2013) who avoided the use of predictors that only include circulation variables such as geopotential height, sea level pressure, zonal and meridional wind components. They argue that circulation variables tend to have a weaker climate change signal than temperature and/or absolute humidity which are related to variations in radiation balance. Thus in downscaling temperature an indicator of the radiative properties of the atmosphere should be considered (Huth, 2004).

Similarly, humidity information need to be taken into account when downscaling precipitation (von Storch et al., 2000) since it improves predictions for present climate and stationarity of the model (Hewitson and Crane, 2006). Besides, local precipitation relies on atmospheric circulation and most GCMs do not simulate relative humidity well (Hanssen-Bauer et al., 2005). However, they also acknowledge the use of signal bearing predictor(s) such as atmospheric moisture when downscaling climate under climate change conditions.

Predictors used in some previous studies involving statistical downscaling of temperature and precipitation are given in Table 3. It is worth noting that this table is not exhaustive but only meant to illustrate predictors used to downscale temperature and precipitation in different regions. Based on predictors shown in Table 3, it is apparent that predictors used for downscaling temperature and precipitation usually constitute a combination of circulation and those carrying radiative properties of the atmosphere. Middle tropospheric variables (at 850 hPa and 750 hPa) are commonly used while upper levels (500 hPa) or more are rarely utilised.

Table 3: Illustration of predictors and methods used in statistical downscaling of temperature and precipitation from different regions (countries)

Predictand	Predictors	Methods	Region/country	References
Temperature	T2m, SLP	Canonical correlational analysis –CCA (EOF –based)	Scandinavia	Benestad, R.E (2001)
Temperature	T850, SLP	Multiple linear regression (MLR), CCA, Singular Value Decomposition (SVD)	Central Europe	Huth, R. (2002)
Temperature Precipitation	T2m, SLP, Z850, U850, V850 T2m, SLP, Z850, U850, V850, Dew point temperature at 2m	Analogue	Western Mediterranean	Grouillet et al., (2016)
Tmax, Tmin Precipitation	U500, Z500, Z850, Q850/R850, Vortices at 500 hPa MSLP, U500, U850, Z500, Q850/R850, Q500/R500	SDSM (regression based)	Northern Canada	Dibike et al., (2008)
Temperature	T550, Z550	Simple linear regression (SLR)	Cordillera Blanca, Peru	Hofer, M. et al., (2015)
Precipitation	SLP	Analogue	Central Sweden	Wetterhall, F. et al. (2005)
precipitation	Q500, Q850, U850, airflow strength at 850hPa	SDSM	Agustan del Norte, Philippine	Burdeos, K.B and Lansigan, F.P (2017)
Tmax precipitation	Z500, T850 T500, Q850, U850	Analogue based on nearest neighbour	Senegal	Manzanas, R.G(2017)

Note:

Predictors: specific humidity (Q), meridional wind component (V), zonal wind component (U), relative humidity (R), temperature at 2 metres (T2m), temperature (T), geopotential height (Z), sea level pressure (SLP/MSLP), dew point temperature at 2m (D2)

Methods: Canonical Correlational Analysis (CCA), Multiple Linear Regression (MLR), Singular Value Decomposition (SVD), Statistical Downscaling Model (SDSM), Empirical Orthogonal Functions (EOF), Self-Organising Maps (SOM), Probability Density Functions (PDF) and Cumulative Density Function (CDF).

Table 3 Continued

Predictand	Predictors	Methods	Region/country	References
Tmax Tmin precipitation	U500, U850, Z850, 850 hPa divergence, 500 hPa airflow strength, Surface zonal velocity U850, T2m, MSLP, surface specific humidity	SDSM	South Wollo Zone, North Central Ethiopia	Legesse, S.A et al.(2013)
precipitation	Large-scale precipitation, specific humidity at 10m	Empirical Orthogonal functions (EOF)	Tanzania	Mtongori, H.I. et al.(2016)
precipitation	Q750, R750, U750, V750, surface temperature	Self-Organising Maps (SOM) and PDF	South Africa	Hewitson,B.C and Crane, R.G (2006)
Rainfall and temperature (Tmin, Tmax)	U700, V700, 500 – 850hPa lapse rate, T2m, 10m U and V winds, relative and specific humidity	SOM and CDF (cumulative distribution functions)	Cape Town/ South Africa	Tadross and Johnston, (2012)
Precipitation	T850, Q850, U850	Analogue	Zambia	Libanda, B et al., (2016)

Note:

Predictors: specific humidity (Q), meridional wind component (V), zonal wind component (U), relative humidity (R), temperature at 2 metres (T2m), temperature (T), geopotential height (Z), sea level pressure (SLP/MSLP), dew point temperature at 2m (D2)

Methods: Canonical Correlational Analysis (CCA), Multiple Linear Regression (MLR), Singular Value Decomposition (SVD), Statistical Downscaling Model (SDSM), Empirical Orthogonal Functions (EOF), Self-Organising Maps (SOM), Probability Density Functions (PDF) and Cumulative Density Function (CDF).

2.7. Selection of Geographical Domain

Local climate variables such as precipitation and temperature are related to conditions taking place over large surrounding space as well local geographical features (Benestad, 2016). Additionally, GCMs have different skill in reproducing observed climatology across space and time. This standpoint justifies the selection of a geographical domain as an important activity in a statistical downscaling process. Wilby et al. (2004) argued that this helps in specifying the location and dimensions of the large-scale predictor fields for downscaling local variables of interest. The domain chosen for downscaling should be large enough to reflect influential processes affecting the region under study.

Although Goodess and Palutikof (1998) contend that the predictive ability of a model is expected to increase with increasing domain size, other studies have shown that too large a domain size can add unnecessary noise and result into producing spurious results. Further, a domain size which is small enough would enable completion of simulations in a reasonable amount of time since time required is proportional to the number of grid points. In order to establish the predictor–predictand relationship, the selected domain should capture synoptic forcing features represented by the GCM (Hewitson and Crane, 1996).

To overcome some of the issues associated with the skill level of various domain sizes, the use of mean sea-level pressure or variables derived from mean sea-level pressure have formed the centrepiece of many downscaling studies due to its relatively conservative variability and hence, predictability (Goodess and Palutikof, 1998; Wilby and Wigley, 1997; Wilby et al., 1998). In contrast, Gutierrez et al. (2013) and Haylock et al. (2006) demonstrated that predictor choice has more influence on the downscaled results than the size of the geographical domain applied. In the case of analogue method, Gutiérrez et al.(2004; 2013) suggest that better results are obtained from smaller domains.

2.8. Projections of Changes in Temperature and Precipitation

2.8.1. Global Level

Analysis of global surface temperature records for the period 1880 to 2012 indicates an average warming of 0.85˚C since the pre-industrial period (IPCC, 2013). Global mean surface air temperature is projected to rise over the 21st century under all assessed emission scenarios

(Trenberth et al., 2007; Collins, 2011). Relative to the 1985 to 2005 average, global mean annual temperature is projected to increase by 0.3 to 2.5°C by 2050 with a higher change over land areas (Daron, 2014a). The Fifth Assessment Report of the IPCC (2013) has established that change in global temperature increases with the increase in RCP scenarios (i.e. from RCP2.6 to RCP8.5) as well as with time. Thus, long-term projections for the period 2081 – 2100 show larger changes that are likely to exceed 1.5^0C of warming under all IPCC emission scenarios with the exception of low emission scenario (Collins et al., 2013). By the end of 21st century, warming is likely to exceed 3^0C under RCP8.5.

Projected changes in future precipitation are characterised by model disagreements in the likely direction and magnitude of change (Hushaw, 2015). Global precipitation is projected to increase steadily over the 21st century under global warming conditions. On average, an increase of about 2 percent and 5 percent under RCP2.6 and RCP8.5 respectively is projected in global precipitation (Collins et al., 2013). Regionally, precipitation is projected to vary since dry regions will become much drier and wet regions wetter (Collins et al., 2013; IPCC, 2014; Kirtman et al., 2013).

2.8.2. Africa

In the last 50 to 100 years, most parts of Africa have experienced an increase in surface temperature of at least 0.5˚C (Hulme et al., 2001; Niang et al., 2014). Observed data shows that minimum temperature is increasing faster than maximum temperature (Boko et al., 2007; Collins, 2011; Cook and Vizy, 2012; Niang et al., 2014). Studies show largest warming for June – August (JJA) season than December – January (DJF) season (Hulme et al., 2001; Collins, 2011). Temperature increases observed in Sahara are larger than for any other region on the continent.

During the 21st century, it is likely that temperature over Africa will rise. The continent is expected to experience higher land warming than the global land average in all seasons. Drier subtropics will warm more than the wetter tropics (Christensen et al., 2007; Niang et al., 2014). Consistent with observed trends, minimum temperatures are projected to increase faster than maximum temperatures (Niang et al., 2014). By mid- and late- 21st century, the increase in temperature over land across Africa is projected to exceed 2˚C and 4˚C under RCP2.6 and RCP8.5 respectively (Niang et al., 2014). Under the medium (A1B) and high (A2) greenhouse

emission scenarios of the Special Report on Emission Scenarios (SRES) (written as SRES A1B and SRES A2) (IPCC, 2000), mean annual temperature increase over the entire Africa is expected to rise by 2˚C by the end of this 21st century relative to the late 20th century (Niang et al., 2014).

Owing to data quality, spatial coverage sparsity and model disagreement, conclusions about trends and changes in precipitation leads to low confidence as compared to temperature (Trenberth et al., 2007; Blamey et al., 2013; Maidment et al., 2014; Niang et al., 2014; Adler et al., 2017). Projected changes in precipitation vary spatially across the continent. This is evident in the projections of precipitation for different regions of Africa as discussed in the subsequent sections.

2.8.3. North Africa

During the 20th century the region has experienced rising surface temperature (National Intelligence Council - NIC, 2009; Collins et al., 2013), with Northern Algeria and Tunisia showing the greatest increase of about 2˚C to 3˚C (NIC, 2009). Projections for the region show notable increase in both annual maximum and minimum temperatures, with minimum temperature increasing faster than maximum temperature under SRES A1B scenario (Collins et al., 2013; Niang et al., 2014).

Droogers et al. (2012) downscaled nine CMIP3 GCMs using the A1B scenario for the Middle East and North Africa (MENA) region for the period up to 2050. For North Africa, in agreement with Terink et al. (2013) the study shows reduced precipitation by 2050. Moderate decrease or no change is projected in winter (October to March) with significant reduction during summer (April to September) (Barkhordarian et al., 2013; Christensen et al., 2013). Drier conditions are projected with rising GHG concentrations with warm and cold seasons experiencing maximum and minimum decreases respectively (Barkhadorian et al., 2013).

Terink et al. (2013) evaluated climate change for 22 MENA countries by downscaling nine GCMs. Two future periods were considered: 2020 – 2030 and 2040 – 2050, with baseline period 2000 to 2009. The study established decrease in projected annual precipitation for most parts of the region. For the Northern African region, largest decreases are projected for Morocco, Tunisia, Central Libya, Southern Egypt, Central and coastal Algeria. However, 15 to

20 percent increase in annual precipitation is projected in some countries such as Djibouti and Yemen.

2.8.4. West Africa

Over West Africa, increase in temperature is projected by both CMIP3 and CMIP5 models. Diffenbaugh and Giorgi (2012) characterised West Africa as a climate change hotspot using CMIP5 models under RCP4.5 and RCP8.5 scenarios. Under SRES A2 and A1B (CMIP3) and RCP 4.5 and RCP 8.5 (CMIP5), temperature increase is projected to rise above the 1986 – 2005 baseline by between 3 to 6°C by the end of the 21st Century (Niang et al., 2014). These temperature projections are consistent with the range of 1.5 to 6.5°C warming found by (Sylla et al., 2016). The warming will vary spatially with Guinean coast projected to be less warm than the Sahel (Blamey et al., 2013). Under RCP 8.5 scenario warming is projected to increase faster into the interior by about 5°C than along the Sahel/Sahara boundary.

There is substantial uncertainty in the projected West African precipitation (Sylla et al. 2016; Riede et al., 2016; Monerie et al., 2017; Obada et al., 2017). This is largely attributed to model disagreement on both direction and magnitude of change (Sylla et al. 2016). The uncertainty is evident through the possible precipitation changes which range from -30 to 30 percent (Sylla et al., 2016) for the entire region and -10 to 10 percent in the Sahel alone (Obada et al., 2017). Studies have established that the range of uncertainty varies directly with RCP forcing and time frame being considered. For instance, precipitation reduction strengthens and extends spatially to East Sahel as time periods shifts from 2036 – 2065 to 2071 – 2100 as well as forcing increases from RCP4.5 to 8.5 (Sylla et al. 2016). Spatially, precipitation is projected to decrease in Senegal, Mali, Northern Guinea and Southern Mauritania. However, some parts of gulf of Guinea, Sierra Leone, Ivory Coast and East Sahel are projected to experience increase in precipitation.

2.8.5. East Africa

Observation datasets show significant increase in temperature but decrease in precipitation over East Africa for the period 1951 – 2010 (Ongoma and Chen, 2017). This is consistent with Daron (2014a) who reports warming signal over East Africa for the period 1963 to 2012. Over

the past 50 years the region has experienced an average increase in temperature of 1.5 to 2˚C and surpassing 3 ˚C during March to August in some areas such as South Sudan.

Anyah and Qiu (2012) assessed temperature and precipitation changes during the 20th and 21st century using a total of 11 CMIP3 model outputs over Greater Horn of Africa (GHA). The study shows that temperature has increased significantly over the GHA since the early 1980s. Based on high (A2) and mid – range (A1B) carbon dioxide emission scenarios, for two time periods; 2046 – 2065 and 2081 – 2100 relative to the 1981 – 2000 period, projections in temperature and precipitation changes were significant. A general increase in both maximum and minimum temperature for all seasons was projected under both scenarios and time periods. According to this study, significant increase in minimum temperature is greater than the increase in maximum temperature.

At seasonal scale, the study established that under A1B scenario, the warming trend in the projected temperature anomaly reaches an average of about 1˚C for all seasons with exception of JJA which attains 1.5˚C by the year 2040. Seasonality in precipitation of GHA is noted in the CMIP3 models under A1B and A2 scenarios. This seasonality is attributed to the migration of Inter-tropical Convergence Zone (ITCZ) as there is remarkable increase in projected precipitation which coincides with ITCZ location. The Southern parts of the GHA are projected to experience slight increase in precipitation during DJF season.

In Ethiopia, Legesse et al. (2013) downscaled projected temperature and precipitation over Wollo zone using the third version of the Hadley Centre Coupled Model (HadCM3) and two SRES emission scenarios; A2 and B2. The SRES B2 is the lower mid-range scenario where the emphasis is on local solutions to economic, social and environmental sustainability with less rapid and more diverse technological change. A statistical downscaling model (SDSM) was applied in this study. Results show increase in temperature and decline in precipitation for the future periods: 2010 – 2039, 2040 – 2069, and 2070 – 2100. Mean annual precipitation is projected to decrease by 14.2 to 43.3 percent by 2080s with respect to the 1980 – 2012 average. However, maximum and minimum temperatures are expected to rise by 6.17˚C and 5.65˚C respectively by 2080s with respect to the 1980 – 2012 average. Daron (2014a) and (Liebmann et al., 2014) have also reported the decrease in rainfall for MAM season during the

period 1963 to 2012 and 1979 to 2012 respectively. In contrast, the short rain seasons (SON) saw slight increase in rainfall especially over Great Lakes Region.

2.8.6. Southern Africa

Various studies have shown that Southern Africa is getting warmer while rainfall trends show mixed signals (New et al., 2006; Collins, 2011; Kruger and Sekele, 2013; Daron, 2014; MacKellar et al., 2014; Niang et al., 2014; Pinto et al., 2015) report temperature increase of about 1˚C to 1.5˚C over the past 50 years with the interior regions experiencing largest changes of up to 2˚C. Furthermore, minimum temperature has been found to be rising faster than maximum temperature over the region. Analysis of rainfall trends over Southern Africa reveals high temporal and spatial variability (Davis, 2011).

Projections of temperature and precipitation over Southern Africa based on both GCMs simulations and downscaled GCM outputs show increase in temperature and decrease in JJA and SON rainfall. Temperature is projected to keep on increasing until 21st century (Davis-Reddy and Vincent, 2017). Some parts of Northern Botswana, Namibia, Western Mozambique, Zimbabwe and Southern Zambia are expected to experience decrease in rainfall while Tanzania and parts of northern Mozambique are expected to be wetter. While annual temperature is projected to increase by 1˚C to 4˚C by 2050, the increase in seasonal temperature is projected to be 0 to 4˚C in summer and no change to 3.54˚C in winter. Under RCP4.5, temperature for DJF season will increase by between 1˚C to 3 ˚C by 2050, with higher emission scenarios having higher increase (Daron, 2014).

2.8.7. Zambia

The country has experienced climatic hazards that include seasonal floods and flush floods, drought, dry spells and extreme temperatures (NAPA, 2007). Since the second half of the 20th century, temperature has been increasing at a rate faster than the global average rate of warming. During the 1950 to 2010 period, the average increase in temperature is approximately 0.6˚C/decade Neubert et al.(2011) whereas the first three decades since 1950 saw an increase of about 0.33˚C/decade (Phiri et al., 2013). From 1960 to 2006 mean annual temperature has risen by 1.3˚C, with an average rate of 0.29 ˚C/decade (McSweeney et al., 2008).

A study for Mt. Makulu by Chisanga et al. (2017a) revealed significant increasing trends for annual maximum and minimum temperatures. Seasonally, DJF and SON were found to have much higher heat spell events with probability of occurrence of 0.78 and 0.98 respectively. Generally, rainfall amounts across Zambia exhibit downward gradient from North to the South of the country (Phiri et al., 2013). Model projections over Zambia indicate an increase of between 1.2 ˚C to 3.4 ˚C in mean annual temperature by 2060 and 1.6 ˚C to 5.5 ˚C by 2090 relative to the 1970 to 1999 average. Hot days and nights are projected to increase while a gradual decrease in number of cold days and nights is expected relative the 1970 to 1999 average. Spatially, Southern and western regions of the country are expected to experience a higher warming trend than the northern and eastern counterparts (McSweeney et al., 2008).

Projections of annual precipitation for Zambia do not indicate large changes (McSweeney et al., 2008). This differs from the projections presented in NAPA (2007), which reported precipitation increase in each of the Agro Ecological Regions (AERs) of the Zambia. In the study of McSweeney et al. (2008), the ensemble of models shows an increase of 15 percent in DJF rainfall and a decrease of 14 percent in SON rainfall by 2090 relative to the baseline period 1970 – 1999. The projected marginal increases of rainfall during DJF and MAM are concentrated in the north-east while the SON decreases are greatest towards the south of the country and little or no change is expected for JJA season. The reductions projected for the SON season are more substantial than any other season. The frequency and intensity of heavy rainfall events are expected to increase during the rainy season.

2.9. Research Gap

Literature reviewed in this study has shown that climate is changing globally and regionally. It is also clear that climate scientists use global climate models to understand how climate would evolve in future. However, the coarse spatial resolution of GCMs renders their outputs inappropriate for direct use in climate change impact and vulnerability assessment at local level. Therefore, the growing demand for higher spatial resolution climate information has necessitated the need for downscaling the coarse GCMs to local scale.

The release of CMIP5 models which formed the basis for the Intergovernmental Panel on Climate Change Fifth Assessment Report (IPCC-AR5) induced more studies globally and regionally. Generally, CMIP5 models have higher resolution than CMIP3 models. Moreover,

they have improved in resolution, parameterization of physical process and model components. However, research seems to indicate that CMIP5 models have not been used to project changes in precipitation and temperature at various meteorological stations located across Zambia. This is evident from earlier studies for Zambia. Yamba et al. (2011) projected changes in precipitation over the Zambezi River Basin using raw outputs of CMIP3 GCMs. Stenek et al. (2011) also used CMIP3 GCMs to downscale precipitation and temperature for Zambia with focus on Kafue River Basin. Recently, Libanda et al. (2016) only assessed predictor variables associated with statistical downscaling or precipitation over Zambia. The study did not downscale the projected change. It appears from literature that despite relative improvements of CMIP5 models compared to CMIP3, there is still limited knowledge regarding projections of precipitation and temperature at local level. Therefore, this study focused on the projection of changes in annual and seasonal climatologies (long-term averages) of precipitation and temperature at meteorological stations across Zambia.

2.10. Chapter Summary

The chapter has presented the two theories on which this study is anchored, namely: Anthropogenic Global Warming (AGW) theory and the principle of uncertainty in Earth's climate. Considerations for selection of large-scale variables and GCMs for downscaling precipitation and temperature have been highlighted as well. The chapter has also brought to light the observed and projected changes in precipitation and temperature at various levels. The gap this research sought to address has been discussed. It has been shown that only scanty literature exists for Zambia on the subject of Statistical downscaling of climate projections from the GCMs outputs. Further, it has been established that despite the increasing demand for high resolution climate information for impact and vulnerability assessment, no study has been undertaken to downscale temperature and precipitation over Zambia as a whole using climate models from CMIP5 archive.

CHAPTER THREE: DESCRIPTION OF THE STUDY AREA

3.1. Overview

This chapter describes the study area and its physical, administrative and demographic characteristics. The study is focused on a total of 19 weather stations of which 11, 13 and 19 stations were utilised for maximum temperature, minimum temperature and precipitation respectively. These weather stations are located across the country. Consequently, the description of the study area is at country level and includes agro-ecological regions.

3.2. Geographical Location of Zambia

Zambia is a landlocked country lying in central Southern Africa extending from longitude 22˚E to 34˚E and latitude 8˚S to 18˚ S with spatial coverage of 752, 615km^2 (Jain, 2007). It lies entirely within the tropics and on the central African high plateau with an average altitude of 1200m above sea level (asl.) (Kanyanga, 2008). It is surrounded by eight neighbouring countries, namely: Angola, Botswana, Democratic Republic of Congo (DRC), Malawi, Mozambique, Namibia, Tanzania and Zimbabwe. Figure 3 (a) shows the location of Zambia and her neighbouring countries.

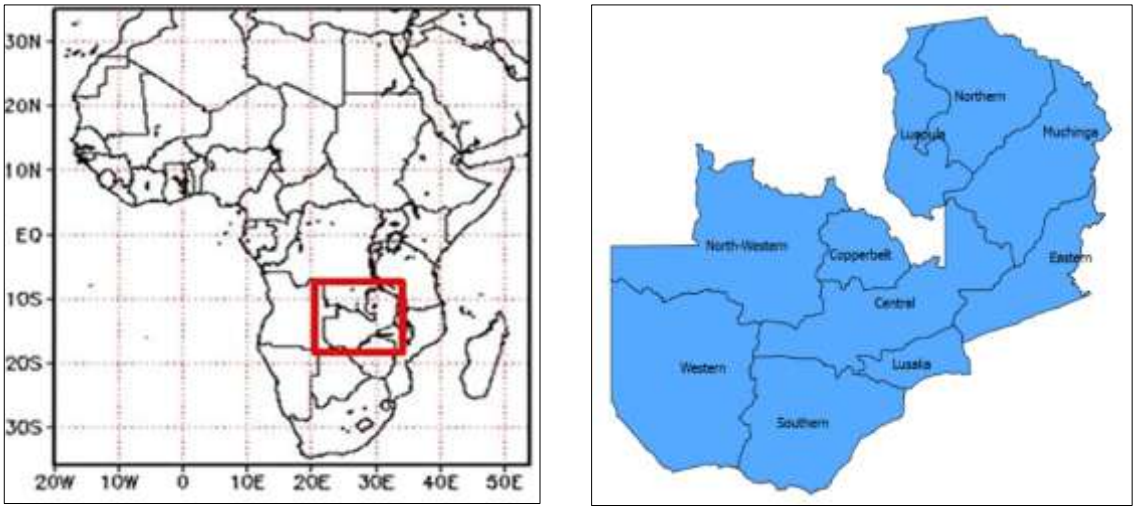

(a) (b)

Figure 3: *Location of Zambia in Africa (red rectangle) (panel a) and provinces of Zambia (panel b).*

Source: Map of Africa from (Libanda et al., 2016) and map of provinces of Zambia from `https://mwana.moh.gov.zm (retrieved on 22/02/2018)`

3.3. Administration and Demographic Characteristics

For administration purposes, Zambia is divided into ten provinces: Central, Copperbelt, Eastern, Luapula, Lusaka, Muchinga, Northern, North-Western, Southern and Western (Figure 3(b)). According to Central Statistics Office (CSO, 2012) Zambia had 150 and 1430 constituencies and wards respectively as of 2010. Since then, new districts have been created. At the time of the study, Zambia had 110 districts.

According to CSO (2012), Zambia's total population of 13,092,666 composed of 49.3 percent and 50.7 percent male and females respectively. Rural population stood at 60.5 percent compared to 39.5 percent of the urban population. Although Zambia is highly urbanised, its population is predominately rural with annual rate of population growth of 2.8 percent during the inter-censal period, 2000 – 2010. The 2010 census saw an increase of 22.6 percent and 51.0 percent in rural and urban populations respectively but is still sparsely populated with a density of 17.4 persons per square kilometre. Of the total population, 45.4 percent were aged below 15 years.

3.4. Climate

Zambia is characterised by a tropical climate with three distinguishable seasons: hot and dry season from mid-August to November, warm and wet season (mid-November to April) and cool and dry season (May to mid-August) (NAPA, 2007; CSO, 2012). Average temperature is 21˚C with coldest and hottest month being July and October respectively. While the range of cold temperature is 3.6 ˚C to 12.0 ˚C with an average of 8.1 ˚C, hot temperature has average of 31.8 ˚C ranging from 27.7 ˚C to 36.5 ˚C (YEC, 1995 quoted in Kasali, 2008). Zambia is characterized by unimodal rainfall during the months of November to March. Rainfall is highly influenced by the migration of the Inter-Tropical Convergence Zone (ITCZ). ITCZ is a tropical rain belt that is formed when the Southeast Trade Winds and Northeast Trade Winds meet near the equator. It oscillates between the Northern and Southern tropics over the course of a year. This phenomenon results into downward gradient of rainfall distribution from the North to the South of the country (Libanda et al., 2016). It may also lead to inter-annual variability in rainfall. The annual rainfall ranges from 700mm to 1400m in the extreme southwest and in the north respectively (Kanyanga, 2008; Kasali, 2008).

Besides ITCZ, El Niño Southern Oscillation (ENSO) has a strong influence on rainfall in Zambia as it brings about inter-annual variations. The northern half of the country experiences drier conditions in the months DJF during La Niña episodes (cold phase) at the same time, the southern part experiences wet conditions. During EL Niño (warm phase) episodes, the opposite pattern occur, with the northern half experiencing wetter conditions than normal and dry conditions in the south (Kanyanga, 2008). Furthermore, northeast trade winds, southeast trade winds, northwest airflow and south airflow are the air masses that largely control the climate of Zambia. Based largely on rainfall pattern and soil type, Zambia is divided into three (I, II and III) distinguishable Agro-Ecological Regions (AERs). Moreover, AER II is further divided into two regions IIa and IIb based mainly on soil types. Figure 4 depicts spatial distribution of the AERs across Zambia and their major attributes displayed in Table 4.

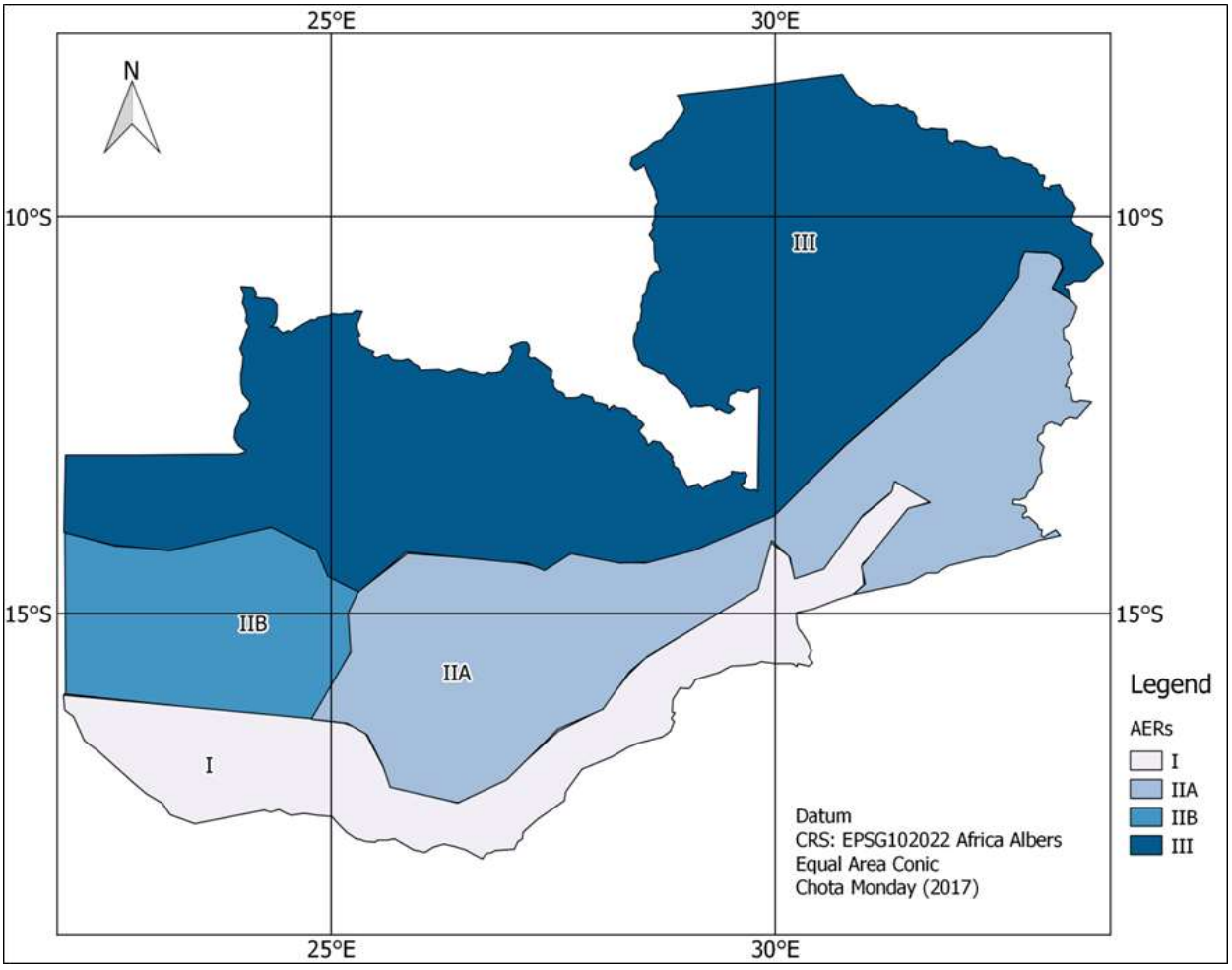

Figure 4: *Agro-Ecological Regions of Zambia (Source: Author)*

Table 4: Distribution and major attributes of AERs

AER	Location	Attributes
I	• Plateau sub-region in Southwest Zambia, Zambezi and South Luangwa valleys	• Semi-arid conditions with annual rainfall less than 800mm • Mean annual temperature of 24.2°C with range 10.3 to 36.5°C. • Altitude: 300 – 900m asl.
II	• Semi-veld plateau of central, Eastern and Southern provinces. • Kalahari sand plateau of western province.	• Semi-arid and typical tropical conditions. • Receives about 800 – 1000mm annual total rainfall. • Mean annual temperature of 21.2°C, with range 6.3 to33.7°C and altitude of 900 – 1300m asl. • 2 subdivisions: IIa and IIb, which differs slightly in terms of amount of rainfall and soil type.
III	• Copperbelt, Northern, North-Western, Luapula and Muchinga (except Chama district –AER II) Provinces	• Part of central African plateau • Typical tropical conditions. • Rainfall above 1000mm annual total rainfall. • Mean annual temperature of 20.7°C, with range 5.7 – 32.1°C. • Altitude: 1100 -2000m asl.

Source: *Adapted from Kanyanga (2008), Kasali (2008) and Jain (2007)*

CHAPTER FOUR: DATA AND METHODOLOGY

4.1. Overview

This chapter describes datasets and methods used in the study. Several stages of the methodology leading to model development and downscaling of GCM projections are presented.

4.2. Datasets

4.2.1. Meteorological Station Data

Station data for the period 1981 – 2010 was acquired from Zambia Meteorological Department (ZMD) which is the main national institution mandated to observe and manage weather and climate data. ZMD manages 39 manual weather stations and 68 automatic weather stations located across the country. Automatic weather stations are very recent (with less than 10 years of daily data). Therefore, this study relied on manual weather stations which have over 50 years of daily data. Due to discontinuities in daily data, only 19 stations were utilised for precipitation, 13 for minimum temperature and 11 for maximum temperature (Figure 5). Independent data quality control was not carried out as ZMD had already done so.

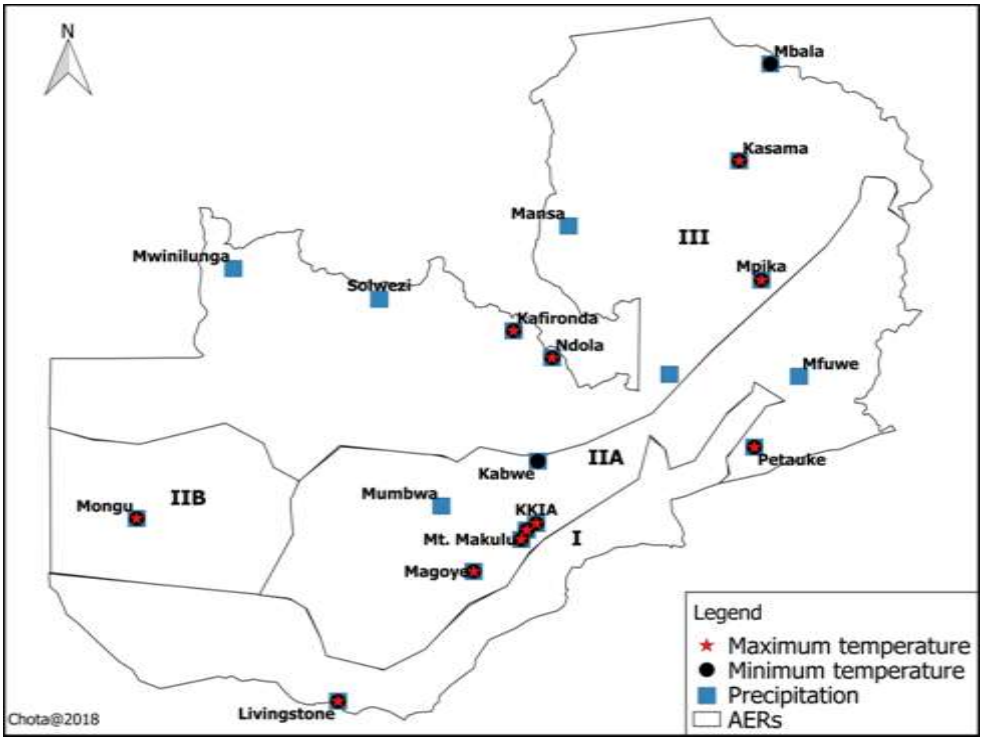

Figure 5: *Location of meteorological stations used in the study*

4.2.2. Gridded Reanalysis Data

ERA-Interim reanalysis dataset (Dee et al., 2011) of the European Centre for Medium Range Weather Forecasts (ECMWF) provided low resolution predictors (large-scale atmospheric variables) necessary for downscaling precipitation and temperature at surface level. This dataset runs from 1979 to date and has spatial horizontal resolution of 0.75° x 0.75°. It consists of daily estimates of both surface and atmospheric variables. Temperature and rainfall are some of the surface variables while wind, air temperature and pressure at various altitudes represent atmospheric variables contained in reanalysis data. This dataset is accessible at `https://www.ecmwf.int/en/forecasts/datasets`. Predictors considered in this study are displayed in Table 5.

Table 5: Predictor variables considered in this study

Name	Code	levels (hPa*)	Units
Geopotential height	Z	1000, 850, 700, 500	m^2s^{-2}
Temperature	T	1000, 850, 700, 500	K
Specific humidity	Q	1000, 850, 700, 500	kgkg^{-1}
U-wind component	U	1000, 850, 700, 500	ms^{-1}
V-wind component	V	1000, 850, 700, 500	ms^{-1}
Mean sea level pressure	SLP	0	Pa
2m Temperature	T2m	0	K

Source: *Statistical Downscaling Portal (`www.meteo.unican.es/downscaling/login.html`).*hPa stands for hectopascals, the SI units for pressure [1 hPa = 1milibar]. Q1000 means specific humidity at 1000hPa height*

4.2.3. Global Climate Model Simulations

Simulations of precipitation and temperature were downscaled from three GCMs of the Fifth Phase Coupled Model Intercomparison Project (CMIP5) under RCP4.5 and RCP8.5. The process of selecting the models is described in detail in Section 4.3.5. Briefly the selection was based on their ability to simulate key climatological features over Southern Africa and Zambia in particular. CMIP5 dataset is available at the website `http://pcmdi9.llnl.gov` maintained by the Earth System Grid Federation which is an international collaboration of several climate modelling centres around the world.

4.3. Methodology

4.3.1. Geographical Domains

Statistical downscaling of GCMs under perfect prognosis approach requires the screening of predictors (large-scale atmospheric variables) (Gutierrez et al., 2013; Ribalaygua et al., 2013). This includes the atmospheric domain surrounding the target region (Zambia in this case). In this study, four geographical domains (Ds) were assessed to determine the atmospheric window over which predictors in the ERA-Interim reanalysis data (also found in GCMs) are most influential on local precipitation and temperature. While Libanda et al. (2016) assessed predictors for downscaling precipitation over a single domain D1, other domains were included in this study for comparison purpose. The assessment of at least one domain is a common practice in climate downscaling (Wilby et al., 2004; Benestad, 2016). This permits the assessment of an atmospheric window over which preferred predictors have influence most. The geographical domains have been defined in such a way that the surrounding areas which have meteorological influence on Zambia are captured. Only one of these four domains was selected on the basis of predictor influence on the local climate. The four Ds and their respective number of grid points in ERA-Interim data are presented in Table 6.

Table 6: Geographical domains considered

Code	Longitude	Latitude	No. of grid points
D1	19 ˚E : 37 ˚E	22 ˚S : 4 ˚S	100
D2	19 ˚E : 37 ˚E	28 ˚S : 2 ˚N	160
D3	13 ˚E : 43 ˚E	22 ˚S : 4 ˚S	225
D4	13 ˚E : 43 ˚E	28 ˚S : 2 ˚N	256

4.3.2. Selection of Predictors

This is a crucial and time consuming step in statistical downscaling of global climate models. Predictor selection in this study was done in two steps. The first step involved carrying out preliminary experiments to assess the influence of each of the predictors (at each level indicated) in Table 5 on local variables: precipitation (PRECIP), minimum temperature (TMIN) and maximum temperature (TMAX). This resulted into 66 experiments (22 for PRECIP, 22 for TMIN and 22 for TMAX). For the purpose of preliminary experiments, reanalysis data was downscaled over a common geographical domain using individual

predictor levels (example, each level of specific humidity: Q1000, Q850, Q700 and Q500). The performance of each of these variables was checked using correlations and KS-*p* values. In the second step, based on the said statistics and expert advice from meteorologists at ZMD, several potential predictor combinations were constituted as displayed in Tables 7 – 9.

Table 7: **Predictor combinations tested for downscaling precipitation**

Code	Combination
V1	T2m, U1000, U850, V850, T850, Q850, Q700
V2	T2m, U1000, U850, V850, T850, Q850
V3	T2m, U850, V850, T850, Q850
V4	T2m, U1000, V850, T850, Q850
V5	Q850, T850, U850, V850
V6	T2m, U850, V850, Q850
V7	U850, T850, Q850
V8	T2m, U850, Q850
V9	Z1000, Z850, U850, V850, T850, Q850
V10	Z1000, U850, V850, T850, Q850
V11	Z850, U850, T850, Q850
V12	T850, Q850, T700, Q700
V13	T850, Q850, T700

Table 8: Predictor combinations tested for downscaling minimum temperature

Code	Combinations
P1	SLP, T1000, T850, Z850, T2m, Q850, Q1000, U700
P2	SLP, T850, U700, Q850, Z850
P3	SLP, T850, U700, Q850
P4	SLP, T1000, U700, Q850
P5	SLP, T850, Q850
P6	SLP, T1000, Q850
P7	SLP, T850, Q1000
P8	SLP, T2m
P9	T2m

Table 9: Predictor combinations tested for downscaling maximum temperature

Code	Combination
T1	SLP, T2m, U1000, T850, U700, Q500
T2	SLP, T2m, T850, U700, Q500
T3	SLP, T850, U700, Q500
T4	SLP, T850, U1000, Q500
T5	SLP, U1000, U700, Q500
T6	SLP, U1000, U700
T7	SLP, T850, Q500
T8	SLP, T850
T9	SLP, T2m
T10	T2m

Note: In each of these combinations, the numbers associated with predictors denote the vertical level (hPa). As an example, T850 refers to air temperature at 850 hPa.

In order to determine the most influential predictor-geographical domain combination, each predictor combination in Tables 7 – 9 was considered over every geographical domain presented in Table 6. This resulted into 52, 36 and 40 predictor-domain combinations for PRECIP, TMIN and TMAX respectively. Each of these combinations represented a possible downscaling model for the respective local climate variables. For each target local variable (PRECIP, TMIN and TMAX), only one predictor-geographical domain combination was finally chosen by analogue method.

In climate science, the term analogue is used to refer to states of the atmosphere that are similar. The method is based on the assumption that similar atmospheric patterns over a region of interest lead to similar meteorological outcomes (Manzanas, 2017). The main limitation of the analogue method is inability to produce a local state that has never been observed in the historical record. In this study, Euclidean distance was used as a measure of similarity between atmospheric patterns following the recommendation by Matulla et al. (2008). For the purpose of predictor selection, the analogue method was implemented as follows.

Observed station dataset for the period 1981 to 2010 was divided into training period (75 percent of data: 1981 – 2002) and testing period (25 percent of data: 2003 – 2010). The

training dataset was used to predict station daily time series for the testing period (2003 – 2010) using the analogue method. For this purpose, a target day *t* was taken from the testing period (2003 – 2010) and the analogous day *u* from the training period (1981 – 2002) based on the minimum Euclidean distance between the predictor combination values for day *t* and *u*, was determined. The surface variable value of the analogous day u is assigned to the target day t as a predicted local-scale value. This procedure is executed for each day in the testing period to produce a predicted daily time series $f_1, f_2, \ldots, f_n$, where *n* denotes the number of days.

Each of the respective predictor combinations in Tables 7 – 9 was used to simulate predicted time series for each of the three local climate variables at each meteorological station. These were then compared with the corresponding daily station observation time series, $o_1, o_2, \ldots, o_n$, from the testing period. The skill for each predictor combination was assessed based on correlation analysis of the observations and corresponding predicted values from reanalysis in the historical period (1981 – 2010). Kolmogorov Smirnov *p* values were also considered for assessing model reliability (dissimilarity). These measures of skill are described in section 4.3.3 below

4.3.3. Performance Measures of Predictor Variables

A number of statistical measures were used to assess performance of each predictor combination listed in Tables 7 – 9 in predicting local variables. Correlation coefficient was used to measure the level of agreement between predicted and observed time series. Pearson's correlation coefficient (rho) was used to check the strength of the predicted values for temperature and Spearman's correlation coefficient (r_s) was used to assess predicted values for precipitation, since it is less sensitive to strong outliers that lie in the tails of both samples. Reliability of predicted values was checked by Kolmogorov Smirnov *p* values (KS-*p* values evaluated the quality of distributional similarity in climatological terms of the predicted and observed time series.

4.3.3.1. Pearson's Correlation Coefficient (rho)

It measures the strength and direction of a linear relationship between the observations (o) and predictions (f). This score ranges from -1 to 1. In this context, a value of 1 describes a perfect positive linear relationship between observations and predictions whereas negative linear relationship is indicated by -1. The closer the value is to 1 or -1, the stronger the linear

correlation. The value of 0 indicates no linear relationship between variables. This measure is sensitive to outliers. For n pairs of observations $o_1, o_2, \ldots, o_n$, and predictions $f_1, f_2, \ldots, f_n$, Pearson correlation coefficient is computed by equation 4.1.

$$\rho_{o,f} = \frac{\sum_{i=1}^{n}(O_i - \bar{O})(f_i - \bar{f})}{\sqrt{\sum_{i=1}^{n}(O_i - \bar{O})^2}\ \sqrt{\sum_{i=1}^{n}(f_i - \bar{f})^2}} \tag{4.1}$$

4.3.3.2. Spearman's Rank Correlation Coefficient (r_s)

This statistic measures the dependence between observations and predicted values using some monotonic function (Gutierrez et al., 2011). Basically, r_s is similar to the *rho* except that the former is computed using the ranks of data unlike the latter which use actual data values. Let $R(O_i)$ denote the rank of i^{th} observation among n observations and $R(f_i)$ denote the rank of i^{th} value among n predicted values. Then the Spearman rank correlation coefficient is calculated by equation 4.2 (Wackerly et al., 2008) which is equivalent to equation 4.1.

$$r_s = \frac{\sum_{i=1}^{n}\left(R(O_i) - \overline{R(O)}\right)\left(R(f_i) - \overline{R(f)}\right)}{\sqrt{\sum_{i=1}^{n}\left(R(O_i) - \overline{R(O)}\right)^2}\ \sqrt{\sum_{i=1}^{n}\left(R(f_i) - \overline{R(f)}\right)^2}} \tag{4.2}$$

A more direct method exists for computing r_s (equation 4.3) and is widely available in literature (Wilks, 2006; Wackerly et al., 2008)

$$r_s = 1 - \frac{6\sum_{i=1}^{n} {d_i}^2}{n(n^2-1)}, \tag{4.3}$$

In equation (4.3), $d_i = R(O_i) - R(f_i)$ is the difference in ranks between the i^{th} pair of data values. Average rank is assigned to tied values prior to computing the d_i's if they occur in the data. The sign of this score shows the direction of association between observations and predicted values. Like rho, it ranges from -1 to 1 and its absolute value tends to 1 as observations and predictions become closer to being perfect monotone functions of each other. A coefficient of 1 or -1 in this case is a consequence of observations and predicted values having a perfect monotone relationship (not necessarily linear relationship). However, compared to the Pearson's correlation, Spearman's correlation coefficient is less sensitive to outliers that may be in the tails of both observations and predictions (Gutierrez et al., 2011). Further, since precipitation may not follow a normal distribution Spearman's correlation is better choice for validating precipitation.

4.3.3.3. Two sample Kolmogorov-Smirnov Test (KS test)

The downscaling model's capability to reproduce the distribution of the target time series was assessed by using a two sample KS test (*p*-value approach). This is a non-parametric test which assesses the null hypothesis that the two samples come from the same distribution. In the context of climate change, this test helps to determine whether the SD method applied is capable of reproducing the observed distribution. Under perfect prognosis approach, it is desirable for the downscaling model to reproduce the observed distribution if it is to be useful for downscaling GCM simulations. The null hypothesis is rejected for *p*-values less than or equal to the significance level of 1 percent. Moreover, a good downscaling model would yield higher *p*-values than others. Larger *p*-values of KS test signify more distribution similarity between observed and downscaled time series than low values. The KS test statistic is calculated using the equation 4.5.

$$D = |F_1(x) - F_2(x)| \tag{4.5}$$

where D is the distance between cumulative density functions of two samples.

4.3.4. Building the Downscaling Model

The downscaling model was built using the analogue method under perfect prognosis approach (Section 2.3). Essentially, predictor combinations (Tables 7 – 9) over each of the four geographical domains (Table 6) served as potential downscaling models. The predictor combination with highest skills over a specific geographical domain was considered as a downscaling model.

4.3.5. Selection of Global Climate Models

The performance of eight CMIP5 Global Climate models (GCMs) over Zambia was assessed based on available literature. Basic information about these eight GCMs is presented in Table 10. Literature was assessed to determine suitability of three GCMs based on their skill to simulate key climatological features such as annual cycles of temperature and precipitation for Zambia.

Table 10: Basic information of GCMs that were assessed in literature

CMIP5 Model ID	Modeling Centre	Resolution Lat. × Lon.	Periods of daily time series available in SDP
CanESM2	Canadian Centre for Climate Modeling and Analysis, Canada.	2.8° × 2.8°	Hist: 1941 – 2000 rcp4.5: 2010 – 2100 rcp8.5: 2010 – 2100
CNRM-CM5	National Centre for Meteorological Research, France	1.4° × 1.4°	Hist: 1941 – 2000 rcp4.5: 2010 – 2100 rcp8.5: 2010 – 2100
GFDL-ESM-2M	NOAA Geophysical Fluid Dynamics Laboratory. USA	2.0° ×2.5	Hist: 1941 – 2000 rcp4.5: 2010 – 2100 rcp8.5: 2010 – 2100
HadGEM2-ES	Met office Hadley Centre, UK	1.25° ×1.875	Hist: 1941 – 2000 rcp4.5: 2010 – 2100 rcp8.5: 2010 – 2100
IPSL-CM5A-MR	Pierre Simon Laplace Institute, France	1.25° ×2.5	Hist: 1941 – 2000 rcp4.5: 2010 – 2100 rcp8.5: 2010 – 2100
MIROC-ESM	Japan Agency for Marine Earth Science and Technology, Atmosphere and Ocean Research Institute, and National Institute for Environmental Studies, Japan.	2.81° ×2.81	Hist: 1941 – 2000 rcp4.5: 2010 – 2100 rcp8.5: 2010 – 2100
MPI-ESM-MR	Max Planck Institute for Meteorology, Germany	1.875° ×1.875	Hist: 1941 – 2000 rcp4.5: 2010 – 2100 rcp8.5: 2010 – 2100
NorESM1-M	Norwegian Climate Centre, Norway	1.89° ×2.5	Hist: 1941 – 2000 rcp4.5: 2010 – 2100 rcp8.5: 2010 – 2100

Source: *www.meteo.unican.es/downscaling/ensembles and Zubler et al. (2016)*

Note: Lat = Latitude, lon = Longitude, rcp = representative concentration pathway and hist = historical.

4.3.6. Downscaling GCMs Scenarios

After selecting the downscaling model using station daily data and ERA-Interim, the analogue method was again used to simulate daily future and baseline values of local variables. For the purpose of downscaling GCM simulations, the model built is applied to GCMs. In this case, the large-scale atmospheric variables from the GCM for a targeted day *t* (within downscaling period, 2020 - 2049) were compared to large scale variables in the reanalysis record (1981 – 2010) using Euclidean distance as a measure of similarity. The surface estimate in the

reanalysis record corresponding to the analogue is the downscaled value for day *t*. At this stage, the analogue method was implemented in the same way as at the predictor selection stage except that the large scale variables for the targeted day t was obtained from the GCMs. Studies that have used the analogue method to downscale precipitation and temperature include Grouillet et al. (2016) and Manzanas (2017).

In this study, daily time series were downscaled from GCM simulations for two time periods: 2020 – 2049 (future period, **F**) and 1971 – 2000 (baseline period, **B**). This was done to compare modelled time series of the past and future simulations. A web based statistical downscaling portal accessed on `https://www.meteo.unican.es/downscaling` was utilised to downscale daily time series for precipitation, minimum temperature and maximum temperature for baseline period (**B**) (1971 – 2000) and future period (**F**) (2020 – 2049) at weather station level from three GCMs constrained by two representative concentration pathways: RCP4.5 and RCP8.5.

4.3.7. Computation of Climate Change Signal and Analysis of Scenarios

Daily time series that were downscaled through the process described in section 4.3.6 were aggregated to seasonal and mean annual values using R Studio version 3.2.2. The climate change signal was computed using delta method. In this method, the change in climate is computed by subtracting mean of the baseline period from the mean of the future period. In the case of precipitation, the difference is expressed in percentage terms. Equations 4.6 and 4.7 were used to compute the climate change signal in temperature and precipitation

$$\Delta_P = \frac{\bar{Y}_F - \bar{Y}_B}{\bar{Y}_B} \times 100\%, \tag{4.6}$$

$$\Delta_T = \bar{Y}_F - \bar{Y}_B \tag{4.7}$$

where Δ_T = change in temperature, Δ_P = change in precipitation,

$$\bar{Y}_i = \text{mean of} \begin{cases} \text{future period, if i} = F \\ \text{baseline period, if i} = B \end{cases}$$

Climate change projections for precipitation and temperature are presented using the ensemble mean of GCMs computed for each RCP. The use of ensemble mean is very common in climate change studies (Mehran et al., 2014; Miao et al., 2014). Studies (Flato et al., 2013; Miao et al., 2014; Pierce et al., 2009; Zubler et al., 2016) show that model ensemble results are better than

those of any single GCM. This is attributed to the presence of information from all participating models and single models tend to be overconfident. It is one way of reducing uncertainty associated with model configuration. Furthermore, the use of more than one scenario allowed a range of plausible future climate change (Cubasch et al., 2013). Uncertainty in the projected mean climate change is expressed quantitatively using model spread (a range of values calculated by various models). IPCC have used model spread as a measure of uncertainty of climate change projections in a number of their reports.

Robustness of the projected changes was ensured by computing ensemble mean of at least two GCMs with the same sign of change. This is one of the methods for determining the robustness of a climate change signal (Collins et al., 2013) and it has been applied in other studies (Osima et al., 2018)

4.4. Chapter Summary

The current chapter has presented methodological aspects of the study with respect to procedures, techniques and tools that were used to assess the objectives and hypothesis framed in Chapter One. Figure 6 summarises the major steps followed in this study to downscale precipitation and temperature.

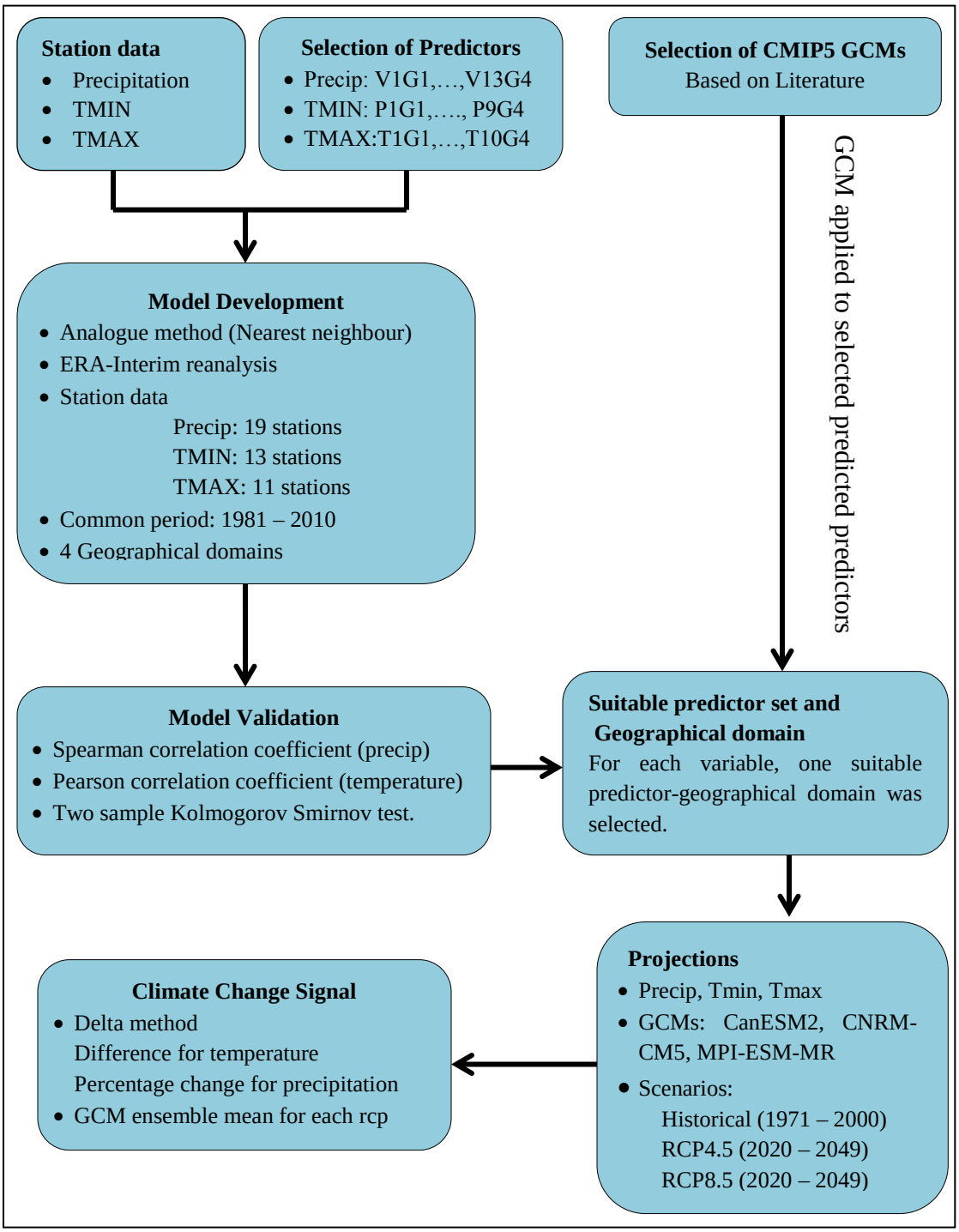

Figure 6: *Graphical representation of downscaling process followed in the study*

CHAPTER FIVE: RESULTS AND DISCUSSION

5.1. Overview

This chapter presents and discusses findings of the study based on the objectives outlined in Section 1.4. The GCMs used in the study are presented in Section 5.2 while predictor combinations selected for downscaling precipitation and temperature are given in Section 5.3, Downscaled precipitation and temperature averaged over the time periods 2020 – 2049 and 1971 – 2000 are presented in Section 5.4. Projected changes in precipitation and temperature for the period 2020 – 2049 relative to 1971 – 2000 are presented in Section 5.5.

5.2. Selection of GCMs from the CMIP5 Archive of Models

Despite relative improvement in terms of spatial resolution and model processes in CMIP5 GCMs (Flato et al., 2013), findings of this study indicate that CMIP5 models have not been extensively utilized in climate change studies over Zambia. Relying on a few studies done for Zambia (Chisanga et al., 2017; Libanda et al., 2016) and largely on Southern Africa (Hewitson et al., 2014; McSweeney et al., 2015; Pinto et al., 2015; Munday and Washington, 2017), three models CanESM2, CNRM-CM5 and MPI-ESM-MR (Table 11) were selected from a pool of 8 CMIP5 models (Table 10). These models have been shown to capture key climatological features such as annual cycles of temperature and precipitation over Southern Africa and Zambia in their simulations of past and present climate. Furthermore, time period available for the study was also taken into account in the selection of models since inclusion of more models would require more computational time.

Table 11: Selected Global Climate Models

Model	Studies in which the model was used
CanESM2	Hewitson et al. (2014); Libanda et al (2016); McSweeney et al.(2015); Munday and Washington (2017);
CNRM-CM5	Dosio et al (2015); Dosio and Panitz (2016); Libanda et al (2016); McSweeney et al. (2015); Munday and Washington (2017);
MPI-ESM-MR	Chisanga et al. (2017b); McSweeney et al. (2015); Munday and Washington (2017).

Libanda et al (2016) showed that CanESM2 and CNRM-CM5 are able to reproduce rainfall distribution over Zambia. This was evidenced by their capability to capture the downward gradient of rainfall distribution from North to South. MPI-ESM-MR was among the four models Chisanga et al. (2017) used in their study aimed at investigating how bias correction methods impact modelled future changes in temperature for Mt. Makulu. McSweeney et al. (2015) also demonstrated that these three GCMs are among models capable of simulating annual cycles of temperature and precipitation for Southern Africa reasonably well.

5.3. Selection of Predictors

The selection of predictors involved the simultaneous choice of large scale variables and geographical domain of great influence on the predictand. This is consistent with Hofer et al. (2015) who argued that the choice of the downscaling geographical domain is an integral part of the process of selecting predictors (large-scale variables). For each predictand, a combination of large scale variables over a domain was selected based on Pearson correlation coefficient for temperature and Spearman correlation for precipitation, and *p*–values of Kolmogorov Smirnov test computed from the observed and predicted daily time series.

5.3.1. Predictors for Precipitation

Predictor combinations listed in Table 7 were considered for precipitation. Validation scores for precipitation are given in Figure 7. A Table of validation scores is also given in Appendix A. Although correlation coefficients are generally low, panel (a) of Figure 7 show relatively higher correlations of predictors with precipitation over domain D1 with predictor combinations V1, V4, V5, V9 and V10 having the highest correlation of 0.47 each. Over D3, the predictor V11 has the same correlation coefficient of 0.47 as those predictors over D1. The geographical domains D1 and D3 have the same spatial average for correlation coefficient of 0.46 whereas D2 and D4 have 0.44. It is worth noting that correlations for precipitation tend to be low under perfect prognosis approach.

The predictors V1, V4, V5, V9 and V10 over D1 and V11 over D3 were shortlisted based on correlation coefficient. The predictor V5 formed by a combination of large scale variables T850, Q850, U850 and V850 was selected for downscaling precipitation over D1 since it outperformed the predictor combinations represented by the codes V1, V4, V9 and V10 over D1 and V11 over D3 in terms of KS *p*–values.

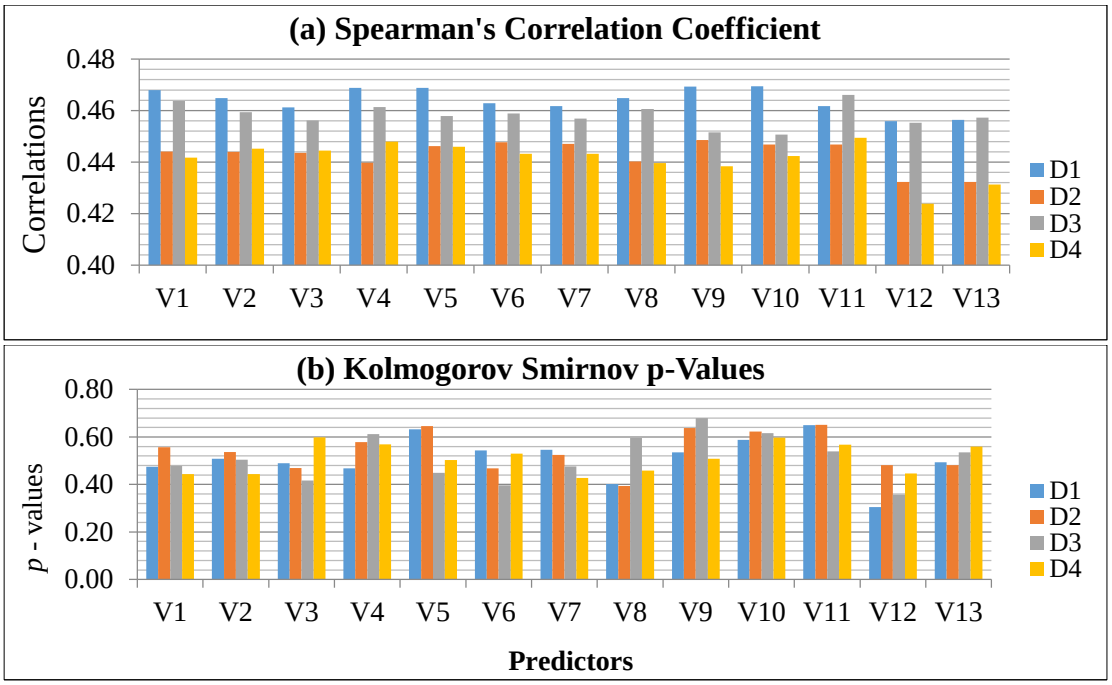

Figure 7: *Validation scores for precipitation (D stands for geographical domain)*

This selection of the domain is consistent with Gutierrez et al. (2013) who argued that for the analogue method, better results are obtained from the smaller domains. However, this is a deviation from the Goodess and Palutikof (1998) who suggested that predictive skill of the model is expected to increase with increasing domain size. Other studies have shown that large sized domains can add unnecessary noise and result into producing spurious results. Furthermore, predictor choice has greater influence on the downscaled results than the size of the domain used (Gutierrez et al., 2013; Haylock et al., 2006).

The chosen predictor combination (V5: Q850, U850, V850 and T850) for downscaling precipitation is slightly different from the combination (Q850, U850, T850) recommended by Libanda et al. (2016). Their combination does not include meridional wind component at 850hPa (V850). The current study has established that inclusion of V850 improves coefficient of correlation and KS-p values. This discrepancy is likely to arise from the small number of predictor combinations that Libanda et al. (2016) tested. The findings of the current study shows that exclusion of circulation variables such as in the combinations V12 (T850, Q850, T700, Q700) and V13 (T850, Q850, T700) yielded lower correlations. This is in accordance with findings of several previous studies (Huth, 2002; Hewitson and Crane, 2006; Brands et

al., 2011; Gutierrez et al., 2013; Benestad, 2016) which contend that inclusion of circulation variables in the downscaling model adds value to projections of local precipitation.

Results also show that inclusion of one or more of the variables T2m, U1000, Q700, Z1000 and Z850 to those making V5 did not improve validation scores for precipitation. Further, the use of T2m in place of T850 as in the case of V6 (T2m, U850, V850, Q805) led to reduction in correlation coefficient and p – value of Kolmogorov Smirnov test. The inclusion of Z1000 to V5 did not alter correlation coefficient but reduced p-value of Kolmogorov Smirnov test for distribution similarity. Under climate change conditions, it is desirable for the downscaling model to reproduce the distribution of the target time series (Gutierrez et al., 2013). As such, preferred p-values of KS-test need to be as large as possible since low KS-p values indicate significant distributional dissimilarities between the observed and downscaled series. Thus, including Z1000 is not favourable since it affects distributional similarity of the observed and predicted time series.

5.3.2. Predictors for Minimum Temperature (Tmin)

Pearson correlation coefficients (rho) for each predictor combination for minimum temperature (Tmin) are generally high over each domain (Figure 8a). With exception of predictor combinations P8 (SLP, T2m) and P9 (T2m), the Pearson correlation coefficient (rho) is largest over the smallest domain D1 for most predictor combinations (P1 – P7). In the case of Kolmogorov Smirnov test (Figure 8b); D1 consistently yielded the highest p values for each predictor combination. Similar to precipitation, the smallest domain, D1 was selected for downscaling minimum temperature since it yielded higher correlations and KS-p values compared to other domains. This confirms the findings of Gutierrez et al (2013). Appendix A gives explicit values of validation scores for minimum temperature.

Comparing the performance of predictors over D1, excluding P8 and P9 based on their low correlation coefficients, results show that predictor combination P1 has the largest correlation coefficient but lowest KS-p value over the domain of choice D1. Although P1 has higher correlation with Tmin (r = 0.79) than any other combination, it was not a preferred predictor choice owing to its low KS-p value (0.54) and being a combination of many large-scale variables. Discarding P1 based on the large number of variables combined is in agreement with

Tareghian and Rasmussen (2013) who warned against using excessive number of predictors as this may lead to multi-collinearity and poor prediction accuracy.

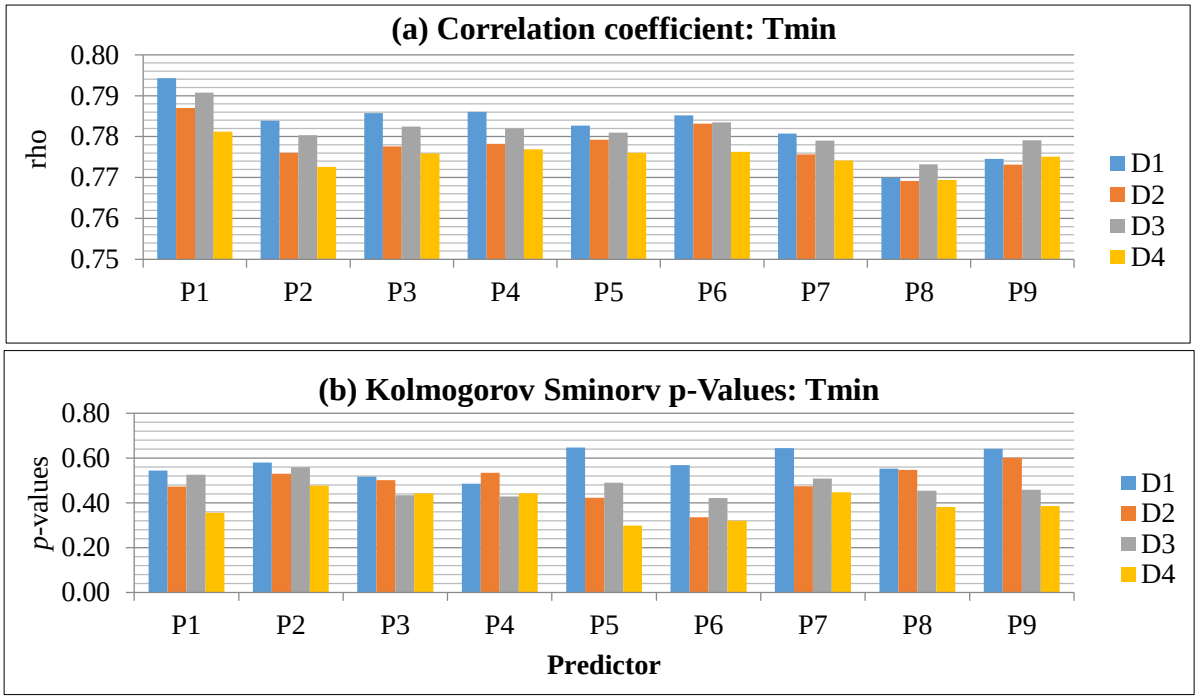

Figure 8: *Validation scores for minimum temperature (TMIN)*

Other predictors with comparable *rho* values over D1 are P2 (0.784), P3 (0.786), P4 (0.786), P5 (0.783), P6 (0.785) and P7 (0.781). Comparing their KS-*p* values over D1, shows that P5 and P7 outperform all others with respective KS-p values of 0.647 and 0.644. Based on correlation coefficient and KS-*p* values, P5 (SLP, T850, Q850) is a predictor set of choice for downscaling minimum temperature. Results also show that exclusion of circulation variables as in predictor sets P5 to P9 leads to larger *p*-values of Kolmogorov Smirnov test. This implies improved distribution similarity between observed and predicted time series for minimum temperature. This is desirable under climate change conditions and consistent with Gutierrez et al. (2013) who established that temperature and/or humidity variables tend to have stronger climate change signal than zonal and meridional wind component in the case of temperature.

5.3.3. Predictors for Maximum Temperature (Tmax)

Figure 9a displays validation scores: *rho* (panel a) and KS-*p* values (panel b) for maximum temperature. Numerical values of validation scores for Tmax are displayed in Appendix A.

Similar to precipitation and minimum temperature, the smallest domain (D1) yields higher correlations for all predictor combinations (Figure 9a). Moreover, with exception of predictor sets T6 (SLP, U1000, U700) and T10 (T2m) whose KS-p values are 0.678 and 0.618 respectively, other predictor sets have low p −values of Kolmogorov Smirnov test. However, T10 composed of T2m only had a better correlation coefficient (rho = 0.757) than T6 which is composed of circulation variables only and had the smallest correlation coefficient (rho = 0.716). Moreover, the removal of temperature variables from the predictor field as it is the case with combinations T5 (SLP, U1000, U700, Q500) and T6 (SLP, U1000, U700) lead to smaller correlation coefficients.

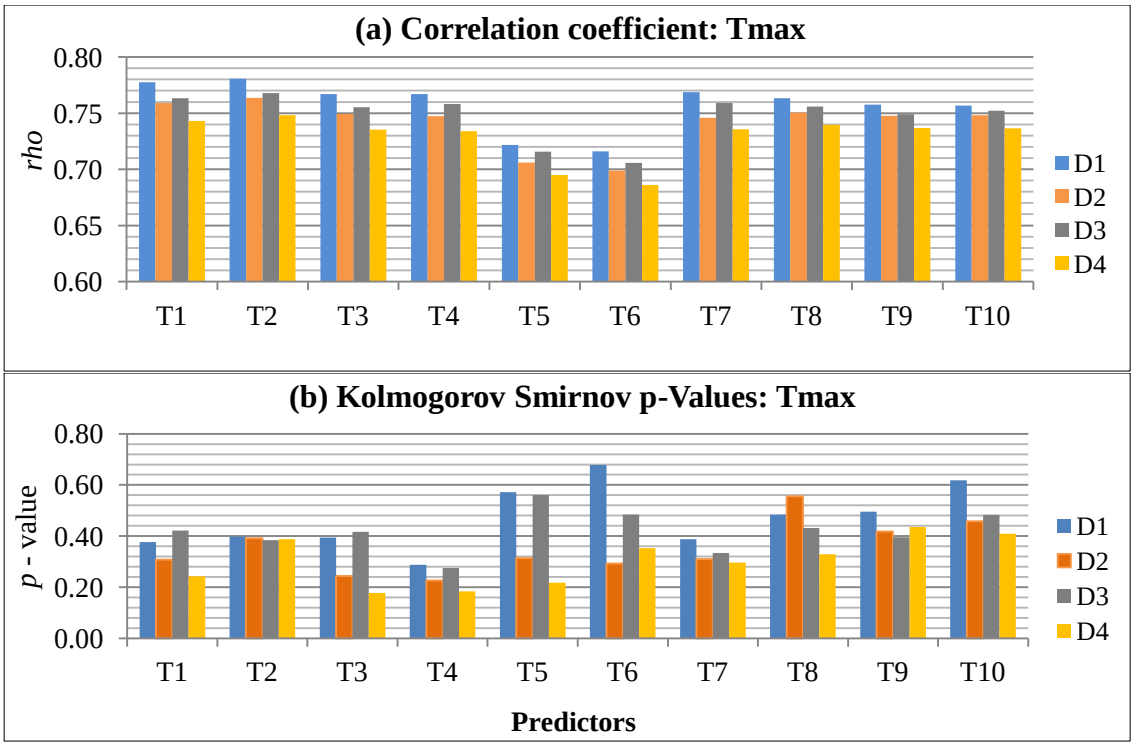

Figure 9: *Validation scores for maximum temperature (TMAX)*

Thus inclusion of temperature variables improves the predictive power of the downscaling model for Tmax. The use of T2m in place of T850 marginally reduces correlation coefficient from 0.763 to 0.758 but increases KS-p value from 0.484 to 0.495. The implication of this is that T2m improves distribution similarity and hence model reliability. This is desirable under climate change conditions. Although the predictor set T7 (SLP, T850, Q500) exhibits high correlations, it has low p values of K-S test. Removing Q500 from T7 slightly reduced the correlation coefficient but increased KS-p value for Tmax. The implication of this is that upper

tropospheric variables improve distributional similarity of observed and predicted time series for Tmax. Therefore, the predictor set T10 (T2m) is preferred for downscaling Tmax since it yielded comparably high correlation and KS-p value over D1. From the foregoing, selected predictors for each predictand are displayed in Table 12. D1 is the geographical domain over which temperature and precipitation were averaged in historical (1971 to 2000) and future periods (2020 to 2049). The choice of the domain D1 is in agreement with Libanda et al. (2016) who used the same domain for assessment of predictors for downscaling precipitation over Zambia. Further, it is confirms the assertion Gutiérrez et al.(2004; 2013), made that better results for downscaled precipitation using analogue method are obtained from the smaller domains.

Table 12: Selected Predictors and their Validation Scores

Code	Predictor combination	Predictand	Rho	KS p – value
V5	T850, Q850, V850, U850	Precip	0.47	0.63
P5	SLP, T850, Q850	Tmin	0.783	0.647
T10	T2m	Tmax	0.757	0.618

5.4 Downscaled Precipitation and Temperature

Results for downscaled precipitation, minimum temperature and maximum temperature at meteorological stations for both historical (1971 – 2000) and future (2020 – 2049) time periods under two concentration pathways (RCP4.5 and RCP8.5) are presented in this section. The presentation and discussion of results is based on an ensemble of GCMs; CanESM2, CNRM-CM5 and MPI-ESM-MR. This approach has been shown to yield better results than those from any single GCM (Flato et al., 2013; Miao et al., 2014; Pierce et al., 2009; Zubler et al., 2016). For precipitation, however, the ensemble mean is computed based on at least two GCMs which have the same sign of the climate change signal. This enables quantification of robustness in projected change in precipitation since it is highly characterised by uncertainty.

5.4.1. Precipitation

Downscaled Mean annual precipitation of the ensemble mean for the historical period 1971 – 2000 and future period 2020 – 2049 under RCP4.5 and RCP8.5 emission scenarios are presented in Figure 10 for meteorological stations given in Figure 5. Numerical values are presented in Appendix B. Results show that stations in the northern part of the country receive

more rainfall compared to those in the Southern part. This is consistent with earlier studies (Libanda et al., 2016; Phiri et al., 2013; Thurlow et al., 2009; NAPA, 2007). With exception of Mansa, Mpika and Serenje, other stations in AER III are projected to have Mean Annual Precipitation (MAP) above 1000mm which agrees with (Kanyanga, 2008; Kasali, 2008; Jain, 2007). For the period 2020 – 2049, stations in the AER III are projected to experience MAP ranging from 916 to 1206mm and 887 to 1203mm under RCP4.5 and RCP8.5 respectively. The smallest and highest MAP for stations in AER III is projected to occur over Serenje and Mwinilunga respectively under both RCPs (Figure 10).

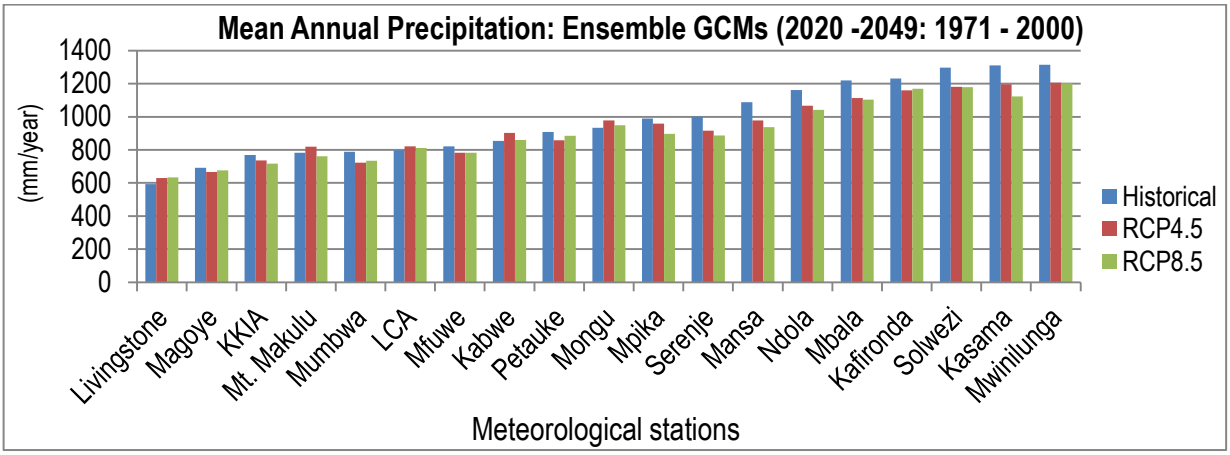

Figure 10: *Downscaled projections of MAP for the baseline period (1971 - 2000) and future (2020 - 2049) time periods using an ensemble of at least two GCMs. LCA means Lusaka City Airport and KKIA mean Kenneth Kaunda International Airport*

Meteorological stations in AER II are projected to experience MAP ranging from 667 to 977mm and 676 to 938 under RCP4.5 and RCP8.5 respectively. The smallest and highest MAP for stations in AER II is projected to occur over Magoye and Mongu respectively under both RCPs (Figure 10).

Projected seasonal precipitation is downscaled for three seasons, namely; December – February (DJF), March – May (MAM) and September – November (SON) using an ensemble of GCMs and two RCPs (RCP4.5 and RCP8.5). Due to lack of rainfall activities during June – August (JJA) season, JJA season was not considered for analysis. Downscaled seasonal precipitation is consistently largest during December – February (DJF) season, ranging from 393 – 810mm (historical), 410 – 729mm (RCP4.5) and 434 – 740 mm (RCP8.5). Livingstone meteorological station consistently exhibit lowest DJF precipitation under both RCPs. Under RCP4.5, the largest DJF precipitation is projected to occur over Kasama whereas Kafironda is

expected to experience the largest DJF precipitation under RCP8.5 scenario (Figure 11). See Appendix C for more information on downscaled projections of seasonal precipitation.

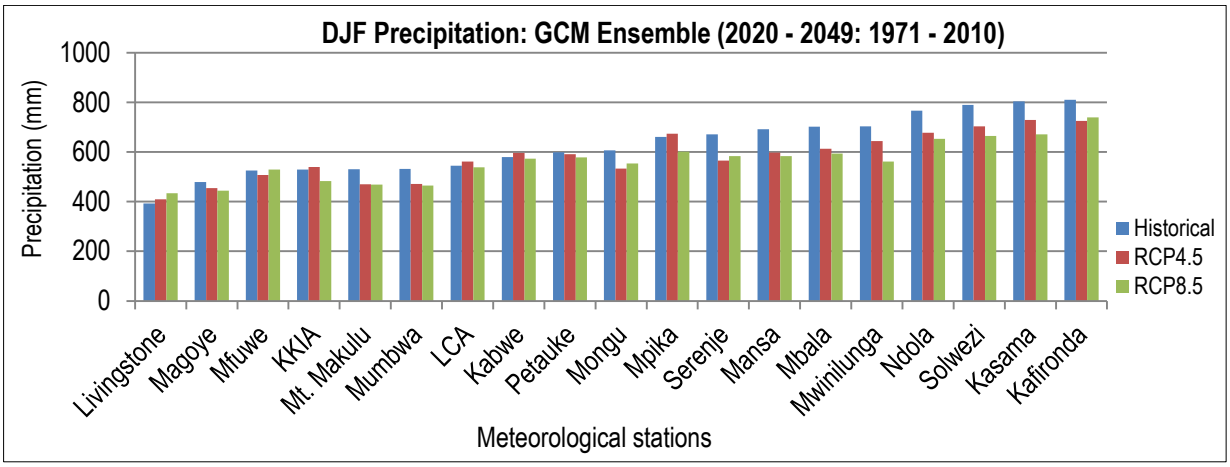

Figure 11: *Downscaled projections of DJF precipitations for the baseline (1971 - 2000) and future (2020 - 2049) time periods using an ensemble of GCMs. LCA means Lusaka City Airport and KKIA isKenneth Kaunda International Airport.*

The downscaled projections of March – May (MAM) precipitation range from 101 – 364mm (historical), 105 – 314mm (RCP4.5) and 85 – 339mm (RCP8.5). Livingstone has the lowest MAM precipitation for historical and under RCP8.5 scenarios. Under RCP4.5 scenario, the lowest downscaled MAM precipitation occurs over Mumbwa weather station. The largest MAM precipitation is consistently projected for Mbala weather station for both RCP4.5 and RCP8.5 scenarios as well as for historical period (Figure 12 and Appendix C).

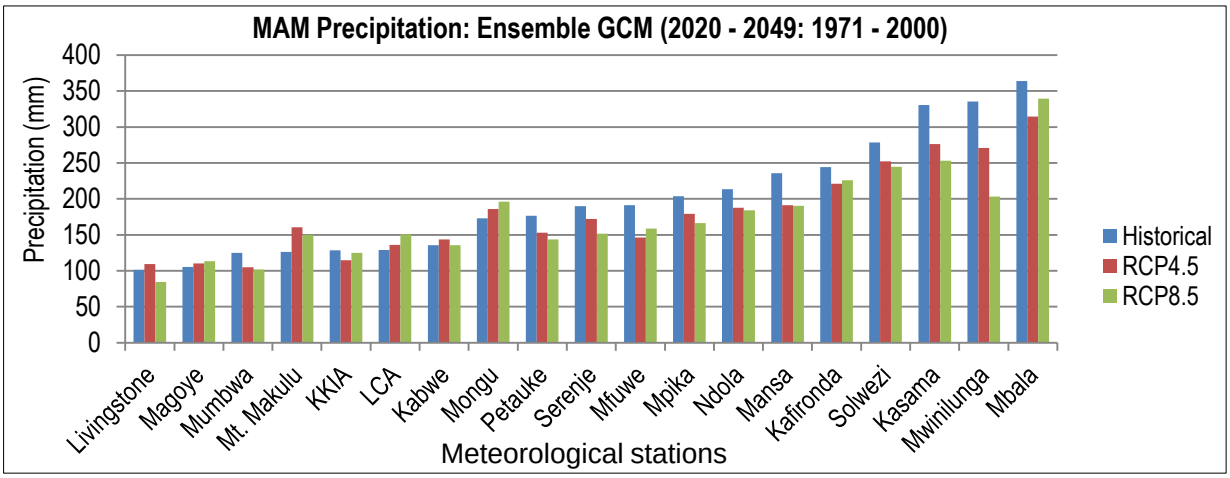

Figure 12: *Downscaled projections of MAM precipitation for the baseline (1971 - 2000) and future (2020 - 2049) time periods using an ensemble of GCMs. LCA means Lusaka City Airport and KKIA mean Kenneth Kaunda International Airport.*

Figure 13 shows downscaled September – November (SON) precipitation for the time periods 1971 – 2000 and 2020 – 2049. The SON precipitation is projected to be largest over Mwinilunga weather station for both time periods and scenarios under consideration. It is projected to range from 97 – 274mm (historical), 94 – 301mm (RCP4.5) and 87 – 254 mm (RCP8.5) across all weather stations used in the study. Kenneth Kaunda International Airport (KKIA) and Mpika weather stations are projected to experience the lowest SON precipitation (Figure 13 and Appendix C).

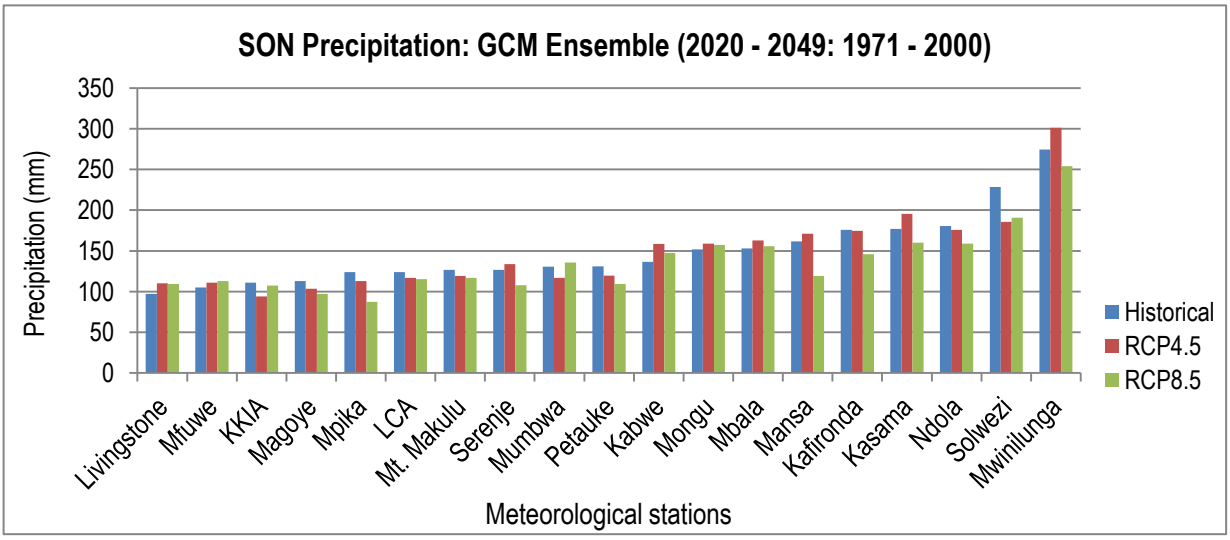

Figure 13: *Downscaled projections of SON precipitation for the baseline (1971 - 2000) and future (2020 - 2049) time periods using an ensemble of GCMs. LCA means Lusaka City Airport and KKIA mean Kenneth Kaunda International Airport*

The downscaled projections of precipitation (Figures 10 – 13) show larger mean annual and seasonal precipitation for meteorological stations in the northern part of the country. Marginal decrease in downscaled projected precipitation is also clear for most stations.

5.4.2. Temperature

The downscaled projected temperature show increasing trends for both minimum temperature and maximum temperature under both RCPs at every station considered. Minimum temperature is projected to increase to 12.0 – 17.8°C (RCP4.5) and 12.2 – 17.9°C (RCP8.5) from the baseline range of 11.4 – 16.9°C. For both time periods and RCPs, the largest minimum temperature and smallest minimum temperature is projected to occur over Petauke and Kafironda respectively (Figure 14a). See Appendix D for more information.

Similar to minimum temperature, the downscaled maximum temperature is projected to increase for all stations under both RCPs. Maximum temperature is projected to increase to 27.9 – 32.3°C (RCP4.5) and 28.2 – 32.4°C (RCP8.5) from the baseline range of 26.4 – 30.6°C. Mpika and Livingstone weather stations are projected to experience the smallest maximum temperature and largest maximum temperature respectively (Figure 14b). For numerical values of maximum temperature, refer to Appendix F.

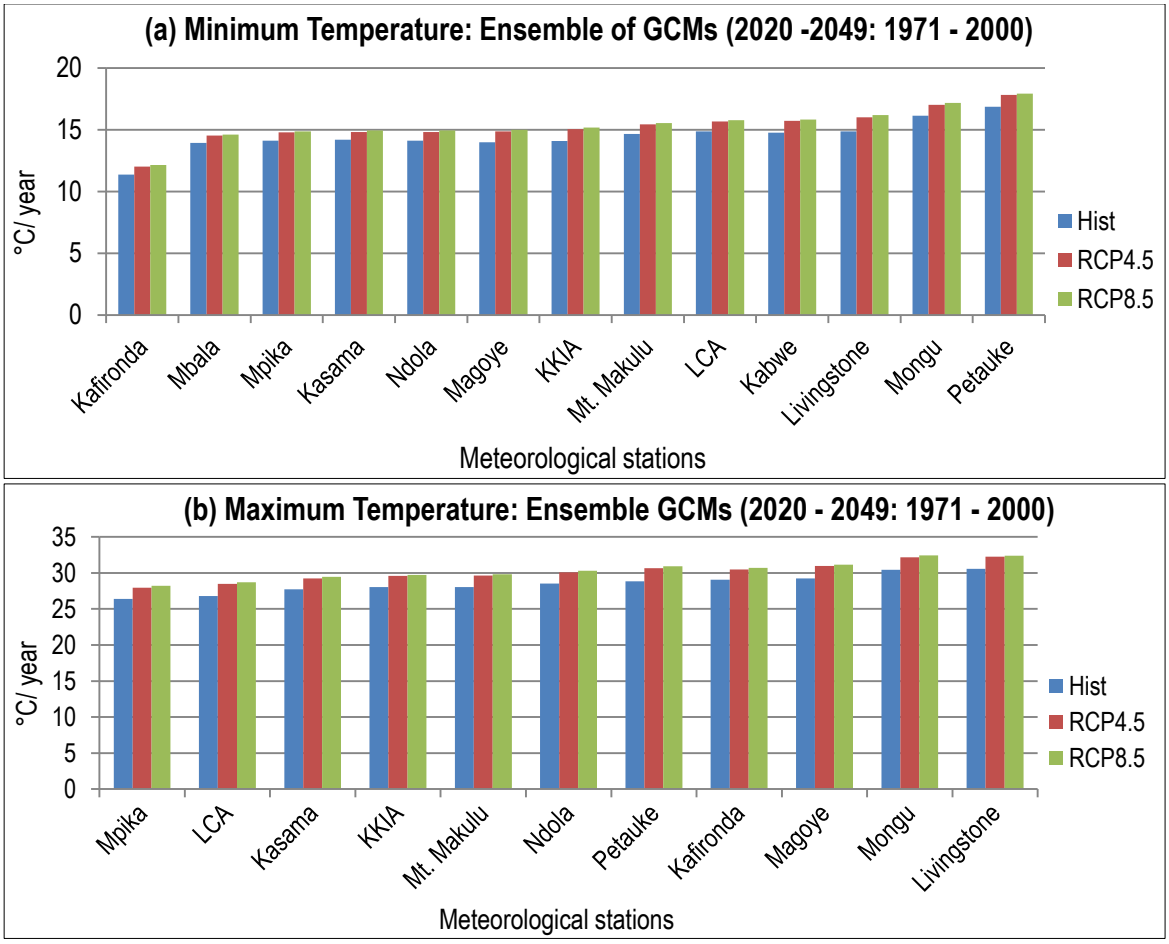

Figure 14: *Downscaled projected mean annual minimum temperature (panel a) and maximum temperature (panel b) for the baseline (1971 – 2000) and future (2020 – 2049) time periods using an ensemble of GCMs. LCA means Lusaka City Airport and KKIA mean Kenneth Kaunda International Airport.*

Downscaled seasonal mean temperatures also indicate an increase in minimum and maximum temperature (Figures 15 – 16). The DJF minimum temperature is projected to be in the range of 15.1 – 19.1°C (Historical), 15.6 – 19.7°C (RCP4.5) and 15.6 – 19.8°C (RCP8.5). The lowest minimum temperature for DJF season is expected to occur over Mbala station for both

scenarios. Mongu and Livingstone stations will experience the largest minimum temperature under RCP4.5 scenario. However, only Mongu station is projected to have the largest minimum temperature under RCP8.5 (Figure 15).

For the MAM, JJA and SON seasons, Kafironda weather station exhibits the smallest minimum temperature for baseline and future time periods under the two concentration pathways (Figure 15). The largest minimum temperature during these three seasons will occur over Petauke under both RCPs. The downscaled projected MAM minimum temperature will increase to 12.9 – 17.7°C under RCP 4.5 and 13.0 – 17.8°C under RCP 8.5 from the baseline minimum temperature ranging between 12.2 and 16.6°C. For JJA season, the projected minimum temperature lies between 4.2 and 13.1°C (historical), 5.4 and 14.4°C (RCP4.5) and 5.6 to 14.6°C (RCP8.5). During the SON season, minimum temperature ranges between 12.5 and 18.9°C (historical), 12.9 and 19.8°C (RCP4.5), and 13.1 to 19.8°C (RCP8.5) (Figure 15).

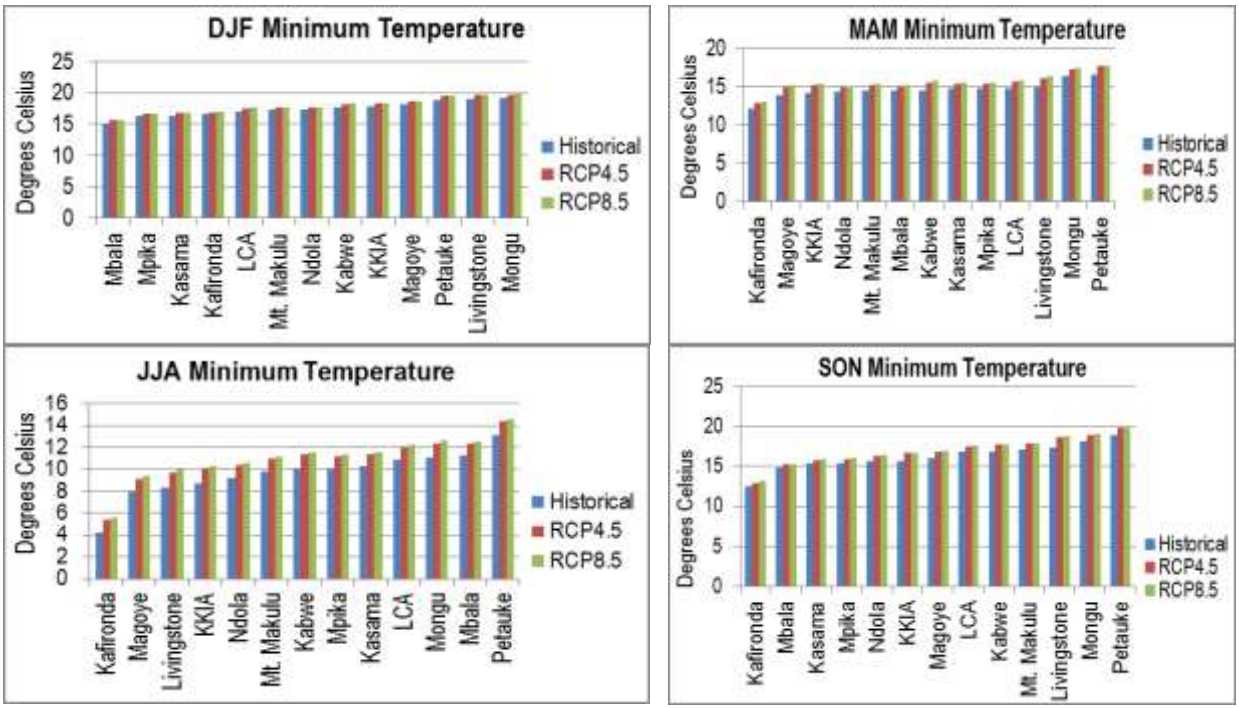

Figure 15: *Downscaled projections of seasonal minimum temperature for the baseline (1971 – 2000) and future (2020 – 2049) time periods using ensemble of GCMs. LCA means Lusaka City Airport and KKIA means Kenneth Kaunda International Airport]*.

The downscaled seasonal maximum temperatures also exhibit increases over every station considered in this study. The lowest maximum temperature is consistently projected to occur over Mpika weather station for all seasons and RCPs. Livingstone is projected to experience the highest maximum temperature during the seasons DJF and MAM under both RCPs with Mongu posed to experience largest maximum temperature during JJA and SON seasons (Figure 16). The DJF maximum temperature is projected to be in the range of, 28.4 – 32.9°C (RCP4.5) and between 28.8 – 33.0°C (RCP8.5). The ranges of maximum temperature for MAM season are 27.2 – 31.5°C (RCP4.5) and 27.5 – 31.7 °C (RCP8.5). The JJA season is projected to experience maximum temperature ranging from 25.2 to 30.3°C under RCP4.5 and 25.4 to 30.7°C under RCP8.5. The SON maximum temperature is projected to range between 31.1 and 35.5 under RCP4.5 and 31.1 to 35.7°C under 8.5 scenarios (Figure 16).

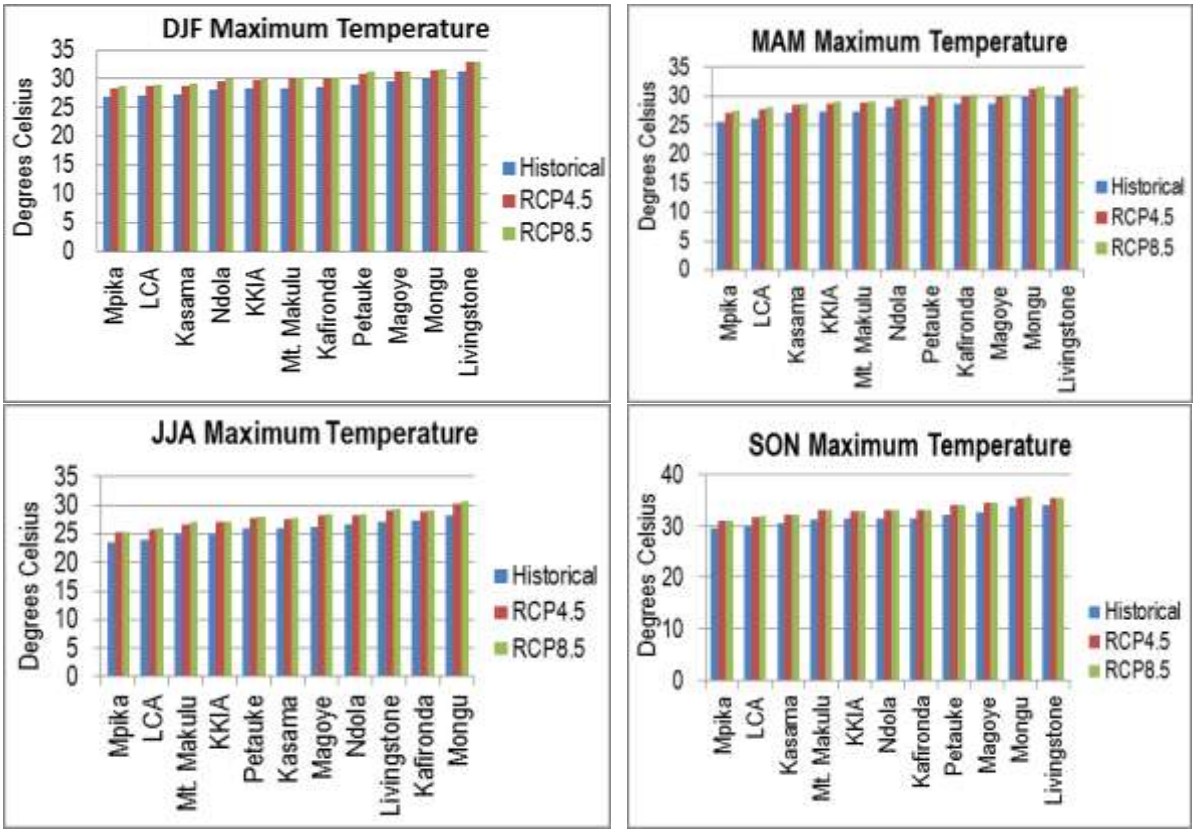

Figure 16: *Downscaled projections of seasonal maximum temperature for the baseline (1971 – 2000) and future (2020 – 2049) time periods using ensemble of GCMs. [LCA means Lusaka City Airport and KKIA means Kenneth Kaunda International Airport.]*

5.5. Projected Changes in Precipitation and Temperature

5.5.1 Projected Changes in Annual Precipitation

Figure 17 shows percentage change in mean annual precipitation (MAP) as projected by an ensemble of GCMs using RCP4.5 emission scenario. The figure shows decrease in MAP for all meteorological stations in AER III, ranging from −10.2 percent (Mansa) to −3.1 percent (Mpika). For AER II, MAP will decrease over stations in the eastern part of the region and increase in western part. A mixed change signal in precipitation ranging between −8.4 percent (Mumbwa) and 5.6 percent (Kabwe) is projected for stations in the central part of region II. Livingstone meteorological station in AER I is projected to experience increase in MAP. The projected change in mean annual precipitation under RCP4.5 across stations ranges from −10.2 percent (Mansa) to 6.4 percent (Livingstone).

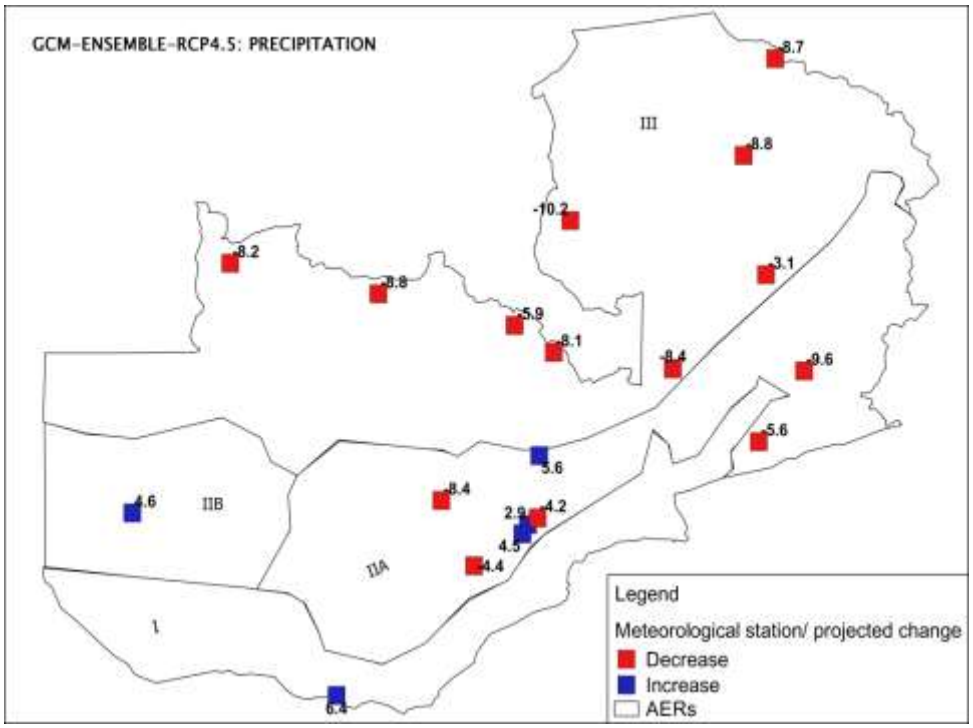

Figure 17: *Projected changes in downscaled MAP for an ensemble of GCMs under RCP4.5 scenario for the period 2020 - 2049 relative to 1971 - 2000.*

In Figure 18, the ensemble average of GCMs under RCP 8.5 projects change in MAP over meteorological stations ranging from −14.4 percent (Kasama) to 7.0 percent (Livingstone). Similar to projections under RCP4.5, precipitation is projected to decrease for all meteorological stations in AER III, ranging from −14.4 percent (Kasama) to −5.1 percent

(Kafironda). For AER II, precipitation will decrease over stations in the eastern part of the region and increase in western part. A mixed change signal in precipitation ranging between −6.8 percent (Mumbwa and KKIA) and 1.7 percent (LCA) is projected for stations in the central part of region II. Livingstone meteorological station in AER I is projected to experience an increase of 7 percent in MAP. The results show larger changes for stations in AER III than those in AERs I and II.

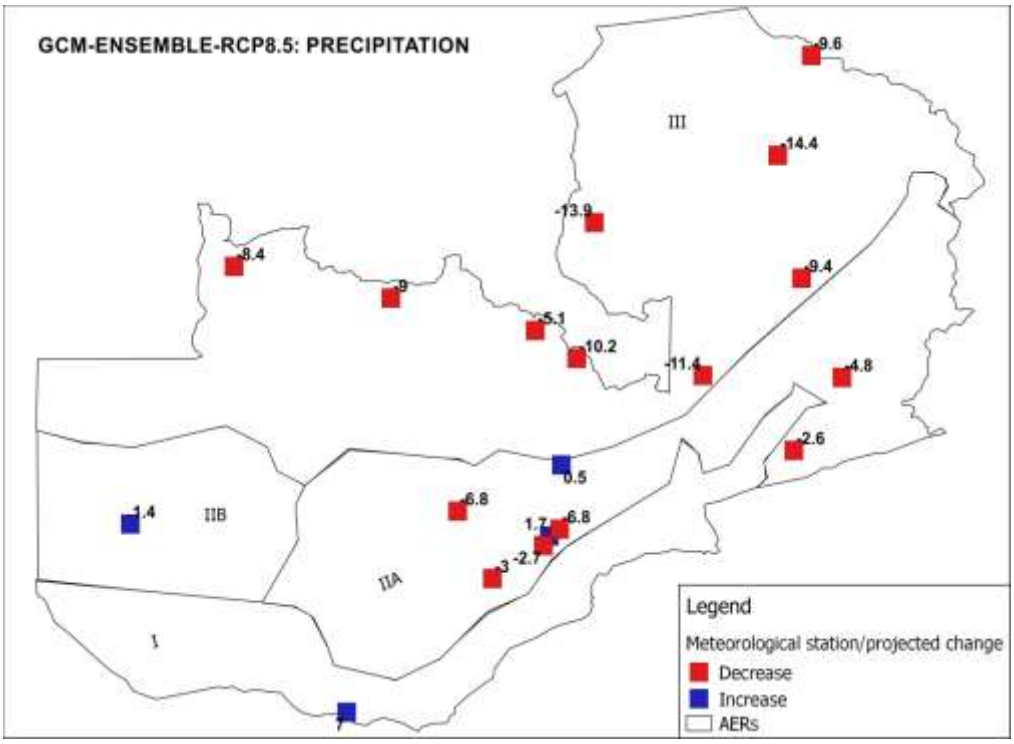

Figure 18: *Projected changes in downscaled MAP for an ensemble of GCMs under RCP8.5 scenario for the period 2020 – 2049 relative to 1971 – 2000.*

Projections show model agreement on decrease of precipitation for stations in the northern region of Zambia. These projections are consistent with the findings for Mpelele (2018) who established decrease in future precipitation for the northern region of the country using dynamical downscaling. However, a mixed signal is projected in precipitation change for the Southern region. The general decreasing pattern in precipitation can be attributed to decrease in DJF rainfall (McSweeney et al., 2008), late start and early cessation of rainy season (NAPA, 2007). This study has projected decrease in mean annual precipitation for all meteorological stations located in AER III with isolated exceptions in AERs I and II where marginal increases have been projected. This result is inconsistent with NAPA (2007) which reported increase in precipitation in the northern part of the country and for each AER of Zambia. This discrepancy

can be attributed to the use of a single climate model, the Hadley Centre Coupled Model version 3 (HADCM3) in the earlier study. The use of one model does not account for uncertainty attributed to model structure. The use of ensemble of models, however, reduces uncertainty in projections that are associated with individual model structure (Flato et al., 2013; Pierce et al., 2009).

5.5.2 Projected Changes in Seasonal Precipitation

Changes in projected seasonal precipitation are reported for DJF, MAM and SON seasons. The season JJA has not been included in the analysis of seasonal precipitation based on lack of rainfall activities during the season. The results indicate that seasonal precipitation varies according to stations and representative concentration pathways. Figure 19 indicates increase in DJF precipitation for Livingstone station under both RCPs during the period 2020 – 2049 relative to 1971 – 2000. Under RCP4.5, increase in DJF precipitation is projected for Kabwe, Livingstone, LCA, KKIA and Mpika with the rest of the stations likely to experience decrease in precipitation. Under RCP8.5, Kafironda, Livingstone, Mfuwe, Mongu and Serenje are projected to experience an increase in DJF precipitation. The rest of the stations are projected to experience a decrease in DJF precipitation (Figure 19). Numerical values for projections of seasonal precipitation for each station are given in Appendix C. The ensemble of models projected changes in DJF precipitation ranging from -15.7 to 4.3 percent and -12.7 to 6.1 percent under RCP4.5 (Appendix H) and RCP8.5 (Appendix I) respectively. These projections are in line with McSweeney et al., 2008). Reduction in DJF precipitation may result into serious crop failure for this is the main season for crop development and growth.

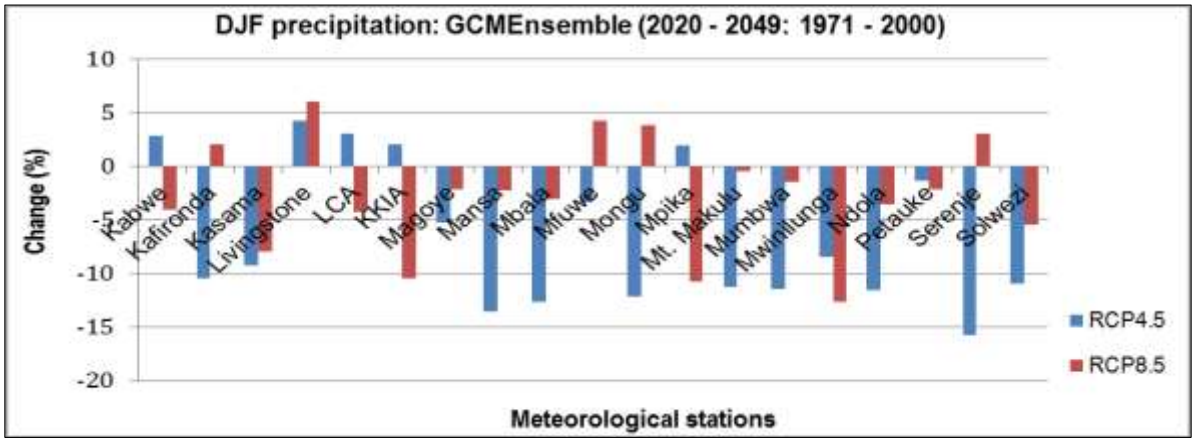

Figure 19: *Projected changes in downscaled DJF precipitation for the period 2020 – 2049 relative to the baseline 1971 – 2000 under RCP4.5 and RCP8.5 scenarios.*

The MAM precipitation for Lusaka city, Magoye, Mongu and Mt. Makulu is projected to increase under both concentration pathways. Livingstone and Kabwe are projected to experience an increase in MAM precipitation under RCP4.5 and a decrease under RCP8.5 scenario. As for the remaining stations, a decrease in MAM precipitation is projected under both RCPs. The largest increase is expected to occur over Mt. Makulu under both scenarios. However, the largest decrease is projected for Mfuwe and Mwinilunga under RCP4.5 and RCP8.5 respectively (Figure 20). The range of projected changes for MAM precipitation is from -23.4 to 27.3 percent and -39.3 to 18.6 percent for RCP4.5 and RCP8.5 respectively (Appendices H and I).

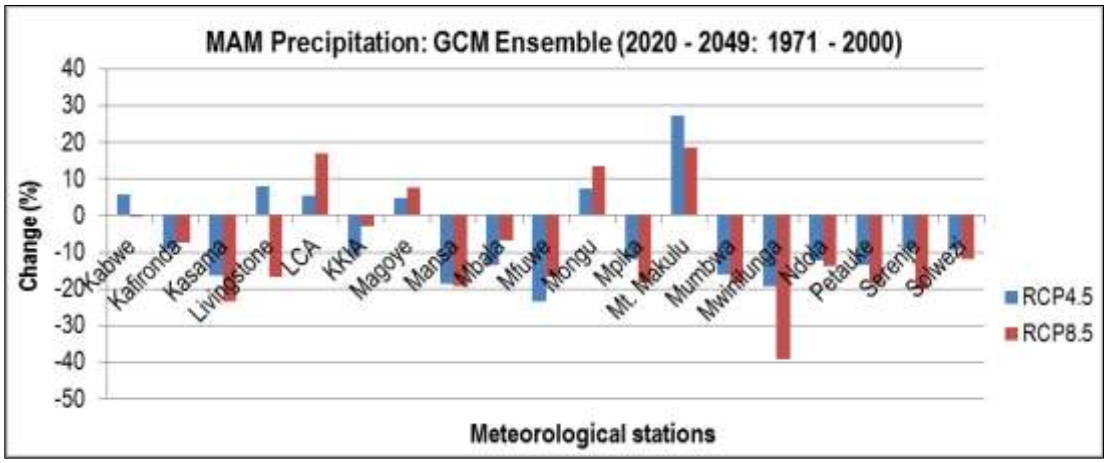

Figure 20: *Projected changes in downscaled MAM precipitation for the period 2020 - 2049 relative to the baseline 1971 - 2000 under RCP4.5 and RCP8.5 scenarios. [LCA - Lusaka City Airport, KKIA - Kenneth Kaunda International Airport]*.

During SON season, the ensemble of models project increase in precipitation under both emission scenarios over Kabwe, Livingstone, Mbala, Mfuwe and Mongu stations. Opposite change signs are projected for Kasama, Mansa, Mumbwa, Mwinilunga and Serenje meteorological stations under the two RCPs (Figure 21). The range of projected changes for SON precipitation is from -18.8 to 16.3 percent and -29.3 to 12.6 percent for RCP4.5 and RCP8.5 respectively (Appendices H and I).

Seasonal projections by the ensemble of models largely indicate drying conditions for SON, DJF and MAM seasons across weather stations in Zambia (Figures 19 – 21). Relatively smaller changes are projected for DJF precipitation while the MAM season exhibits larger changes relative to the baseline means. Results of this study deviate from that of previous study

(McSweeney et al., 2008) which projected increase in DJF rainfall. However, it conforms to the decreasing SON seasonal precipitation projected for Zambia (McSweeney et al., 2008). The decrease in projected precipitation could be in terms of amounts, onset and cessation of the raining season. The decrease in DJF precipitation has profound implications on Zambia's agriculture sector which is largely rain-fed (Jain, 2007) and on water resources management.

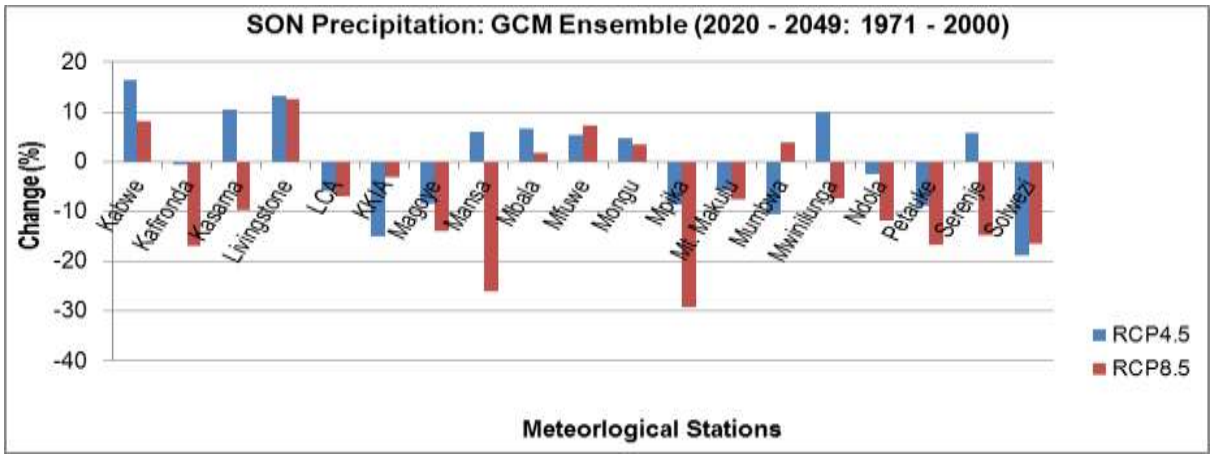

Figure 21: *Projected changes in downscaled SON precipitation for the period 2020 - 2049 relative to the baseline 1971 - 2000 under RCP4.5 and RCP8.5 scenarios. [LCA: Lusaka city airport, KKIA: Kenneth Kaunda International.]*

The general picture is that precipitation is projected to decrease in the northern and eastern parts of Zambia, increase in the western and Southern parts and mixed signals in the central region. The projected decrease in mean annual precipitation has implication on availability and management of water resources, agriculture, health, and hydroelectric power generation.

The projected decrease in precipitation has far reaching hydrological and agricultural implications especially that Zambia already experiences precipitation deficit which is attributed to relatively high temperatures and hence excess potential evapo-transpiration (NAPA, 2007).

5.5.3 Projected Changes in Minimum Temperature

Projected changes in minimum temperature using the ensemble of models under RCP4.5 and RCP8.5 emission scenarios are displayed in Figure 22 and Figure 23 respectively. The ensemble average of three GCMs projects increase in minimum temperature over every station under both emission scenarios. Livingstone will likely experience the largest increase of 1.15°C and 1.32°C under RCP4.5 (Figure 22) and RCP8.5 (Figure 23) respectively. The least

increase of 0.59°C and 0.69°C is projected over Mbala under the two scenarios. Consistent with individual models, the ensemble of GCMs under both scenarios project increases that tend to get larger towards the Southern part of the country. Regardless of the emission scenario considered, minimum temperature is projected to increase by 0.59 – 1.32°C across meteorological stations. See Appendix D for more information.

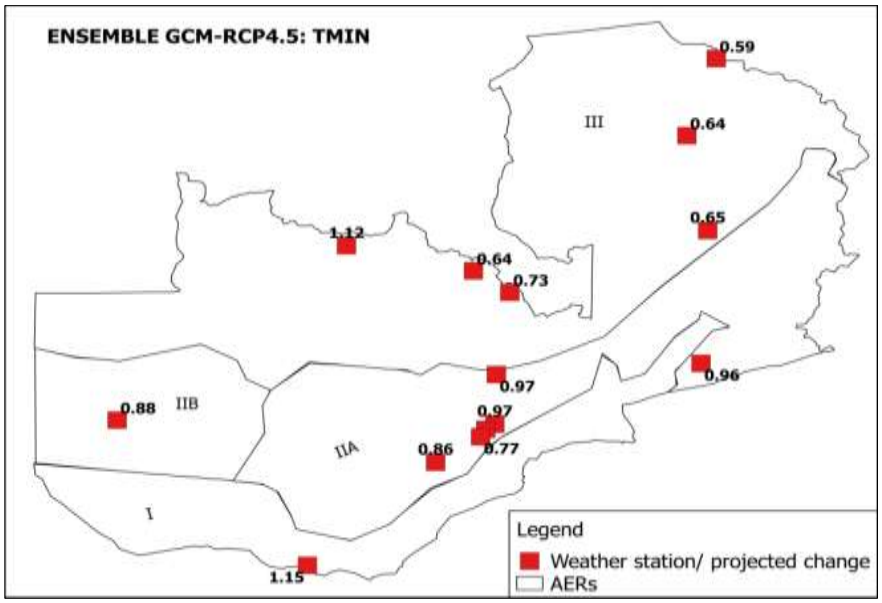

Figure 22: *Projected changes in downscaled mean TMIN for ensemble of GCMs under RCP4.5 scenario for the period of 2020 – 2049 relative to 1971 – 2000.*

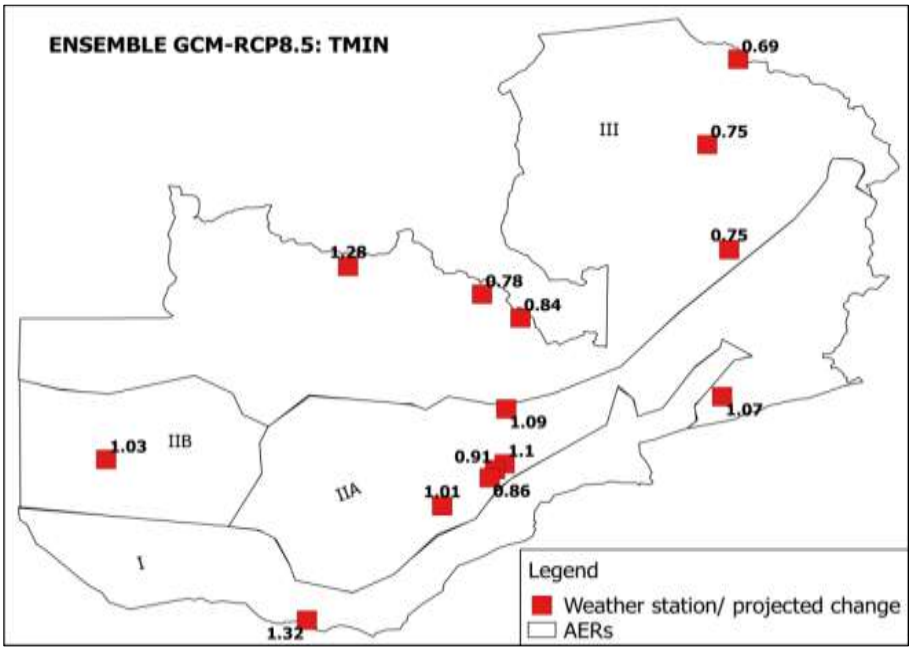

Figure 23: *Projected changes in downscaled mean TMIN for ensemble of GCMs under RCP8.5 scenario for the period of 2020 – 2049 relative to 1971 – 2000.*

5.5.4. Projected Changes in Maximum Temperature

Ensemble average changes in maximum temperature for the period 2020 – 2049 with respect to the period 1971 – 2000 for RCP4.5 and RCP8.5 scenarios are shown in Figure 24 and 25 respectively. Maximum temperature is projected to increase over every station under both scenarios. However, larger increases in maximum temperature are seen under RCP8.5 scenario than RCP4.5. Petauke will very likely experience the largest increase of 1.85°C and 2.08°C under RCP4.5 and RCP8.5 scenarios respectively. Least increases of 1.45°C (RCP4.5) and 1.63°C (RCP8.5) are projected over Kafironda. Maximum temperature is projected to increase by 1.45°C to 2.08°C across meteorological stations regardless of the emission scenario. Consistent with individual models, the ensemble of GCMs under both scenarios projects increases that tend to get larger towards the Southern part of the country (Figures 24 – 25).

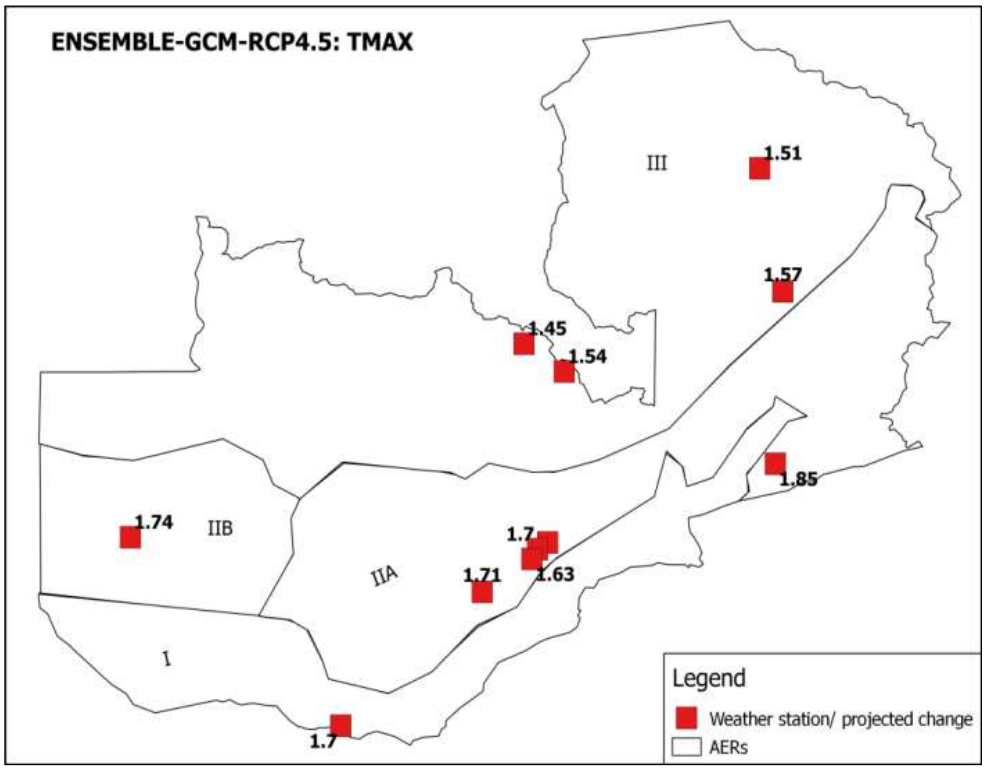

Figure 24: *Projected changes in downscaled mean TMAX for ensemble of GCMs under RCP4.5 scenario for the period of 2020 – 2049 relative to 1971 – 2000.*

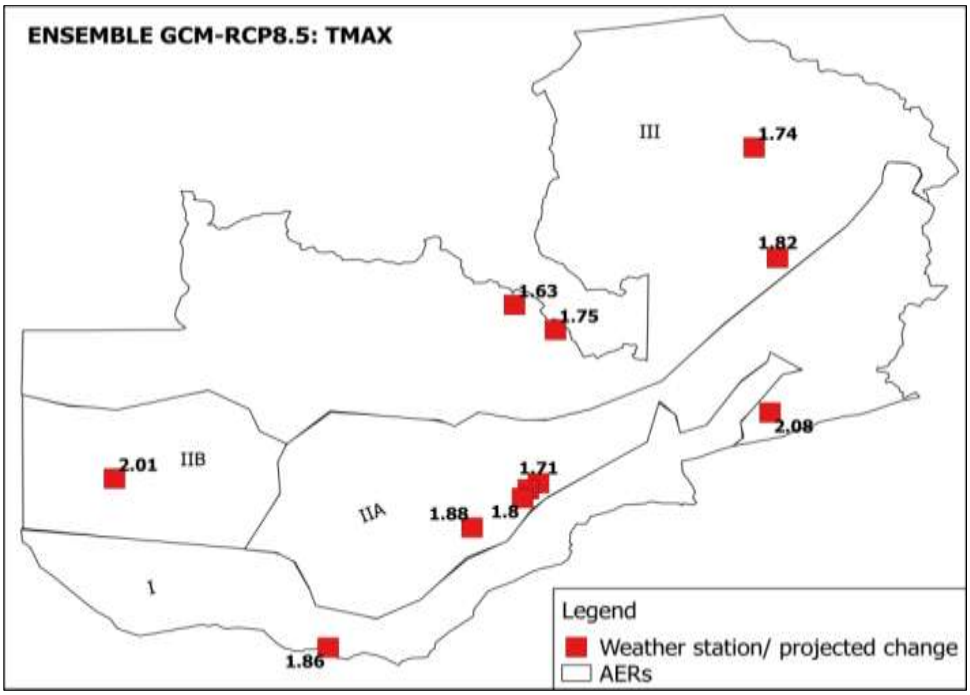

Figure 25: *Projected changes of downscaled TMAX from the ensemble of three GCMs under RCP8.5 scenarios for the period 2020 - 2049 relative to 1971 – 2000.*

5.5.5. Projected Seasonal Temperature Changes

On seasonal basis, the ensemble of models projects increase in both minimum temperature and maximum temperature for the seasons SON, DJF, MAM and JJA at all weather stations under both emission scenarios. The increase gets bigger with the increase in concentration of emissions (Figure 26 – 27). Thus, changes are bigger under RCP8.5 than RCP4.5 for most stations. For minimum temperature, the largest and smallest increases at each station are projected to occur during JJA and DJF seasons respectively under the two future emission scenarios (Figure 26).

The Ensemble mean shows that for DJF season, Kafironda will experience the smallest increase of 0.26°C and 0.29°C in mean minimum temperature under RCP4.5 and RCP8.5 respectively. Similarly, Mbala is projected to experience the smallest rise in mean minimum temperature of 0.47°C (RCP4.5) and 0.57°C (RCP8.5) during MAM season, 1.04°C (RCP4.5) and 1.21°C (RCP8.5) in JJA, and 0.38°C (RCP4.5) and 0.42°C (RCP8.5) for SON (Figure 26). Apart from JJA season under RCP4.5, Livingstone is consistently projected to experience the highest increase for DJF, MAM and SON season under both scenarios. Under RCP4.5 scenario, seasonal mean minimum temperature for Livingstone will rise by 0.68°C (DJF),

1.25°C (MAM) and 1.30°C (SON). For JJA season, the largest increase of 1.41°C is projected to occur over Kabwe station (Figure 26a). As for RCP8.5, the ensemble of models project increases of 0.74°C (DJF), 1.50°C (MAM), 1.68°C (JJA) and 1.35°C (SON) in minimum temperature for 2020 – 2049 relative to 1971 – 2000 (Figure 26b) over Livingstone. These changes may have implications on tourism sector in the

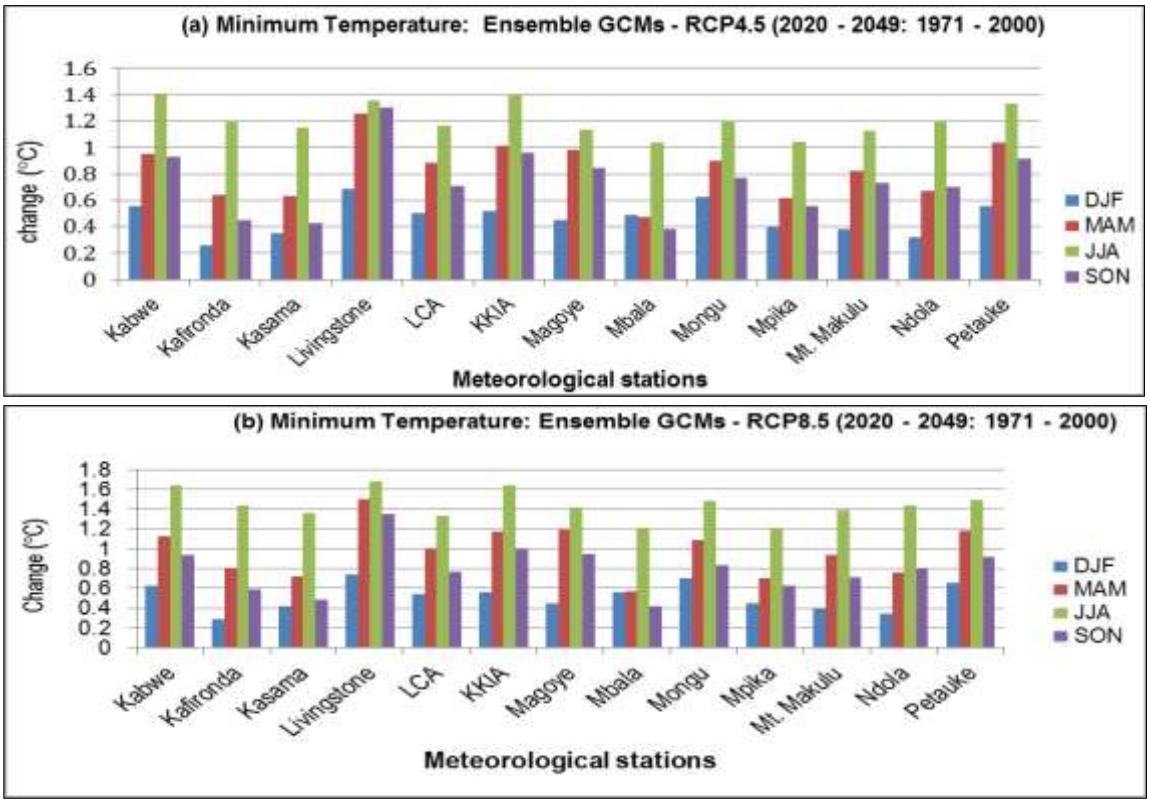

Figure 26: *Projected changes of downscaled seasonal minimum temperature using the ensemble of three GCMs under RCP4.5 and RCP8.5 emission scenarios for the period 2020 - 2049 relative to 1971 – 2000.*

The Ensemble mean projects seasonal mean maximum temperature to increase by 1.45 – 1.85°C (DJF), 1.37 – 1.84°C (MAM), 1.56 – 2.07°C (JJA) and 1.35 – 1.86°C (SON) under RCP4.5 emission scenario (Figure 27a). The increase in seasonal maximum temperature under RCP8.5 is projected to be in the range of 1.59 and 2.22°C (DJF), 1.61 and 2.21°C (MAM), 1.81 and 2.39°C (JJA) and 1.35 and 1.95°C (SON) (Figure 27b). For most weather stations, largest warming is projected to occur during JJA season under both scenarios. The results show that changes in maximum temperature tend to get larger towards Southern part of the country.

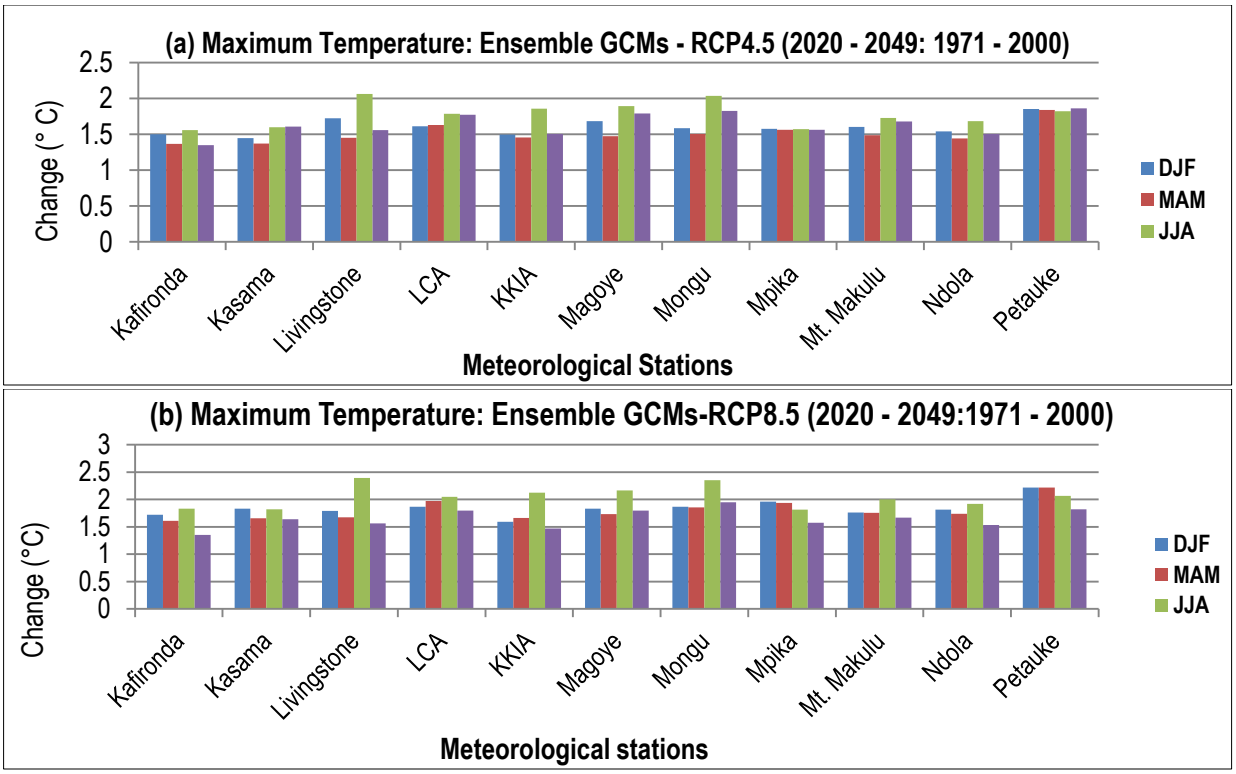

Figure 27: *Projected changes of downscaled seasonal maximum temperature using the ensemble of three GCMs under RCP4.5 (panel a) and RCP8.5 (panel b) emission scenarios for the period 2020 - 2049 relative to 1971 - 2000.*

In agreement with previous studies (McSweeney et al., 2008; NAPA, 2007) the current study has projected increase in annual and seasonal temperature across all meteorological stations under both emission scenarios (Figures 17 – 27). The projected changes indicate smaller increases for stations in the northern part of Zambia compared to those in the southern part. Thus, continued increase in temperature may have implications on various sectors of the economy and adversely impact livelihoods. Therefore, it is necessary to enhance implementation of climate change policy.

5.6. Chapter Summary

The chapter has presented and discussed research findings in relation to the objectives of the study. Besides, findings have been compared to previous similar studies. Temperature has been projected to increase for every station under both RCP4.5 and RCP8.5 emission scenarios at both annual and seasonal scales. Projections for precipitation, however, are less certain across meteorological stations although the level of model agreement is high in the projected decrease in annual and seasonal precipitation for the northern part of the country

CHAPTER SIX: CONCLUSIONS AND RECOMMENDATIONS

6.1. Overview

This chapter presents conclusions drawn from the findings of the study. It also brings out recommendations that focus on national policy issues and future research.

6.2. Conclusions

The primary goal of this study was to project changes in precipitation and temperature at meteorological stations located across Zambia for the period 2020 – 2049 relative to the baseline period 1971 – 2000.

A non-parametric analogue method based on nearest neighbour was used to downscale three Global Climate Models whose horizontal spatial resolution is about 100 to 300 km per grid box. These GCMs were constrained by two representative concentration pathways; RCP4.5 and RCP8.5. The assessment of literature demonstrates that three CMIP5 GCMs, namely; CanESM2, CNRM-CM5 and MPI-ESM-MR are capable of simulating the past and present climate for Southern Africa and Zambia in particular. These models have been used in a number of studies for Zambia but more often for Southern Africa.

The study has established that the exclusion of circulation variables from the predictor field for downscaling precipitation leads to low predictive power of the downscaling model. For the purpose of downscaling precipitation, atmospheric temperature at 850hPa (T850) has better predictive power than temperature at 2 metres (T2m). Results show that replacing T850 by T2m in predictor combinations for precipitation led to reduction in both correlations and p – values of the Kolmogorov Smirnov test. Generally, middle tropospheric atmospheric variables were found to be suitable for downscaling precipitation. Therefore, the predictor combination consisting of Q850, T850, U850 and V850 was used to downscale precipitation. In the case of temperature, the exclusion of circulation variables improved the skill of the downscaling model. The removal of at least one of the temperature variables T2m and T850 from predictor fields for temperature resulted into lower correlations of observations and predicted values. SLP, Q850 and T850 constituted the preferred predictor combination for downscaling minimum temperature. Moreover, T2m was used to downscale maximum temperature.

Precipitation is projected to decrease for all stations located in the AER III and for most stations in the AERs I and II. The results indicate that precipitation will decrease over most stations in AERIII under both RCPs. However, a mixed climate change signal for precipitation is projected for few stations in AER III. While some meteorological stations in AERs I and II are projected to experience marginal increase in precipitation, most of them are expected to have reduced precipitation. Under RCP4.5, the ensemble of models projects changes in seasonal precipitation ranging from -15.7 to 4.3 percent (DJF), -23.4 to 27.3 percent (MAM) and -18.8 to 16.3 percent (SON). Moreover, seasonal precipitation changes are projected to range from -12.7 to 6.1 percent (DJF), -39.3 to 18.6 percent (MAM) and -29.3 to 12.6 percent (SON) under RCP8.5 scenario.

Clear increase in minimum temperature and maximum temperature is projected at all stations used in the study. The increase in temperature tends to be larger for stations located in the Southern part of the country. Regardless of the emission scenario considered, minimum temperature is projected to increase by 0.59 to 1.32°C across meteorological stations. Maximum temperature is projected to increase by 1.45°C to 2.08°C across meteorological stations regardless of the emission scenario.

On a seasonal scale, temperature is projected to increase across all stations during each season. The smallest increase in minimum temperature is projected to occur during DJF season with JJA expected to experience the largest increase for every station under both emission scenarios. In the case of maximum temperature, the smallest increase is projected to occur during MAM season for most stations. Besides, largest increases are projected for JJA season under both emission scenarios for the majority of stations.

6.3. Recommendations

6.3.1 Policy Recommendations

Impacts of climate change permeate societies and many economic sectors. The projected increase in temperature and decrease in precipitation are expected to exacerbate water deficit, crop failure and lower hydropower generation. Livestock would be deprived of grazing land and stressed by high temperature. To minimize the adverse impacts that could result from the

projected changes in precipitation and temperature, the following policy recommendations are proposed.

i. The Government of the Republic of Zambia through line ministries and other stakeholders should promote irrigation farming. This would supplement crop water demand which is predominantly rain-fed.
ii. Although Zambia is making head ways in the adoption and promotion of alternative sources of energy such as wind and solar, there is need to expedite the implementation process and expand the solar power grids. This would greatly cushion the power shortage which the country experiences during years of low rainfall and subsequent reduction of water in Kariba dam.
iii. There is need to create climate data sharing protocol between the Ministry of Transport and Communications through Zambia Meteorological Department and local Universities. This will make climate data accessible for educational purposes and students pursuing studies related to weather/climate will have the experience of working with real climate data.
iv. Strengthen institutional capacity in weather/climate monitoring. This will in turn reinforce early warning systems and emergency planning.

6.3.2. Recommendations for Future Research.

The research has served its purpose of providing high resolution climate information at local scale. It has provided an understanding of how precipitation and temperature are likely to change at various meteorological stations across Zambia for the period 2020 – 2049 relative to baseline 1971 – 2000. Nevertheless, some opportunities for future research were identified during the investigation.

The study has only projected mean climate change for precipitation, minimum temperature and maximum temperature at annual and seasonal time scales. Future studies can investigate climate variability and extreme weather events for the period 2020 – 2049. Understanding plausible changes in extreme weather indices could motivate formulation of strategies aimed at mitigating and adapting to adverse impacts of extreme weather/climate events.

An assessment of GCMs performance in reproducing past and present climate for Zambia was not carried out. The current study solely relied on model performance as reported in literature. An independent assessment of models would have provided insights into performance of individual GCMs when assessed against gridded observed datasets. Future research, therefore, should be dedicated to an independent assessment of an ensemble of models suitable for downscaling climate over Zambia under multiple concentration pathways.

Future studies may consider testing several statistical downscaling methods and compare their results. This would provide a pool of methods suitable for climate downscaling activities in Zambia.

The study was confined to projections of changes in precipitation and temperature without assessing possible impacts on specific sectors such agriculture, energy, water resources, health and wildlife. It is therefore recommended that future studies should consider assessing impacts of the projected changes in climate on specific sectors.

REFERENCES

Adler, R.F., Gu, G., Sapiano, M., Wang, J., and Huffman, G. J. (2017). Global Precipitation: Means, Variations and Trends During the Satellite Era (1979–2014). *Surveys in Geophysics*. Springer Netherlands, **38**(4), 679–699.

Anyah, R. O. and Qiu, W. (2012). Characteristic 20th and 21st Century Precipitation and Temperature Patterns and Changes over the Greater Horn of Africa. *International Journal of Climatology*, **32**(3), 347–363.

Arslan, A., McCarthy, N., Lipper, L., Asfaw, S., Cattaneo, A., and Kokwe, M. (2015). *Food Security and Adaptation Impacts of Potential Climate Smart Agricultural Practices in Zambia*. Food and Agriculture Organisaion of The United Nations. Rome.

Barkhordarian, A., Storch, H. Von and Bhend, J. (2013). The Expectation of Future Precipitation Change over the Mediterranean Region is Different from what we Observe. *Climate Dynamics*, **40**, 225–244.

Bast, J. L. (2010). *Seven Theories of Climate Change*. Chicago, IIlinois: The Heartland Institute.

Benestad, R. (2016). Downscaling Climate Information. *Oxford Research Encyclopedia of Climate Science*. doi: 10.1093/acrefore/9780190228620.013.27.

Benestad, R. E. (2001). A Comparison Between Two Empirical Downscaling Strategies. *International Journal of Climatology*, **21**(13), 1645–1668.

Blamey, R., Copp, L., Jack, C., Loveday, B., and Sutherland, K. (2013). *Background Report on the Status and Possible Evolution of Climate Projections in West Africa.* USAID- African and Latin American Resilience to Climate Change Report.

Boko, M., Niang, I., Nyong, A., Vogel, C., Githeko, A., Medany, M., Osman-Elasha, B., Tabo, R., and Yanda, P. (2007). Africa. In *Climate change 2007: Impacts, Adaptation and Vulnerability. Contribution of Working Group II to the Fourth Assessment Report of the Intergovernmental Panel on Climate Change*. Cambridge UK: Cambridge University Press. 433–467.

Brands, S., Taboada, J.J., Cofino, A., Sauter, T., and Schneider, C. (2011). Statistical Downscaling of Daily Temperatures in the NW Iberian Peninsula from Global Climate Models: Validation and Future Scenarios. *Climate Research*, **48**, 163–176.

Breach, P. A., Simonovic, S. P. and Yang, Z. (2016). Global Climate Model Selection for Analysis of Uncertainty in Climate Change Impact Assessments of Hydro-Climatic Extremes. *American Journal of Climate Change*, **5**(5), 502–525.

Burdeos, K. B. and Lansigan, F. P. (2017). Statistical Downscaling of Future Precipitation Scenarios for Agusan del Norte. *Climate, Disater and Development Journal*, **2**(2), 13–22.

Casanueva, A., Herrera, S., Fernandez, J., and Gutierrez, J.M. (2016). Towards a Fair Comparison of Statistical and Dynamical Downscaling in the Framework of the EURO-CORDEX Initiative. *Climatic Change*, **137**(3–4), 411–426.

Chisanga, C. B., Phiri, E. and Chinene, V. R. N. (2017). Climate Change Impact on Maize (Zea mays L.) Yield using Crop Simulation and Statistical Downscaling Models: A Review. *Scientific Research and Essays*, **12**(18), 167–187.

Chisanga, C.B., Phiri, E., and Chinene, V.R.N. (2017a). Statistical Downscaling of Precipitation and Temperature Using Long Ashton Research Station Weather Generator in Zambia: A Case of Mount Makulu Agriculture Research Station. *American journal of Climate Change*, **6**, 487–512.

Chisanga, C. B., Phiri, E. and Chinene, V. R. N. (2017b).Statistical Bias Correction of Fifth Coupled Model Intercomparison Project Data from the CGIAR Research Program on Climate Change , Agriculture and Food Security - Climate Portal for Mount Makulu, Zambia. *British Journal of Applied Science & Technology*, 21(4), 1–16.

Chong-Hai, Y. X. and Ying. (2012). Preliminary Assessment of Simulations of Climate Changes over China by CMIP5 Multi-Models. *Atmospheric and Oceanic Science Letters*, **5**(6), 489–494.

Christensen, J. H., Hewitson, B., Busuioc, A., Chen, A., Gao, X., Held, I., Jones, R., Kolli, R.K., Kwon, W.-T., Laprise, R., Magana Rueda, V., Mearns, L., Menendez, C.G., Raisanen, J., Rinke, A., Sarr, A., and Whetton, P. (2007). Regional Climate Projections. In *Climate Change 2007: The Physical Science Basis. Contribution of Working Group I to the Fourth Assessment Report of the Intergovernmental Panel on Climate Change*. United Kingdom and New York, NY, USA.: Cambridge University Press, 847–940.

Christensen, J. H., Krishna Kumar, K., Aldrian, E., An, S.-I., Cavalcanti, I.F.A., de Castro, M., Dong, W., Goswami, P., Hall, A., Kanyanga, J.K., Kitoh, A., Kossin, J., Lau, N.-C., Renwick, L., Stephen, D.B., Xie, S.-P and Zhou, T. (2013). Climate Phenomena and their Relevance for Future Regional Climate Change. In *Cimate Change 2013: The Physical science Basis. contribution of Working Group I to the Fifth Assessment Report of the Interovernmental Panel on Climate Change*. Cambridge, United Kingdom and New York, NY, USA.: Cambridge University Press, 1217–1308.

Chylek, P., Li, J., Dubey, M.K., Wang, M., and Lesins, G. (2011). Observed and Model Simulated 20th Century Arctic Temperature Variability: Canadian Earth System Model CanESM2. *Atmospheric Chemistry and Physics Discussions*, **11**(8), 22893–22907.

Collins, J. M. (2011). Temperature variability over Africa. *Journal of Climate*, **24**(14), 3649–3666.

Collins, M., Knutti, R., Arblaster, J., Dufresne, J.-L., Fichefet, T., Friedlingstein, P., Gao, X., Gutowski, W.J., Johns, T., Krinner, G., Shongwe, M., Tebaldi, C., Weaver, A.J. and Wehner, M.. (2013). Long-term Climate Change: Projections, Commitments and Irreversibility. In Stocker, T., Qin, D., Plattner, G., Tignor, M., Allen, S., Boschung, J., and Midgley, P.(eds). *IPCC Fifth Assessment Report*. Cambridge: Cambridge University Press, 1029–1136.

Cook, K. H. and Vizy, E. K. (2012). Impact of climate change on mid-twenty-first century growing seasons in Africa. *Climate Dynamics*, **39**(12), 2937–2955.

Coulibaly, P., Dibike, Y. B. and Anctil, F. (2005). Downscaling Precipitation and Temperature with Temporal Neural Networks. *Journal of Hydrometeorology*, **6**(4), 483–496.

CSO. (2012). *2010 Census of Population and Housing: National Analytical Report*. Lusaka: Central Statistics Office.

Cubasch, U., Wuebbles, D., Chen, D., Facchini, M.C, Frame, D., Mahowald, N., and Winther, J.-G. (2013). Introduction. In Stock, T.F., Qin, D., Plattner, G.-K., Tignor, M., Allen, S., Boschung, J.,Nauels, A., Xia, Y., Bex, V. and Midgley, P. (eds). *Climate Change 2013. The Physical Science Basis. Contribution of Working Group I to the Fifth Assessment Report of the Intergovernmental Panel on Climate Change*. Cambridge, 119–158.

Curry, J. (2017). *Climate Models for the Layman*. The Global Warming Policy Foundation (Briefing 24). London.

Curry, J. A. and Webster, P. J. (2011). Climate Science and the Uncertainty Monster. *Bulletin of the American Meteorological Society*, **92**(12), 1667–1682.

Daron, J.D. (2014). *Regional Climate Messages: Southern Africa*. Scientific Report from the CARIAA Adaptation at Scale in Semi-Arid Regios (ASSAR) Project, December 2014.

Daron, J. D. (2014a). *Regional Climate Messages: East Africa*. Scientific report from the CARIAA Adaptation at Scale in Semi-Arid Regions (ASSAR) Project, December 2014.

Davis-Reddy, C. and Vincent, K. (2017) *Climate Risk and Vulnerability: A Handbook for Southern Africa*. (2nd Ed.). Pretoria, South Africa: Council for Scientific and Industrial Research.

Davis, C. L. (2011) *Climate risk and vulnerability: A Handbook for Southern Africa*. Pretoria: Council for Scientific and Industrial Research.

Dee, D. P., Uppalaa, S. M., Simmonsa, A. J., Berrisforda, P., Polia, P., Kobayashib, S., Andraec, U., Balmasedaa, M.A, Balsamoa, G., Bauera, P., Bechtolda, P., Beljaarsa, A.C.M., van de Bergd, L., Bidlota, J., Bormanna, N., Delsola, C., Dragania, R., Fuentesa, M., Geera, L. Haimbergere, A.J., Healya, S.B., Hersbacha, H., H´olma, E.V., Isaksena, L., K˚allbergc, P., K¨ohlera, M., Matricardia, M., McNallya, A.P., Monge-Sanzf, B.M., Morcrettea, J.-J., Parkg, B.-K., Peubeya, C., deRosnaya, P., Tavolatoe, C., Th´epauta, J.-N. and Vitarta F. (2011). The ERA-Interim Reanalysis: Configuration and Performance of the Data Assimilation System. *Quarterly Journal of the Royal Meteorological Society*, **137**(656), 553–597.

Dibike, Y. B., Gachon, P., St-Hilaire, A., Ouarda, T.B.M.J., Nguyen, V.T.V. (2008). Uncertainty Analysis of Statistically Downscaled Temperature and Precipitation Regimes in Northern Canada. *Theoretical and Applied Climatology*, **91**, 149–170.

Diffenbaugh, N. S. and Giorgi, F. (2012). Climate Change Hotspots in the CMIP5 Global Climate Model Ensemble. *Climatic Change*, **114**, 813–822.

Droogers, P., Immerzeel, W., Terink, W., Hoogeveen, J., Bierkens, M.F.P., van Beek, L.P.H., and Debele, B. (2012). Water Resources Trends in Middle East and North Africa Towards 2050. *Hydrology and Earth System Sciences*, **16**(1), 1–14.

Emori, S., Taylor, K., Hewitson, B., Zermoglio, F., Juckes, M., Lautenschlager, M. and Stockhause, M. (2016). *CMIP5 data provided at the IPCC Data Distribution Centre. Fact Sheet of the Task Group on Data and Scenario Support for Impact and Climate Analysis (TGICA) of the Intergovernmental Panel on Climate Change (IPCC)*. Available at: http://www.ipcc-data.org/docs/fact_sheets_process_document_Oct2011.pdf.

Evans, J. P. (2011). CORDEX – An International Climate Downscaling Initiative. In *19th International Congress on Modelling and Simulation*. Perth, Australia.

Eyring, V., Bony, S., Meehl, G.A., Senior, C.A., Stevens, B., Stouffer, R.J. and Taylor, K.E. (2016). Overview of the Coupled Model Intercomparison Project Phase 6 (CMIP6) Experimental Design and Organization. *Geosceintific Model Development*, **9**, 1937–1958.

Fenech, A., Comer, N. and Gough, B. (2002). Selecting a Global Climate Model for Understanding Future Projections of Climate Change. In *Linking Climate Models to Policy and Decision Making*. Prince Edward Island. UPEI Climate Lab,133–145.

Flato, G., Marotzke, J., Abiodun, B., Braconnot, P., Chou, S.C., Collins, W., Cox, P., Driouech, F., Emori, S., Eyring, V., Forest, C., Gleckler, P. , Guilyardi, E. , Jakob, C., Kattsov, V., Reason, C and Rummukainen, M. (2013). Evaluation of Climate Models. In *Climate Change 2013: The Physical Science Basis. Contribution of Working Group I to the Fifth Assessment Report of the Intergovernmental Panel on Climate Change*, 741–866 [Stocker, T., Qin, D., Plattner, G., Tignor, M., Allen, S., Boschung, J., and Midgley, P.(eds)]. Cambridge: Cambridge University Press.

Girod, B., Wiek., A., Mieg, H., and Hulme, M. (2009). The Evolution of the IPCC's Emissions Scenarios. *Environmental Science and Policy*, **12**(2), 103–118.

Goodess, C. M. and Palutikof, J. P. (1998). Developement of daily Rainfall Scenarios for South East Spain Using a Circulation-Type Approach to Downscaling. *International Journal of Climatology*, **10**, 1051–1083.

Grouillet, B., Ruelland, D., Ayar, P.V., and Vrac, M. (2016). Sensitivity Analysis of Runoff Modeling to Statistical Downscaling Models in the Western Mediterranean. *Hydrology and Earth System Sciences*, **20**(3), 1031–1047.

Gutierrez, J. M., San-Martin, D., Cofino, A.S., Herrera, S., Manzanas, R.G., and Frias, M.D. (2011). User Guide of the ENSEMBLES Downscaling Portal (version 2). *Technical Notes*. Spain: Santander Meteorology Group (CSIC-UC).

Gutiérrez, J. M., San-Martin, D., Brands, S., Manzanas, R.G., and Herrera, S. (2013). Reassessing statistical downscaling techniques for their robust application under climate change conditions. *Journal of Climate*, **26**(1), 171–188.

Gutiérrez, J. M., Cofiño, A. S. and Cano, R. (2004). Clustering Methods for Statistical Downscaling in Short-Range Weather Forecasts. *Monthly Weather Review*. 132, 2169–2183. Hanssen-Bauer, I., Achberger, C., Benestad, R.E., Chen, D., and Forland, E.J. (2005). Statistical Downscaling of Climate Scenarios over Scandinavia. *Climate Research*, **29**(3), 255–268.

Haylock, M. R., Cawley, G.C., Harpham, C., Wilby, R.L, and Goodess, C.M. (2006). Downscaling heavy precipitation over the United Kingdom: A Comparison of Dynamical and Statistical Methods and their Future Scenarios. *International Journal of Climatology*, **26**(10), 1397–1415.

Hewitson, B. C., Daron, J., Crane, R.G, Zermoglio, M.F., and Jack, C. (2014). Interrogating Empirical-Statistical Downscaling. *Climatic Change*, **122**(4), 539–554.

Hewitson, B. C. and Crane, R. G. (2006) 'Consensus Between GCM Climate Change Projections with Empirical Downscaling: Precipitation Downscaling over South Africa', *International Journal of Climatology*, **26**(10), 1315–1337.

Hewitson, B. and Crane, R. (1996). Climate Downscaling: Techniques and Application. *Climate Research*, **7**, 85–95.

Hofer, M., Marzeion, B. and Molg, T. (2015). A Statistical Downscaling Method for Daily Air Temperature in Data-Sparse, Glaciated Mountain Environments. *Geoscientific Model Development*, **8**(3), 579–593.

Hulme, M., Doherty, R., Ngara, T., New, M., and Lister, D. (2001). African Climate Change: 1900-2100. *Climate Research*, **17**, 145–168.

Hushaw, B. J. (2015). Global Precipitation Part I : Trends & Projections'. Climate Smart Land Network. Center for Conservation Sciences: Climate Smart Land Network. Available at: http://climatesmartnetwork.org/wpcontent/uploads/2015/05/Global_Precipitation.pdf. Accessed on 20/10/2017.

Huth, R. (2002). Statistical Downscaling of Daily Temperature in Central Europe. *Journal of Climate*, **15**(13), 1731–1742.

Huth, R. (2004). Sensitivity of Local Daily Temperature Change Estimates to the Selection of Downscaling Models and Predictors, *Journal of Climate*, **17**(3), 640–652.

IPCC (2000) *Summary for Policymakers: Emissions Scenarios. A Special Report of Working Group III of the Intergovernmental Panel on Climate Change*. IPCC. doi: 92-9169-113-5.

IPCC (2013) *Summary for Policymakers. In : Climate Change 2013: The Physical Science Basis. Contribution of Working Group I to the Fifth Assessment Report of the Intergovernmental Panel on Climate Change*. [Stocker, T., Qin, D., Plattner, G., Tignor, M., Allen, S., Boschung, J., and Midgley, P (eds.)].Cambridge, United Kingdom: Cambridge University Press.

IPCC (2014) *Summary for Policymarkers, Climate Change 2014: Mitigation of Climate Change. Contribution of Working Group III to the Fifth Assessment Report of the Intergovenrment Panel on Climate Change*. [Edenhofer, O., Pichs-Madruga, R., Sokona, Y., Farahani, E. Kadner, S., Seyboth, K., Adler, A., Baum, I., Brunner, S., Eickemeier, P., Kriemann, B., Savolainen, J., Schlomer, S., von Stechow, C., Zwickel, T., and Minx, J.C. (eds.)]. Cambridge, United Kingdom: Cambridge University Press.

Jain, S. (2007) *An Empirical Economic Assessment of Impacts of Climate Change on Agriculture in Zambia. Policy Research Working Paper*. WPS 4291: World Bank.

Kanyanga, J. K. (2008) *EL NIÑO Southern Oscillation (ENSO) and Atmospheric Transport over Southern Africa.* Thesis (PhD). University of Johannesburg.

Kasali, G. (2008) *Capacity Strengthening in the Least Developed Countries(LDCs) for Adaptation to Climate Change (CLACC): Climate Change and Health in Zambia*. CLACC Working Paper 2. International Institute for Environment and Development.

Kirtman, B., Power, S.B., Adedoyin, J.A. Boer, G.L., Bojariu, R., Camilloni, I., Doblas-Reyes, F.J., Fiore, A.M., Meehl, G.A., Prather, M., Sarr, A., Schar, C., Sutton, F.J., van Oldenborgh, G.J., Vecchi, G., and Wang, H.J. (2013). Near-Term Climate Change: Projections and Predictability. In *Climate Change 2013: The Physical Science Basis. Contribution of Working Group I to the Fifth Assessment Report of the Intergovenermnetal Panel on Climate Change*. [Stocker, T., Qin, D., Plattner, G., Tignor, M., Allen, S., Boschung, J., and Midgley, P (eds.)].Cambridge, United Kingdom: Cambridge University Press.

Kruger, A. C. and Sekele, S. S. (2013). Trends in Extreme Temperature Indices in South Africa : 1962 – 2009. *International Journal of Climatology*, **33**, 661–676.

Legesse, S. A., Rao, P. V. V. P. and Rao, M. M. N. (2013). Statistical Downscaling of Daily Temperature and Rainfall Data From Global Circulation Models: in South Wollo Zone , North Central Ethiopia. *National Monthly Referred Journal of Research in Science & Technology*, **2**(7), 27–39.

Libanda, B., Allan, D., Noel, B., Luo, W., Chilekana, N., and Nyasa, L. (2016). Predictor Selection Associated With Statistical Downscaling of Precipitation over Zambia. *Asian Journal of Physical and Chemical Sciences*, **1**(2), 1–9.

Liebmann, B., Hoerling, M.P., Funck, C., Blade, I., Dole, R.M., Allured, D., Quan, X., Pegion, P.and Eischeid, Z.K.(2014). Understanding Recent Eastern Horn of Africa Rainfall Variability and Change. *Journal of Climate*, **27**(23), 8630–8645.

Luo, Q, Wen., L., McGregor, J.L., and Timbal, B. (2013). A Comparison of Downscaling Techniques in The Projection of Local Climate Change and Wheat Yields. *Climatic Change*, **120**, 249–261.

Lutz, A. F., Maat, H.W., Biemans, H., Shrestha, A.B., Wester, P., Immerzeel, W.W. (2016). Selecting Representative Climate Models for Climate Change Impact Studies: An Advanced Envelope-Based Selection Approach. *International Journal of Climatology*, **36**(12), 988–4005.

MacKellar, N., New, M. and Jack, C. (2014). Observed and Modelled Trends in Rainfall and Temperature for South Africa: 1960-2010. *South African Journal of Science*, **110**, 1–13.

Maidment, R. I., Grimes, D, Allan, R.P., Tarnavsky, E., Stringer, M., Hewitson, T., Roebeling, R., and Black, E. (2014). The 30 year TAMSAT African Rainfall Climatology And Time series (TARCAT) data set. *Journal of Geophysical Research: Atmospheres*, **119**, 10619–10644.

Manzanas, R. (2017). Assessing the Suitability of Statistical Downscaling Approaches for Seasonal Forecasting in Senegal. *Atmospheric Science Letters,* **18**(9), 381–386.

Manzanas R.G (2016). *Statistical Downscaling of Precipitation in Seasonal Forecasting: Advantages and Limitations of Different Approaches*. Thesis (PhD). University of Cantabria.

Maraun, D., Wetterhall, F., Ireson, A. M., Chandler, R. E., Kendon, E. J., Widmann, M., Brienen, S., Rust, H. W., Sauter, T., Theme, M., Venema, V. K. C., Chun, K. P., Goodess, C. M., Jones, R. G., Onof, C., Vrac, M., Thiele-Eich, I. (2010). Precipitation Downscaling Under Climate Change: Recent Developements to Bridge the Gap Between Dynamical Models and the End User. *Reviews of Geophysics*, **48**, 1–38.

Matulla, C., Zhang, X., Wang, X. L., Wang, J., Zorita, E., Wagner, S., and Storch, H. (2008). Influence of Similarity Measures on the Performance of the Analogue Method for Downcaling Daily Precipitation. *Climate Dynamics,* **30**, 133 - 144.

McSweeney, C.F., Jones, R.G., Lee, R.W. and Rowell, D.P. (2015). Selecting CMIP5 GCMs for Downscaling over Multiple Regions. *Climate Dynamics*, **44**, 3237 - 3260.

McSweeney, C. F., Jones, R. G. and Booth, B. B. B. (2012). Selecting Ensemble Members to Provide Regional Climate Change Information, *Journal of Climate*, **25**(20), 7100–7121.

McSweeney, C., New, M. and Lizcano, G. (2008). UNDP Climate Change Country Profile: Zambia. School of Geography & Environment. University of Oxford & Tyndal Centre for Climate Change Research.

Meehl, G. A., Boer, G.J., Covey, C., Latif, M., and Stouffer, R.J. (2000). The Coupled Model Intercomparison Project (CMIP): Meeting Summary. *Bulletin of the American Meteorological Society*, **2**, 313–318.

Mehran, A., Aghakouchack, A. and Phillips, T. J. (2014). Evaluation of CMIP5 Continental Precipitation Simulations Relative to Satellite-Based Gauge-Adjusted Observations. *Journal of Geophysical Research: Atmospheres*, **119**, 1695–1707.

Miao, C., Duan, Q., Qiaohong, S., Yong, H., Kong, D., Yang, T. and Gong, W. (2014). Assessment of CMIP5 Climate Models and Projected Temperature Changes over Northern Eurasia. *Environmental Research Letters*, **9**(5), 1–12.

Monerie, P. A., Sanchez-Gomez, E., Pohl, B., Robson, J., and Dong, B. (2017). Impact of Internal Variability on Projections of Sahel Precipitation Change. *Environmental Research Letters*, **12**, 1–12.

Moss, R. H., Edmonds, J.A., Hibbard, K.A., Manning, M.R., Rose, S.K., van Vuuren, D.P., Carter, T. R., Emori, S., Kainuma, M., Kram, T., Meehl, G. A., Mitchell, J. F. B., Nakicenovic, N., Riahi, K., Smith, S.J., Stouffer, R.J., Thomson, A.M., Weyant, J.P. and Wilbanks, T.J. (2010). The Next Generation of Scenarios for Climate Change Research and Assessment, *Nature*, **463**(7282), 747–756.

Mpelele, E. B. (2018). *Statistical Projections of Climate Change for Zambia Based on Simulations of Regional Climate Models*. Unpublished Dissertation (MSc). University of Zambia.

Mtongori, H. I., Stordal, F. and Benestad, R. E. (2016). Evaluation of Empirical Statistical Downscaling Models' Skill in Predicting Tanzanian Rainfall and their Application in Providing Future Downscaled Scenarios, *Journal of Climate*, **29**(9), 3231–3252.

Munday, C. and Washington, R. (2017). Circulation Controls on Southern African Precipitation in Coupled Models: The Role of the Angola Low. *Journal of Geophysical Research: Atmospheres*, **122**(122), 861–877.

Nakicenovic, N., Alcamo, J., Davis, G., Vries, B., de Fenhann, J., Gaffin, S., and Zhou, D. (2000). IPCC Special Report on Emissions Scenarios: A special Report of Working Group III of the Intergovernmental Panel on Climate Change. *Emissions Scenarios*. Cambridge: Cambridge University Press.

NAPA (2007) *Formulation of the National Adaptation Programme of Action on Climate Change (Final Report).* Lusaka, Zambia: Ministry of Tourism, Environment and Natural Resources.

Neubert, S., Krumsiek, A., Schulte, A., Tatge, A. and Zeppenfeld, L. (2011). *Agricultural Development in a Changing Climate in Zambia: Increasing resilience to climate change and economic shocks in crop production*. Bonn, Germany: German Development Institute

New, M., Hewitson, B., Stephenson, D.B., Tsiga, A., Kruger, A., Manhique, A., Gomez, B., Coelho, C.A.S., Masisi, D.N., Kalulanga, E., Mbambala, E., Adesina, F., Saleh, H., Kanyanga, J.K., Adosi, J., Bulane, L., Fortuna, L., Mdoka, M.L. and Lojoie, R. (2006). Evidence of Trends in Daily Climate Extremes over Southern and West Africa. *Journal of Geophysical Research*, **111**, 1–11.

Niang, I., Ruppel, O.C., Abdrabo, M.A., Essel, A., Lennard, C., Padgham, J. and Urquhart, P. (2014). Africa. In *Climate Change 2014: Impacts, Adaptation, and Vulnerability. Part B: Reional Aspects. Contribution of Working Group II to the Fifth Assessment Report of the Intergovernmental Panel on Climate Change*[Barrors, V.R., Field, C.B., Dokken, D.J., Mastrandrea, M.D., Mach, K.J., Bilir, T.E., Chatterjee, M., Ebi, K.L., Estrada, Y.O, Genova, R.C., Girma, B., Kissel, E.S., Levy, A.N., MacCracken, S., Mastrandrea, P.R. and White, L.L. (eds.)]. Cambridge, United Kingdom: Cambridge University Press.

NIC. (2009). *North Africa: The Impact of Climate Change to 2030 (selected Countries), A Commissioned Research Report*. Natioanal Intelligence Council.

Obada, E., Alamou, E., Zandagba, J., Chabi, A. and Afouda, A. (2017). Change in Future Rainfall Characteristics in the Mekrou Catchment (Benin), from an Ensemble of 3 RCMs (MPI-REMO, DMI-HIRHAM5 and SMHI-RCA4). *Hydrology*, **4**(1), 14.

Ongoma, V. and Chen, H. (2017). Temporal and Spatial Variability of Temperature and Precipitation over East Africa from 1951 to 2010. *Meteorology and Atmospheric Physics*, **129**(2), 131–144.

Ongoma, V., Chen, H. and Gao, C. (2017a). Projected Changes in Mean Rainfall and Temperature over East Africa Based on CMIP5 Models. *International Journal of Climatology*. wileyonlinelibrary.com, doi: 10.1002/joc.5252. Accessed on 10/01/2018.

Osima, S., Indasi, V.S., Zaroug, M., Edris, H.S., Gudoshava, M., Misiani, H.O, Nimusiima, A., Onyah, R.O., Otieno, G., Oqwang, B.A., Jain, S., Kondowe, A.L., Mwangi, E., Lennard, C., Nikulin, G. and Dosio, A. (2018). Projected Climate over the Greater Horn of Africa under 1.5 °c and 2 °c Wlobal Warming. *Environmental Research Letters*, **13** 065004, doi.org/10.1088/1748-9326/aaba1b. Accessed on 29/10/2018

Phiri, J., Moonga, E., Mwangase, O. and Chipeta, G. (2013). *Adaptation of Zambian Agriculture to Climate Change: A Comprehensive Review of the Utilisation of the Agro-Ecological Regions - A Review for Policy Makers.* Luasaka: Zambian Academy of Science.

Pierce, D. W., Barnnet, T.P., Santer, B. D., and Gleckler, P.J. (2009). Selecting Global Climate Models for Regional Climate Change Studies. *Proceedings of the National Academy of Sciences*, **106**(21), 8441–8446.

Pinto, I.. Lennard, C., Tadross, M., Hewitson, B., Dosio, A., Nikulin, G., Panitz, H.-J. and Shongwe, M.E. (2015). Evaluation and Projections of Extreme Precipitation over southern Africa from two CORDEX Models. *Climate Change*. doi: 10.1007/s10584-015-1573-1. accessed on 16/08/2016.

Ribalaygua, J., Torres, L., Portoles, J., Monjo, R., Gaitan, E. and Pino, M.R. (2013). Description and Validation of a Two-Step Analogue/Regression Downscaling Method. *Theoretical and Applied Climatology*, **114**, 253–269.

Riede, J. O., Posada, R., Fink, A.H. and Kaspar, F. (2016). What's on the 5th IPCC Report for West Africa. In: Yaro, J. A. and Hesselberg, J. (eds). *Adaptation to Climate Change and Variability in Rural West Africa*. Switzerland: Springer International Publishing. 7–24.

Roehrig, R., Bouniol, D., Guichards, F., Hourdin, F., Redelsperger, J.-L. (2013). The Present and Future of the West African Monsoon: A Process-Oriented Assessment of CMIP5 Simulations along the AMMA Transect. *Journal of Climate*, **26**(17), 6471–6505.

Stenek, V., Boysen, D., Buriks, C., Bohn, W. and Evans, M. (2011). *Climate Risk and Business: Hydropower - Kafue Gorge Lower-Zambia*. Washington, DC: International Finance Corporation (IFC) of the World Bank Group.

Sylla, B. M., Nikiema, P.M., Gibba, P., Kebe, I. and Klutse, N. A.B. (2016). Climate Change over West Africa: Recent Trends and Future Projetcions. In: Yaro, J. A. and Hesselberg, J. (eds) *Adaptation to Climate Change and Variability in Rural West Africa*. Springer International, 25 - 40.

Tadross, M. and Johnston, P. (2012). *Sub-Saharan African Citites: A five-City Network to Pioneer Climate Adaptation through Participatory Research & Local Action (Climate Change Projections for Dar es Salaam - Adding value through downscaling)*. CapeTown: Climate System Aanalysis Group.

Tareghian, R. and Rasmussen, P. F. (2013). Statistical Downscaling of Precipitation using Quantile Regression, *Journal of Hydrology*, **487**, 122–135.

Taylor K.E., Stouffer, R.J. and Meehl, G. (2012). An Overview of CMIP5 and The Experiment Design. *Bulletin of the American Meteorological Society*, **3**, 485–498.

Terink, W., Immerzeel, W. W. and Droogers, P. (2013). Climate Change Projections of Precipitation and Reference Evapotranspiration for the Middle East and Northern Africa until 2050. *International Journal of Climatology*. Wileyonlinelibrary.com, doi: 10.1002/joc.3650. Accessed on 10/01/2018.

Thurlow, J., Zhu, T. and Diao, X. (2009) *The Impact of Climate Variability and Change on Economic Growth and Poverty in Zambia.* International Food Policy Research Institute. Discussion Paper 00890.

Trenberth, K. E., Jones, P.D., Ambenje, P., Bojariu, R., Easterling, D., Klein Tank, A., Parker, D., Rahimzadeh, F., Renwick, J.A., Rusticucci, M., Soden, B. and Zhani P. (2007). Observations: surface and atmospheric climate change. In: *Climate Change 2007: The Physical Science Basis. Contribution of Working Group I to the Fourth Assessment Report of the Intergovernmental Panel on Climate Change*[Solomon, S., Qin, D., Manning, M., Chen, Z., Marquis, M., Averyt, K.B., Tignor, M. and Miller, H.L. (eds.)]. Cambridge, United Kingdom: University of Cambridge Press, 235–336.

Trzaska, S. and Schnarr, E. (2014). A Review of Downscaling Methods for Climate Change Projections. *United States Agency for International Development by Tetra Tech ARD*, 1 - 42.

UNFCCC (1992). United Nations Framework Convention on Climate Change FCCC/Informal/84,270–277. doi: 10.1111/j.1467-9388.1992.tb00046.x. Accessed on 15/11/2017.

von Storch, H., Hewitson, B. and Mearns, L. (2000). Review of Emperical Downscaling Techniques. In: Iversen, T. and Hoiskar, B. A. (eds.) *Regional climate development under global warming. General Technical Report.* Torbjornrud: Conference Proceedings RegClim Spring Meeting, 29–46.

Vuuren, D. P. Van, Edmonds, J., Kainuma, M., Riahi, K., Nakicenovic, N., Smith, S.J. and Rose, S.K. (2011). The Representative Concentration Pathways: An Overview. doi: 10.1007/s10584-011-0148-z. Accessed on 15/06/2017.

Wackerly, D. D., Mendenhall, W. and Scheaffer, R. (2008). *Mathematical Statistics with Applications*. 7th edn. Belmont: Thomson Brooks/Cole.

Wayne, G. P. (2013).The Beginner's Guide to Representative Concentration Pathways, *Skeptical Science*. Available at https://skepticalscience.com. Accessed on 07/11/2017

Wetterhall, F., Halldin, S. and Xu, C. Y. (2005). Statistical Precipitation Downscaling in Central Sweden with the Analogue Method, *Journal of Hydrology*, **306**, 174–190.

Wibig, J., Maraun, D., Benestad, R., Kjellstrom, E., Lorenz, P. and Christensen O.B.(2015). Projected Change - Models and Methodology. In Bolle H-J., M. Menenti, V. Sebastiano (Eds.) *Regional Climate Studies: Second Assesssment of Climate Change for the Baltics Sea Basin*. Geesthacht: Springer Internal Publishing AG, 189–215.

Wilby, R. L., Charles, S.P., Zorita, E., Timbal, B., Whetton, P. and Mearns, L.O. (2004). *Guidelines for Use of Climate Scenarios Developed from Statistical Downscaling Methods.* Task Group on Data and Scenario Support for Impacts and Climate Analysis (TGICA): IPCC

Wilby, R. L., Hassan, H. and Hanaki, K. (1998). Statistical Downscaling of Hydrometeorological Variables using General Circulation Model Output. *Journal of Hydrology*, **205**,1–19.

Wilby, R. L. and Wigley, T. M. L. (1997). Downscaling General Circulation Model Output: A Review of Methods and Limitations. *Progress in Physical Geography*, **21**(4), 530–548.

Wilby, R. L. and Wigley, T. M. L. (2000). Precipitation Predictors for Downscaling: Observed and General Circulation Model Relationships. *International Journal of Climatology*, **20**(6), 641–661.

Wilks, D. S. (2006). *Statistical Methods in the Atmospheric Sciences*. 2nd ed. *International Geophysics Series*. (D. Dmowska, D. Hartmann, and H. Rossby, eds.). Burlington, USA.

Yamba, F. D., Walimwipi, H., Jain, S., Zhou, P., Cuamba, B. and Mzezewa, C. (2011). Climate Change/Variability Implications on Hydroelectricity Generation in the Zambezi River Basin. *Mitigation and Adaptation Strategies for Global Change*, **16**(6), 617–628.

Yang, W., Seager, R., Cane, M.A. and Liniger, M.A. (2015). The Rainfall Annual Cycle Bias over East Africa in CMIP5 Coupled Climate Models. *Journal of Climate*, **28**(24), 9789–9802.

Zubler, E. M., Fischer, A.M., Frob, F., and Liniger, M.A. (2016). Climate Change Signals of CMIP5 General Circulation Models over the Alps – Impact of Model Selection. *International Journal of Climatology*, **36**, 3088–3104.

APPENDICES

Appendix A: Validation scores for precipitation and temperature

Variable	Predictor Code	Correlation coefficient				Kolmogorov Smirnov *p*−values			
		Geographical domains				Geographical domains			
		D1	D2	D3	D4	D1	D2	D3	D4
PRECIP	V1	0.468	0.444	0.464	0.442	0.474	0.557	0.479	0.443
	V2	0.465	0.444	0.459	0.445	0.509	0.537	0.505	0.443
	V3	0.461	0.444	0.456	0.445	0.489	0.469	0.417	0.598
	V4	0.469	0.440	0.461	0.448	0.467	0.579	0.611	0.568
	V5	**0.469**	0.446	0.458	0.446	**0.633**	0.645	0.449	0.503
	V6	0.463	0.448	0.459	0.443	0.543	0.467	0.397	0.530
	V7	0.462	0.447	0.457	0.443	0.546	0.525	0.477	0.427
	V8	0.465	0.440	0.461	0.440	0.402	0.394	0.595	0.459
	V9	0.469	0.449	0.452	0.438	0.535	0.637	0.679	0.509
	V10	0.469	0.447	0.451	0.442	0.587	0.623	0.616	0.597
	V11	0.462	0.447	0.466	0.449	0.649	0.651	0.539	0.567
	V12	0.456	0.432	0.455	0.424	0.305	0.482	0.358	0.446
	V13	0.456	0.432	0.457	0.431	0.494	0.482	0.535	0.560
TMIN	P1	0.794	0.787	0.791	0.781	0.544	0.473	0.525	0.355
	P2	0.784	0.776	0.780	0.773	0.580	0.531	0.559	0.477
	P3	0.786	0.778	0.782	0.776	0.580	0.531	0.559	0.477
	P4	0.786	0.778	0.782	0.777	0.485	0.535	0.428	0.443
	P5	0.783	0.779	0.781	0.776	**0.647**	0.423	0.490	0.298
	P6	0.785	0.783	0.783	0.776	0.568	0.335	0.421	0.320
	P7	0.781	0.776	0.779	0.774	0.644	0.474	0.509	0.448
	P8	0.770	0.769	0.773	0.769	0.553	0.547	0.454	0.381
	P9	0.775	0.773	0.779	0.775	0.642	0.602	0.459	0.386
TMAX	T1	0.777	0.759	0.763	0.743	0.376	0.308	0.422	0.243
	T2	0.781	0.763	0.768	0.748	0.398	0.392	0.385	0.387
	T3	0.767	0.749	0.755	0.735	0.395	0.244	0.417	0.177
	T4	0.767	0.747	0.758	0.734	0.288	0.227	0.275	0.184
	T5	0.722	0.706	0.716	0.695	0.571	0.315	0.561	0.218
	T6	0.716	0.699	0.706	0.686	0.678	0.293	0.484	0.352
	T7	0.769	0.746	0.759	0.736	0.388	0.311	0.335	0.296
	T8	0.763	0.750	0.756	0.740	0.484	0.556	0.432	0.329
	T9	0.758	0.748	0.749	0.737	0.495	0.418	0.395	0.435
	T10	**0.757**	0.748	0.752	0.736	**0.618**	0.458	0.483	0.410

Note:

- PRECIP, TMIN and TMAX refer to precipitation, minimum temperature and maximum temperature respectively.
- Predictor codes are as defined in tables
- The geographical domains are as defined in Table 6.

Appendix B: 30 year period historical and future mean annual precipitation and projected changes for the ensemble of GCMs under RCP4.5 and RCP8.5 emission scenarios.

Station	Location		Historical	RCP4.5		RCP8.5	
	Lat. (°C)	Lon.(°C)	Mean	Mean (mm)	Mean Δ%	Mean (mm)	Mean Δ%
Kabwe	14.4	28.5	854	902	5.56	859	0.53
Kafironda	12.6	28.1	1232	1159	-5.92	1169	-5.14
Kasama	10.2	31.1	1311	1196	-8.80	1123	-14.4
Livingstone	17.8	25.8	592	630	6.38	634	7.01
LCA	15.4	28.3	798	821	2.88	812	1.69
KKIA	15.3	28.4	769	737	-4.16	717	-6.76
Magoye	15.9	27.6	697	667	-4.40	676	-2.98
Mansa	11.1	28.9	1089	977	-10.2	938	-13.9
Mbala	8.9	31.6	1220	1114	-8.71	1103	-9.60
Mfuwe	13.3	31.9	822	743	-9.56	783	-4.76
Mongu	15.3	23.2	934	977	4.56	974	4.21
Mpika	11.9	31.4	989	959	-3.10	948	1.44
Mt. Makulu	15.5	28.2	783	819	4.52	762	-2.71
Mumbwa	15.1	27.2	788	722	-8.44	734	-6.84
Mwinilunga	11.7	24.4	1314	1206	-8.22	1203	-8.50
Ndola	12.9	28.7	1161	1067	-8.09	1042	-10.2
Petauke	14.3	31.3	909	858	-5.59	885.7	-2.56
Serenje	13.2	30.2	1001	916	-8.44	886.7	-11.4
Solwezi	12.2	26.4	1297	1182	-8.82	1180	-9.03

Appendix C: 30 year seasonal mean for baseline and future periods for precipitation (mm) using ensemble of models under RCP4.5 and RCP8.5 scenarios.

Station	DJF			MAM			SON		
	Hist.	RCP4.5	RCP8.5	Hist.	RCP4.5	RCP8.5	Hist.	RCP4.5	RCP8.5
Kabwe	580	597	573	136	144	135	136	159	148
Kafironda	810	725	740	244	221	226	176	175	146
Kasama	803	729	671	330	276	253	177	195	160
Livingstone	393	410	434	101	109	85	97	110	109
LCA	545	562	538	129	136	151	124	117	115
KKIA	529	539	483	129	115	125	111	94	107
Magoye	479	454	444	105	110	113	113	103	97
Mansa	691	598	584	236	191	190	162	171	119
Mbala	701	613	594	364	314	339	153	163	156
Mfuwe	525	508	529	191	146	159	105	111	113
Mongu	606	533	554	173	186	196	152	159	157
Mpika	660	673	601	203	179	166	124	113	87
Mt. Makulu	530	471	469	126	161	150	127	119	117
Mumbwa	532	471	464	125	105	102	131	117	136
Mwinilunga	703	644	562	335	271	203	274	301	254
Ndola	766	678	654	214	188	184	180	176	159
Petauke	599	591	578	177	153	144	131	120	109
Serenje	672	566	584	190	172	151	127	134	108
Solwezi	790	703	665	278	252	245	228	185	191

Appendix D: 30 year mean (°C) for baseline and future periods for minimum temperature and projected changes (°C) using an ensemble of models.

Station	Location		Historical	RCP4.5		RCP8.5	
	Lat. (°S)	Lon. (°E)	Mean	Mean	Mean Δ	Mean	Mean Δ
Kabwe	14.4	28.5	14.76	15.72	0.9658	15.84	1.086
Kafironda	12.6	28.1	11.38	12.02	0.6408	12.16	0.7841
Kasama	10.2	31.1	14.20	14.84	0.6402	14.95	0.7479
Livingstone	17.8	25.8	14.87	16.02	1.151	16.19	1.32
LCA	15.4	28.3	14.87	15.68	0.8179	15.78	0.9144
KKIA	15.3	28.4	14.08	15.06	0.9725	15.18	1.096
Magoye	15.9	27.6	14.00	14.86	0.8553	15.01	1.006
Mbala	8.9	31.6	13.93	14.52	0.5941	14.62	0.6899
Mongu	15.3	23.2	16.15	17.02	0.8761	17.18	1.032
Mpika	11.9	31.4	14.13	14.79	0.6548	14.88	0.7504
Mt. Makulu	15.5	28.2	14.67	15.44	0.7691	15.53	0.8602
Ndola	12.9	28.7	14.11	14.83	0.7259	14.95	0.8391
Petauke	14.3	31.3	16.86	17.83	0.963	17.93	1.066

Appendix E: 30 year seasonal mean for baseline and future periods for minimum temperature (°C) using ensemble of models

Station	**DJF**			**MAM**			**JJA**			**SON**		
	Hist.	RCP4.5	RCP8.5	Hist.	RCP4.5	RCP8.5	Hist.	RCP4.5	RCP8.5	Hist.	RCP4.5	RCP8.5
Kabwe	17.7	18.2	18.3	14.6	15.6	15.8	10.0	11.4	11.6	16.8	17.7	17.7
Kafiro	16.7	16.9	17.0	12.2	12.9	13.0	4.21	5.41	5.64	12.5	12.9	13.1
Kasama	16.4	16.8	16.8	14.8	15.4	15.5	10.3	11.4	11.6	15.4	15.8	15.9
L/stone	19.0	19.7	19.7	14.9	16.1	16.4	8.31	9.67	10.0	17.4	18.7	18.8
LCA	17.0	17.5	17.6	14.8	15.7	15.8	10.9	12.0	12.2	16.8	17.5	17.6
KKIA	17.8	18.3	18.4	14.2	15.2	15.4	8.71	10.1	10.3	15.7	16.7	16.7
Magoye	18.2	18.7	18.7	14.0	14.9	15.2	7.95	9.09	9.4	16.0	16.8	16.9
Mbala	15.1	15.6	15.6	14.6	15.1	15.2	11.3	12.3	12.5	14.8	15.2	15.2
Mongu	19.1	19.7	19.8	16.4	17.3	17.5	11.1	12.3	12.6	18.1	18.9	19.0
Mpika	16.3	16.7	16.7	14.8	15.4	15.5	10.1	11.2	11.4	15.4	15.9	16.0
Mt Mak	17.3	17.7	17.7	14.5	15.3	15.4	9.84	11.0	11.2	17.1	17.8	17.8
Ndola	17.3	17.6	17.7	14.4	15.0	15.1	9.19	10.4	10.6	15.6	16.3	16.4
Petauke	18.9	19.5	19.6	16.6	17.7	17.8	13.1	14.4	14.6	18.9	19.8	19.8

Note: *Kafiro* represents *Kafironda* weather station and *Mt. Mak* represents *Mt. Makulu* station.

Appendix F: 30 year mean (°C) for historical and future periods for maximum temperature and projected changes (°C) using an ensemble of models

Station	Location		Historical	RCP4.5		RCP8.5	
	Lat.(°S)	Lon.(°E)	Mean	Mean	Mean Δ	Mean	Mean Δ
Kafironda	12.6	28.1	29.05	30.49	1.445	30.68	1.629
Kasama	10.2	31.1	27.70	29.21	1.508	29.44	1.736
Livingstone	17.8	25.8	30.55	32.25	1.701	32.40	1.856
LCA	15.4	28.3	26.78	28.49	1.701	28.71	1.921
KKIA	15.3	28.4	28.02	29.60	1.58	29.73	1.713
Magoye	15.9	27.6	29.25	30.96	1.71	31.13	1.880
Mongu	15.3	23.2	30.41	32.15	1.74	32.42	2.007
Mpika	11.9	31.4	26.37	27.94	1.57	28.19	1.822
Mt. Makulu	15.5	28.2	28.02	29.65	1.625	29.82	1.797
Ndola	12.9	28.7	28.53	30.07	1.543	30.28	1.751
Petauke	14.3	31.3	28.83	30.67	1.845	30.9	2.079

Appendix G: 30 year seasonal mean for historical and future periods for maximum temperature (°C) using an ensemble of models

Station	DJF			MAM			JJA			SON		
	Hist.	RCP4.5	RCP8.5	Hist.	RCP4.5	RCP8.5	Hist.	RCP4.5	RCP8.5	Hist.	RCP4.5	RCP8.5
Kafiro	28.5	30.0	30.2	28.6	30.0	30.2	27.3	28.8	29.1	31.8	33.2	33.2
Kasama	27.3	28.8	29.2	27.1	28.4	28.7	26.0	27.6	27.8	30.5	32.1	32.1
L/stone	31.2	32.9	33.0	30.0	31.5	31.7	27.0	29.1	29.4	34.0	35.5	35.5
LCA	27.1	28.7	28.9	26.2	27.8	28.1	23.9	25.7	25.9	30.1	31.8	31.9
KKIA	28.3	29.8	29.9	27.3	28.7	29.0	25.1	27.0	27.2	31.4	32.9	32.9
Magoye	29.5	31.2	31.3	28.6	30.0	30.3	26.3	28.2	28.4	32.7	34.5	34.5
Mongu	29.9	31.4	31.7	29.8	31.3	31.7	28.3	30.3	30.7	33.7	35.5	35.7
Mpika	26.8	28.4	28.8	25.6	27.2	27.5	23.6	25.2	25.4	29.5	31.1	31.1
Mt Mak	28.4	30.0	30.2	27.4	28.9	29.1	25.0	26.7	27.0	31.3	33.0	33.0
Ndola	28.1	29.6	29.9	28.0	29.4	29.7	26.6	28.3	28.5	31.5	33.0	33.0
Petauke	29.0	30.9	31.2	28.2	30.0	30.4	25.9	27.8	28.0	32.2	34.0	34.0

Note: *Kafiro* represents *Kafironda* weather station and *Mt. Mak* represents *Mt. Makulu* station.

Appendix H: Projected changes in seasonal mean precipitation, minimum temperature and maximum temperature using ensemble of three models under RCP4.5 scenario

Station	Precipitation (%)			Minimum temperature (°C)				Maximum temperature (°C)			
	DJF	MAM	SON	DJF	MAM	JJA	SON	DJF	MAM	JJA	SON
Kabwe	2.87	5.76	16.3	0.56	0.96	1.41	0.93	-	-	-	-
Kafironda	-10.5	-9.48	-0.71	0.26	0.64	1.20	0.45	1.50	1.37	1.56	1.35
Kasama	-9.21	-16.4	10.4	0.35	0.63	1.15	0.42	1.45	1.37	1.60	1.61
Livingstone	4.27	7.89	13.1	0.68	1.25	1.36	1.30	1.73	1.45	2.07	1.56
LCA	3.09	5.50	-5.87	0.50	0.89	1.17	0.71	1.61	1.63	1.79	1.77
KKIA	2.00	-11.0	-15.1	0.51	1.01	1.39	0.96	1.50	1.46	1.86	1.51
Magoye	-5.21	4.90	-8.53	0.45	0.98	1.13	0.84	1.68	1.48	1.89	1.79
Mansa	-13.6	-18.8	5.87	-	-	-	-	-	-	-	-
Mbala	-12.6	-13.6	6.60	0.49	0.47	1.04	0.38	-	-	-	-
Mfuwe	-3.37	-23.4	5.43	-	-	-	-	-	-	-	-
Mongu	-12.1	7.48	4.75	0.63	0.90	1.20	0.77	1.59	1.51	2.04	1.83
Mpika	1.96	-12.0	-8.76	0.40	0.62	1.04	0.56	1.58	1.56	1.57	1.56
Mt Makulu	-11.2	27.3	-5.61	0.38	0.83	1.13	0.73	1.60	1.49	1.73	1.68
Mumbwa	-11.4	-16.0	-10.6	-	-	-	-	-	-	-	-
Mwinilunga	-8.49	-19.2	9.78	-	-	-	-	-	-	-	-
Ndola	-11.5	-12.1	-2.52	0.32	0.67	1.20	0.70	1.54	1.44	1.68	1.51
Petauke	-1.36	-13.4	-8.87	0.56	1.04	1.34	0.91	1.85	1.84	1.82	1.86
Serenje	-15.7	-9.24	5.80	-	-	-	-	-	-	-	-
Solwezi	-11.0	-9.30	-18.8	-	-	-	-	-	-	-	-

Note: The dash (−) implies absence of the variable at a meteorological station

Appendix I: Projected changes in seasonal mean precipitation, minimum temperature and maximum temperature using ensemble of three models under RCP8.5 scenario

Station	Precipitation (%)			Minimum temperature (°C)				Maximum temperature (°C)			
	DJF	MAM	SON	DJF	MAM	JJA	SON	DJF	MAM	JJA	SON
Kabwe	-4.06	-0.26	8.18	0.63	1.13	1.64	0.94	-	-	-	-
Kafironda	2.04	-7.46	-17.0	0.29	0.81	1.43	0.59	1.72	1.61	1.83	1.35
Kasama	-7.98	-23.4	-9.65	0.42	0.72	1.36	0.48	1.83	1.65	1.82	1.64
Livingstone	6.08	-16.6	12.6	0.74	1.50	1.68	1.35	1.79	1.67	2.39	1.56
LCA	-4.26	16.8	-6.87	0.55	1.00	1.33	0.77	1.87	1.97	2.05	1.8
KKIA	-10.4	-2.91	-3.13	0.56	1.17	1.64	1.00	1.59	1.66	2.13	1.47
Magoye	-2.15	7.73	-14.0	0.45	1.20	1.42	0.95	1.83	1.73	2.16	1.79
Mansa	-2.30	-19.3	-26.1	-	-	-	-	-	-	-	-
Mbala	-3.02	-6.76	1.73	0.56	0.57	1.21	0.42	-	-	-	-
Mfuwe	4.28	-16.9	7.24	-	-	-	-	-	-	-	-
Mongu	3.88	13.5	3.51	0.70	1.09	1.49	0.84	1.87	1.86	2.35	1.95
Mpika	-10.7	-18.3	-29.3	0.44	0.70	1.22	0.63	1.96	1.94	1.81	1.58
Mt Makulu	-0.41	18.6	-7.66	0.40	0.94	1.39	0.71	1.76	1.75	2.00	1.67
Mumbwa	-1.47	-18.5	3.89	-	-	-	-	-	-	-	-
Mwinilunga	-12.7	-39.3	-7.40	-	-	-	-	-	-	-	-
Ndola	-3.57	-13.8	-11.9	0.35	0.76	1.43	0.81	1.81	1.74	1.92	1.53
Petauke	-2.18	-18.8	-16.7	0.65	1.18	1.50	0.92	2.22	2.21	2.07	1.82
Serenje	3.10	-20.2	-14.9	-	-	-	-	-	-	-	-
Solwezi	-5.42	-12.0	-16.5	-	-	-	-	-	-	-	-

Note: The dash (−) implies absence of the variable at a meteorological station

APPENDIX J: R script for computing annual and seasonal means at each station

Note:

- Computation were executed using R version 3.5.0 (2018-04-23)
- X represents any of the variables: PRECIP, TMIN or TMAX,
- r is the number of rows to be skipped in a data frame
- "station" the name station should be replaced by the station ID e.g. "KAFIRO01" for KAFIRONDA

```
#########################################################################
Options (digits=4## controls number of significant digits to print
library(plyr)## for implementing the split-apply-combine pattern in R
library (dplyr) ## for data manipulation
library(lubridate) ##for working with dates
library(hydroTSM)##daily, monthly, seasonal
library(scales)## to access breaks/formatting functions
library(zoo)## manipulation of regular and irregular time series of
       ##numeric vectors/matrices
setwd("~/CHOTA MSc/Software (2018)/RStudio wd dissertation/DOWNSCALED
SCENARIOS/X")
################################## Historical ##################
###loading the model cnrm_cm5_hist
X_cnrm_cm5_hist <- read.csv("~/Documents/CHOTA MSc/Software
(2018)/RStudio wd dissertation/DOWNSCALED SCENARIOS/X/CNRM-
CM5/hist_t2m/a1p10 - a1p10_X - Analogues (default) - CNRM-CM5 -
historical_r1i1p1.csv", skip = r)
head(X_cnrm_cm5_hist## reading the first few rows in the data frame

###Converting date to R date format
X_cnrm_cm5_hist$Date <- as.Date(X_cnrm_cm5_hist$Date, "%d/%m/%Y",
na.rm = TRUE)

###STATION_X: Selecting a STATION from the data frame
X_cnrm_cm5_hist <- subset (X_cnrm_cm5_hist, select=c("Date",
"station"))
head(X_cnrm_cm5_hist)
colnames(X_cnrm_cm5_hist) <- c("Date","X_cnrm_cm5_hist")

###loading the model CanESM2_hist
X_CanESM2_hist<-read.csv("~/Documents/CHOTAMSc/Software(2018)/RStudio
wd dissertation/DOWNSCALED
SCENARIOS/X/CanESM2/hist/a1p10_X - Analogues (default) - CANESM2 -
historical_r1i1p1.csv", skip = r)

### Converting date to R date format
X_CanESM2_hist$Date <- as.Date(X_CanESM2_hist$Date, "%d/%m/%Y", na.rm
= TRUE)
head(CanESM2_hist)
```

```
###STATION_X: Selecting a station from the data frame
X_CanESM2_hist <- subset(X_CanESM2_hist, select=c("Date", "station"))
head(X_CanESM2_hist)
colnames (X_CanESM2_hist) <- c("Date","X_CanESM2_hist")

###loading the MPI-ESM-MR
X_MPI_ESM_MR_hist<- read.csv("~/Documents/CHOTAMSc/Software
(2018)/RStudio wd dissertation/DOWNSCALED SCENARIOS/X/MPI-ESM -
MR/Hist-t2m/a1p10 - a1p10_X - Analogues (default) - MPI-ESM-MR -
historical_r1i1p1.csv", skip = r)
head(X_MPI_ESM_MR_hist)

### Converting date to R date format
X_MPI_ESM_MR_hist$Date <- as.Date(X_MPI_ESM_MR_hist$Date, "%d/%m/%Y",
na.rm = TRUE)
head(X_MPI_ESM_MR_hist)

### STATION_X: Selecting one STATION from the data frame
X_MPI_ESM_MR_hist <- subset(X_MPI_ESM_MR_hist, select=c("Date",
"station"))
colnames(X_MPI_ESM_MR_hist) <- c("Date","X_MPI_ESM_MR_hist")

###Combining the datasets using column bind function
STATION_X_hist <- cbind(X_cnrm_cm5_hist, X_CanESM2_hist[,2],
X_MPI_ESM_MR_hist[,2])
colnames(STATION_X_hist) <-
c("Date","X_cnrm_hist","X_CanESM2_hist","X_mpi_esm_mr_hist")

###Calculate row means
STATION_X_hist$ens_X_hist <- rowMeans(STATION_X_hist[,2:4],
na.rm=TRUE)
head(STATION_X_hist)
###Make new variables, year and month
STATION_X_hist<-transform(STATION_X_hist,
month=as.numeric(format(Date,"%m")),year=as.numeric(format(Date,"%Y")
, na.rm = TRUE))
head(STATION_X_hist)

### Number of years in the time slice
nyrs <- yip("1971-01-01", "2000-12-31", date.fmt= "%Y-%m-%d",
out.type = "nmbr")
nyrs

###Converting to zoo file
STATION_X_hist.zoo <- zoo(STATION_X_hist[,2:5], STATION_X_hist$Date)
head(STATION_X_hist)
```

Long term annual mean tmin/tmax temperature

```
STATION_X_annual_his<-annualfunction(STATION_X_hist.zoo,FUN=mean,
na.rm=TRUE)
STATION_X_annual_his
write.csv(STATION_X_annual_his,file = "STATION_X_annual_his.csv",
row.names = FALSE)
```

Long term mean monthly values of X

```
STATION_X_monthly_his<- monthlyfunction(STATION_X_hist.zoo, FUN=mean,
na.rm=TRUE)
STATION_X_monthly_his
write.csv(STATION_X_monthly_his, file = "STATION_X_monthly_his.csv",
row.names = TRUE)
```

###seasonal_means

```
STATION_X_seasonal_hist <- seasonalfunction(STATION_X_hist.zoo,
FUN=mean, na.rm=TRUE)
STATION_X_seasonal_hist
write.csv(STATION_X_seasonal_hist, file =
"STATION_X_seasonal_hist.csv", row.names = TRUE)
```

NOTE: For annual and seasonal precipitation use the function SUM and divide by nyrs.

```
  e.g. STATION_pr_annual <-
annualfunction(STATION_pr_hist.zoo,FUN=sum,
       na.rm=TRUE)/nyrs
```

```
################################### RCP45############################
```

###loading the cnrm_cm5_rcp45

```
X_cnrm_cm5_rcp45 <- read.csv("~/Documents/CHOTA MSc/Software(2018)
/RStudio wd dissertation/DOWNSCALED SCENARIOS/X/CNRM-CM5/rcp45-
t2m/a1p10 - a1p10_X - Analogues (default)-CNRM-CM5 rcp45_r1i1p1.csv",
skip = r)
head(X_cnrm_cm5_rcp45)
```

Converting date to R date format

```
X_cnrm_cm5_rcp45$Date <- as.Date(X_cnrm_cm5_rcp45$Date, "%d/%m/%Y",
na.rm = TRUE)
```

###STATION_X

```
X_cnrm_cm5_rcp45 <- subset(X_cnrm_cm5_rcp45, select=c("Date",
"station"))
colnames(X_cnrm_cm5_rcp45) <- c("Date","X_cnrm_rcp45")
```

```
###loading the model CanESM2_rcp45
X_CanESM2_rcp45 <- read.csv("~/Documents/CHOTA MSc/Software
(2018)/RStudio wd dissertation/DOWNSCALED SCENARIOS/X/CanESM2
/rcp4.5/a1p10_X - Analogues (default) - CANESM2 - rcp45_r1i1p1.csv",
skip = r)
head(X_CanESM2_rcp45)

### Converting date to R date format
X_CanESM2_rcp45$Date <- as.Date(X_CanESM2_rcp45$Date, "%d/%m/%Y",
na.rm = TRUE)

###STATION_X
X_CanESM2_rcp45 <-  subset(X_CanESM2_rcp45, select=c("Date",
"station")) colnames(X_CanESM2_rcp45) <- c("Date","X_CanESM2_rcp45")

### loading the MPI-ESM-MR
X_MPI_ESM_MR_rcp45 <-
read.csv("file:///C:/Users/ENOCK/Documents/CHOTA MSc/Software
(2018)/RStudio wd dissertation/DOWNSCALED SCENARIOS/X/MPI-ESM -
MR/rcp45-t2m/a1p10 - a1p10_X - Analogues (default) - MPI-ESM-MR -
rcp45_r1i1p1.csv", skip = r)
head(X_MPI_ESM_MR_rcp45)

###Converting date to R date format
X_MPI_ESM_MR_rcp45$Date <- as.Date(X_MPI_ESM_MR_rcp45$Date,
"%d/%m/%Y", na.rm = TRUE)

###STATION_X
X_MPI_ESM_MR_rcp45 <-  subset(X_MPI_ESM_MR_rcp45, select=c("Date",
"station"))

###Rename columns
colnames(X_MPI_ESM_MR_rcp45) <- c("Date","X_MPI_ESM_MR_rcp45")

#####Combining the datasets using column bind function
STATION_X_rcp45<-cbind(X_cnrm_cm5_rcp45,X_CanESM2_rcp45[,2],
X_MPI_ESM_MR_rcp45[,2])
colnames(STATION_X_rcp45)<c("Date","X_cnrm_rcp45","X_CanESM2_rcp45","
X_mpi_esm_mr_rcp45")

### Calculate row means
STATION_X_rcp45$ens_X_rcp45 <- rowMeans(STATION_X_rcp45[,2:4],
na.rm=TRUE)

###Make new variables, year and month
STATION_X_rcp45<transform(STATION_X_rcp45,month=as.numeric(format(Dat
e,"%m")),year=as.numeric(format(Date,"%Y"), na.rm = TRUE))
```

```
###Number of years in the time slice
nyrs <- yip("1971-01-01", "2000-12-31", date.fmt= "%Y-%m-%d",
out.type = "nmbr")

###Converting to zoo file
STATION_X_rcp45.zoo <- zoo(STATION_X_rcp45[,2:5],
STATION_X_rcp45$Date)

### Calculating Long term annual mean in X
STATION_X_annual_rcp45 <-annualfunction (STATION_X_rcp45.zoo,
FUN=mean, na.rm=TRUE)
STATION_X_annual_rcp45
write.csv(STATION_X_annual_rcp45, file =
"STATION_X_annual_rcp45.csv", row.names = FALSE)

###Calculating change in long term annual mean tmin/tmax
STATION_annual_change_X_rcp45<-(STATION_X_annual_rcp45)-
(STATION_X_annual_his)
STATION_annual_change_X_rcp45
write.csv(STATION_annual_change_X_rcp45,file="STATION_annual_change_X
_rcp45.csv", row.names = FALSE)

### Long term monthly minimum/maximum temperature
STATION_X_monthly_rcp45<-
monthlyfunction(STATION_X_rcp45.zoo,FUN=mean, na.rm=TRUE)
STATION_X_monthly_rcp45
write.csv(STATION_X_monthly_rcp45, file =
"STATION_X_monthly_rcp45.csv", row.names = TRUE)

### Long term monthly minimum/maximum temperature change
STATION_X_monthly_change_rcp45<-((STATION_X_monthly_rcp45)-
(STATION_X_monthly_his))
STATION_X_monthly_change_rcp45
write.csv(STATION_X_monthly_change_rcp45,file="STATION_X_monthly_chan
ge_rcp45.csv", row.names = TRUE)

###seasonal_means
STATION_X_seasonal_rcp45 <- seasonalfunction(STATION_X_rcp45.zoo,
FUN=mean, na.rm=TRUE)
STATION_X_seasonal_rcp45
write.csv(STATION_X_seasonal_rcp45, file =
"STATION_X_seasonal_rcp45.csv", row.names = TRUE)

###seasonal changes in temperature
STATION_seasonal_X_change_rcp45<-(STATION_X_seasonal_rcp45-
STATION_X_seasonal_hist)
STATION_seasonal_X_change_rcp45
```

```
write.csv(STATION_seasonal_X_change_rcp45,file="STATION_seasonal_X_ch
ange_rcp45.CSV", row.names = TRUE)

NOTE: For precipitation use the function SUM and divide by nyrs
      e.g. STATION_pr_annual <-annualfunction(STATION_pr_hist.zoo,
FUN=sum, na.rm=TRUE)/nyrs
################################## RCP85 ############################

###loading the model cnrm_cm5_rcp85
X_cnrm_cm5_rcp85 <- read.csv("~/Documents/CHOTA MSc/Software
(2018)/RStudio wd dissertation/DOWNSCALED SCENARIOS/X/CNRM-CM5/rcp85-
t2m/a1p10 - a1p10_X - Analogues (default) - CNRM-CM5 -
rcp85_r1i1p1.csv", skip = r)
head(X_cnrm_cm5_rcp85) ## To display the first 6 rows of the
dataframe

### Converting date to R date format
X_cnrm_cm5_rcp85$Date <- as.Date(X_cnrm_cm5_rcp85$Date, "%d/%m/%Y",
na.rm = TRUE)

###STATION_X
X_cnrm_cm5_rcp85 <- subset(X_cnrm_cm5_rcp85, select=c("Date",
"station"))
colnames(X_cnrm_cm5_rcp85) <- c("Date","X_cnrm_rcp85")

####loading the CanESM2_rcp85
X_CanESM2_rcp85<-read.csv("~/Documents/CHOTA MSc/Software(2018)
/RStudio wd dissertation/DOWNSCALEDSCENARIOS/X/CanESM2/rcp8.5/a1p10_X
- Analogues (default) - CANESM2 -rcp85_r1i1p1.csv", skip = r)
head(X_CanESM2_rcp85)

### Converting date to R date format
X_CanESM2_rcp85$Date <- as.Date(X_CanESM2_rcp85$Date, "%d/%m/%Y",
na.rm = TRUE)

###STATION_X
X_CanESM2_rcp85 <-  subset(X_CanESM2_rcp85, select=c("Date",
"station"))

#Rename columns
colnames(X_CanESM2_rcp85) <- c("Date","X_CanESM2_rcp85")

### loading the MPI-ESM-MR_rcp85
X_MPI_ESM_MR_rcp85 <- read.csv("~/CHOTA MSc/Software (2018)/RStudio
wd dissertation/DOWNSCALED SCENARIOS/X/MPI-ESM -MR/rcp85-t2m/a1p10 -
a1p10_X - Analogues (default) - MPI-ESM-MR - rcp85_r1i1p1.csv", skip
= r)
```

```
head(X_MPI_ESM_MR_rcp85)

### Converting date to R date format
X_MPI_ESM_MR_rcp85$Date<- as.Date(X_MPI_ESM_MR_rcp85$Date,"%d/%m/%Y",
na.rm = TRUE)

###STATION_X
X_MPI_ESM_MR_rcp85 <- subset(X_MPI_ESM_MR_rcp85, select=c("Date",
"station"))

###Rename columns
colnames(X_MPI_ESM_MR_rcp85) <- c("Date","X_MPI_ESM_MR_rcp85")

###Combining the datasets using column bind function
STATION_X_rcp85<-cbind(X_cnrm_cm5_rcp85,X_CanESM2_rcp85[,2],
X_MPI_ESM_MR_rcp85[,2])
head(STATION_X_rcp85)
colnames(STATION_X_rcp85)<-
c("Date","X_cnrm_rcp85","X_CanESM2_rcp85","X_mpi_esm_mr_rcp85")
head(STATION_X_rcp85)

###Calculate row means
STATION_X_rcp85$ens_X_rcp85 <- rowMeans(STATION_X_rcp85[,2:4],
na.rm=TRUE)
head(STATION_X_rcp85)

###Make new variables, year and month
STATION_X_rcp85<-transform(STATION_X_rcp85,
month=as.numeric(format(Date,"%m")),year=as.numeric(format(Date,"%Y")
, na.rm = TRUE))

###Number of years in the time slice
nyrs <- yip("2020-01-01", "2049-12-31", date.fmt= "%Y-%m-%d",
out.type = "nmbr")

###Converting to zoo file
STATION_X_rcp85.zoo <- zoo(STATION_X_rcp85[,2:5],
STATION_X_rcp85$Date)
head(STATION_X_rcp85.zoo)

### Calculating long term annual mean temperature
STATION_X_annual_rcp85 <-annualfunction (STATION_X_rcp85.zoo,
FUN=mean, na.rm=TRUE)
STATION_X_annual_rcp85
write.csv(STATION_X_annual_rcp85,file="STATION_X_annual_rcp85.csv",
row.names = FALSE)

###Calculating change in long term annual mean in temperature
```

```
STATION_annual_change_X_rcp85<-STATION_X_annual_rcp85-
STATION_X_annual_his
STATION_annual_change_X_rcp85
write.csv(STATION_annual_change_X_rcp85,file="STATION_annual_change_X
_rcp85.csv", row.names = FALSE)
```

###seasonal_means

```
STATION_X_seasonal_rcp85<- seasonalfunction (STATION_X_rcp85.zoo,
FUN=mean, na.rm=TRUE)
STATION_X_seasonal_rcp85
write.csv(STATION_X_seasonal_rcp85, file =
"STATION_X_seasonal_rcp85.csv", row.names = TRUE)
```

NOTE: for precipitation use the function SUM and divide by nyrs

```
      e.g. STATION_pr_annual <-annualfunction (STATION_pr_hist.zoo,
                                FUN=sum, na.rm=TRUE)/nyrs
```

computing long term changes in average seasonal temperature

```
STATION_seasonal_X_change_rcp85<-STATION_X_seasonal_rcp85-
STATION_X_seasonal_hist
STATION_seasonal_X_change_rcp85
write.csv(STATION_seasonal_X_change_rcp85,file="STATION_seasonal_X_ch
ange_rcp85.CSV", row.names = TRUE)
```

NOTE: For precipitation, express the change as a percentage.